8-2013

# Altered ovarian cancer metabolism increases neuronal n-acetylaspartate to promote tumor growth

Behrouz Zand

**Altered ovarian cancer metabolism increases neuronal n-acetylaspartate to promote tumor growth**

Behrouz Zand, M.D.

APPROVED:

_____
Anil K. Sood, M.D.

_____
Menashe Bar Eli, M.D.

_____
Gary Gallick, Ph.D.

_____
Eric Wagner, Ph.D.

_____
Peiying Ying, Ph.D.

APPROVED:

_____
Dean, the University of Texas- Health Science Center at Houston
Graduate School of Biomedical Science

# Altered ovarian cancer metabolism increases the neuronal n-acetylaspartate to promote tumor growth

**Thesis**

**Presented to the Faculty of**

**The University of Texas**

**Health Science Center at Houston**

**And**

**The University of Texas**

**M.D. Anderson Cancer Center**

**Graduate School of Biomedical Sciences**

**In Partial Fulfillment**

**Of the Requirements**

**For the Degree of MASTER OF SCIENCE**

**By**

**Behrouz Zand, M.D.**

**August 2013**

## Dedication

To my parents, who have always taught me that higher education is one of the most important virtues to strive for in one's life. To my wife Sara, who has been nothing short of 100% supportive of my work and endeavors rain or shine. To my son Aria, who has changed my life more than I would have ever imagined before.

**Altered ovarian cancer metabolism increases the neuronal n-acetylaspartate to promote tumor growth**

Publication No._____

Behrouz Zand, M.D.

Supervisory Professor: Anil K. Sood, M.D.

**Background**: Altered metabolism is a well-established trait in many cancers, and is an emerging hallmark of cancer. Recent resurgence of cancer metabolism studies has identified dysregulated metabolic pathways that produce novel oncometabolites in various cancers. However, large scale studies of dysregualted high grade serous epithelial ovarian cancers (HGSOC) are unknown.

**Materials and Methods:** Following IRB approval, metabolic profiling of 101 HGSOC patients and 15 normal ovaries were obtained using GC/LC mass spectrometry from 2 U.S. academic centers to identify highly up-regulated metabolites. Samples from a cohort of 135 and 208 patients from a single institution were evaluated for gene expression and protein expression of NAT8L, respectively. Gene expression of NAT8L and clinical outcomes were further investigated from publicly available databases from the cancer genomics atlas (TCGA) using www.cbioportal.org, and two previously published melanoma gene expression profiles. Reverse Phase Protein Array (RPPA) and gene expression array were evaluated in HeyA8 ovarian cancer cell lines to investigate the protein and gene expression changes associated with NAT8L siRNA. *In vitro* and *in vivo*

experiments of NAT8L siRNA were investigated to evaluate its effects on cancer proliferation, apoptosis, cell cycle, and invasion/migration.

**Results**: A total of 313 metabolites were identified between these two groups, of which 172 were significantly altered ($p<0.05$) between HGSOC and normal ovary tissues. NAA was one of the most significant alterations in HGSOC compared to the normal ovary with a greater than 28 fold elevation in ovarian cancer compared to the normal ovary ($p=2.30E-11$). NAA levels in HGSOC were strongly correlated with its biosynthetic enzyme NAT8L gene expression levels ($r=0.52$, $p<0.0001$), and not with its degradation enzyme ASPA ($r= -0.11$, $0=0.30$). Patients with higher levels of NAA had worse overall survival (1295 days) compared to patients with low NAA levels (not reached) ($p=0.038$). Two separate HGSOC gene expression cohorts revealed that high expression of NAT8L is associated with worse median overall survival in HGSOC (35 months, 40 months) compared to low NAT8L gene expression (45 months, 52 months) ($p=0.03$, $p=0.005$). High NAT8L protein expression was associated with poor overall survival in ovarian cancer with 3.86 years overall survival compared to 9.09 years with low NAT8L expression ($p<0.001$). Furthermore, high NAT8L gene expression was found to have significantly worse overall survival in invasive breast, lung squamous, colon, uterine, melanoma and kidney renal cell cancers.

HeyA8 and A2780 cell lines showed that NAT8L siRNA significantly increased total apoptosis compared to control (NT) siRNA by 38.53% ($p<0.001$) and 37.85% ($p<0.001$), respectively. HeyA8 cells treated with paclitaxel and NAT8L siRNA had a 29.83% increase in apoptosis compared to paclitaxel and NT siRNA

treated cells ($p<0.001$). HEYA8 and A2780 cells treated with NAT8L siRNA had a significantly decreased cell proliferation by 23.65% ($p<0.001$) and 19.13% ($p<0.001$), respectively. HEYA8 cells treated with NAT8L siRNA had an 8.4% increase in the number of cells with G1 phase ($p<0.001$), and an 11.65% decrease in the number cells in the S phase ($p<0.001$). Knockdown of NAT8L in HEYA8 cells significantly decreased migration and invasion by 91% and 92%, respectively ($p<0.001$). In HEYA8 orthotopic ovarian cancer mouse models, DOPC NAT8L siRNA had significantly decreased tumor burden by 69.17% ($p<0.01$), respectively. Furthermore, NAT8L siRNA + paclitaxel had significantly less tumor burden compared to NT siRNA ($p<0.001$), paclitaxel + NT siRNA ($p=0.004$), and NAT8L siRNA alone ($p=0.032$). We observed similar effects in A2780, SKOV3 orthotopic ovarian cancer mouse models and orthotopic A375-SM melanoma mouse model.

Genomic analysis of HEYA8 cells transfected with NAT8L siRNA compared to NT siRNA showed 1961 significantly different gene expression data ($p<0.001$). Hierarchical cluster analysis of RPPA from NAT8L siRNA and NT siRNA had 171 significantly different protein expression data ($p<0.05$). Computational network analysis (NetWalker) showed significant decreases in a large number of genes involved in mitosis and the M phase of the cell cycle, regulation of catabolic processes, and regulation of cell death being altered.

**Conclusion**: HGSOC metabolic profiling revealed highly altered metabolism compared to the normal ovary. NAA is one of the most up-regulated metabolites in HGSOC. High levels of NAA are associated with worse overall survival in HGSOC. Furthermore, high expression of its biosynthetic gene (NAT8L) is associated with

worse overall survival in HGSOC, invasive breast, lung squamous, colon, uterine, melanoma and renal cell cancers. Inhibiting NAA production decreases tumor growth, and tilts the cancer cell to a more catabolic steady state. Therefore, our data indicate that targeting cancer's NAA production maybe an effective therapeutic approach.

**Table of Contents**

**List of figures**

**List of Tables**

## Background and Introduction

### Ovarian Cancer

In the U.S., ovarian cancer is the fifth most common cause of cancer related deaths in women [1]. Approximately 22,280 women in the U.S. will be diagnosed, and 15,500 will die in one year of ovarian cancer [1]. Despite drug developments, ovarian cancer remains a high mortality cancer with diagnosis in late stage of disease and high tumor burden[2]. This high mortality is due the incidence of recurrence remaining high, and little has changed over 30 years [3,4].

Treatment of primary ovarian cancer is a combination of tumor cytoreductive surgery and combination intravenous paclitaxel and carboplatin chemotherapy. The role of surgery is important to extend overall survival with the ultimate goal of cytoreduction to no residual disease [5,6,7]. Patients with primary ovarian cancer have a 70-80% chemotherapy response rate; however, 40-50% will recur within two years. Various chemotherapy route administration and dose adjustment have been attempted to improve outcomes. For example, the administration of intraperitoneal (I.P.) chemotherapy has been shown to increase overall survival in patients with residual disease < 1 cm after surgery[8]. However, it remains controversial as direct comparison doses to intravenous chemotherapy is not available, and toxicity of I.P. remains a major issue[2]. Given the poor survival and high recurrence of ovarian cancer with little improvement in patient outcomes despite cytotoxic drug developments over the years, the focus is turning on understand the tumor biology to identify new targets in therapy.

## Cancer Metabolism

Altered metabolism is a well-established trait in many cancers, and is an emerging hallmark essential to cancer's biology[9]. In order to better understand cancer metabolism, knowledge of unicellular microbes and proliferating cell in multicellular organisms can better illustrate the effect of environmental nutrition on cell functioning. Under adequate nutrition availability, unicellular organisms such as microbes and proliferating cells in multicellular organisms have evolutionary pressure to replicate new cells. These cells and unicellular organisms will uptake nutrients to provide carbon, nitrogen, and free energy to build new cells. Glucose is the main nutrient metabolized by these cells, and through glycolysis will excrete carbons through lactate, ethanol, or other organic acids such as acetate or butyric acid[10]. In periods of nutrient deficiency or cell starvation, these cells will alter their metabolism to provide maximum amount of free energy for cell survival and temporarily halt cell replication[10].

In multicellular organisms, most cells are exposed to a constant supply of nutrients. To prevent uncontrolled cell proliferation, these cells need growth factor stimulation of signaling receptors to stimulate uptake of nutrients. Cancer cells overcome this by specific gene mutations that can alter receptor signaling pathways. These pathways can be constitutively active allowing for constant nutrient uptake and metabolism that promote cell survival and growth[10]. Therefore, altered cancer metabolism presents a promising approach to anti-cancer therapy development, and this has caused a resurgence of research revealing new metabolic pathways not seen in non-cancerous cells.

Glycolysis and Warburg Effect

Under adequate oxygen supply, differentiated or non-proliferating cells metabolize glucose to $CO_2$ by oxidizing pyruvate in the tricarboxylic acid cycle (TCA cycle). This results in reduction of nicotinamide adenine dinucleotide (NADH). NADH fuels oxidative phosphorylation to maximize ATP production[10]. In anaerobic conditions, differentiated cells primarily rely on glycolysis for energy production, and therefore produce large amounts of lactate. However, cancer cells, normal proliferating cells, and unicellular microbes rely heavily on glycolysis and produce large amounts of lactate even in the presence of adequate oxygen supply. This alteration of cell metabolism in cancer cells compared to non-cancerous cells was first reported by Otto Warburg in 1956[11]. This "Warburg effect" of high glucose consumption and high lactate production has clinically been taken advantage of by fluorodeoxyglucose positron emission tomography (FDG-PET) scans [12].

The metabolism of one molecule of glucose using oxidative phosphorylation in the TCA cycle yields 36 ATP molecules, whereas under glycolysis, glucose only yields 2 ATPs[13]. So why do cancer cells rely heavily on glycolysis even when oxygenation is plentiful? One explanation is that cancer cells are highly proliferative and require large amounts of biomass (lipids, amino acids, and nucleotides) to divide therefore these cells demand more than just ATP. There is accumulating evidence that a "Supply-Based" model is more likely in cancer cells [14]. In this model, growth factor signaling directly increases nutrient uptake and alters

metabolism to maximize biomass production independent of ATP. Thus, ATP is a secondary process in proliferating cancer cells. An example of this is shown by Van Heiden et al. for the major cell membrane molecule, palmitate[10]. Palmitate synthesis requires 7 molecules of ATP, 16 carbons from 8 molecules of acetyl-coA, and 28 electrons from 14 molecules of reduced nicotinamide adenine dinucleotide phosphate (NADPH). A glucose molecule can either provide 36 ATPs via oxidative phosphorylation, 30 ATPs and 2 molecules of NADPH though pentose phosphate pathway, or 6 carbons in the form of acetyl-CoA for macromolecular synthesis. Therefore, proliferating cells demands for glucose are inclined more for NADPH and acetyl-CoA production for palmitate synthesis, and not ATP from oxidative phosphorylation. Furthermore, the commitment of glucose into maximal ATP production by oxidative phosphorylation would increase ATP/ADP ratio therefore inhibiting NADPH and acetyl-CoA production. Therefore, glucose consumption in proliferating and cancer cells is more so needed for acetyl-CoA production for lipid synthesis, diversion to PPP for ribose production for nucleotide synthesis, and glycolytic intermediates for non-essential amino acid production.

Mitochondria and cancer

The mitochondria genome includes one to two thousand nuclear DNA gene, and thousands of copies of mitochondrial DNA inside the mitochondria[15]. The mitochondrial DNA contains the 13 most important genes for oxidative phosphorylation while the nuclear DNA contains the rest including genes for mitochondrial metabolic regulation[15]. The mitochondria has many essential cellular functions and regulates energy production, oxidation-reduction (redox)

status, cytoplasmic calcium levels, reactive oxygen species (ROS) production, biosynthetic precursors such as acetyl-CoA, and apoptosis[15]. It is clear that many cancer cells do not have dysfunctional mitochondria as a well-functioning mitochondrion is needed for cell viability and growth [16,17]. Mitochondrial DNA mutations can alter cell metabolism and enhance tumorigenesis by impairing oxidative phosphorylation and adapting the cell's bioenergetics state for proliferation[18]. Mutations in mitochondrial nuclear DNA genes can also contribute to tumorigenicity. Mutations in succinate dehydrogenase (SDH), fumurate hydratase (FH), and IDH1 and IDH2 can increase levels of succinate, fumurate, and R-2-hydroxyglutarate [(R)-2-HG][19,20,21]. This can inhibit various alpha-ketoglutarate dioxygenase levels and activate NRF2 response leading to increased tumorigenicity [20,22].

Altered cancer metabolism can increase ROS produced by mitochondria. Mitochondrial ROS is a potent mitogen, and if apoptosis is inhibited, high ROS can cause neoplastic transformation [23,24]. Furthermore mitochondrial ROS can stabilize hypoxia inducible factors (HIF), nuclear factor kappa-B (NF-Kβ), and FOS-JUN transcription factors thereby increasing cell proliferation [15,25]. Cancer cell ROS can also affect the tumor microenvironment whereby it inactivates caveolin-1 in the surrounding stromal fibroblasts. This increases fibroblast mitophagy reducing its mitochondrial function, and increases fibroblast lactate production. The over production of lactate in fibroblasts can fuel cancer cells to aid in proliferation and growth. [26]

Lipogenesis in cancer

Most non-cancerous mammalian cells get lipids from the blood stream, and *de novo* lipogenesis occurs mainly in liver, adipocytes, and lactating breasts[27]. Cancer cells can synthesize lipids similar to embryonic cells by reactivating *de novo* lipogenesis [28,29]. The increase in lipid synthesis has important consequences to cancer cell survival and growth. One consequence of lipogenesis is for the massive biomass accumulation. In fact, inhibition of lipid synthesis has been shown to decrease cancer cell proliferation and tumor growth [30,31,32,33]. Fatty acids contribute to phospholipids (phosphotidylcholine, phosphotidylethalamine) for cell membrane synthesis, and phospholipids are associated with poor survival in several cancers [34,35].

There is evidence that lipid synthesis confers resistance in cancer cells to oxidative stress. Cancer cells have high rates of saturated and mono-unsaturated fatty acid synthesis, and this has been shown to reduce cell death induced by oxidative stress or chemotherapy agents[36]. Inhibition of lipid synthesis may seem promising to combine with chemotherapy agents to improve the efficacy of its cytotoxicity.

Increased lipid synthesis may also confer cell resistance to the effects of energy stress. Some tumors rely on lipid oxidation as a source of energy production by using mitochondrial beta-oxidation to produce ATP via OXPHOS [37,38]. Activation of beta-oxidation seems to be needed for cancer cell viability during times of energy stress [39,40].

The regulation of lipid synthesis is mainly done by Sterol Regulatory Element Binding Transcription Factor (SREBPs)[41]. There are three isoforms that regulate lipogenesis: SREBP1a, SREBP1c, and SREBP2[42]. SREBP1a is most abundant in cultured cells [43]. Although there are overlaps, SREBP1s mainly regulate fatty acid, phospholipid, and triaceylglyceride synthesis, and SREBP2 main regulates cholesterol synthesis [41]. Cancer tissues show elevated level of SREBPs[27]. Regulation of SREBPs can be positively regulated by PI3K/AKT/mTOR, loss of retinoblastoma (Rb), and mutant p53 [44,45,46]. Negative regulation of SREBPs is seen with high phosphotidlycholine or AMPK activity [47,48].

Amino acids and Cancer metabolism

Amino acids (AA) are carbon molecules that contain amino and acid groups that have variable side chains giving them different biochemical functions [49]. There are 300 known amino acids, but only 20 of them serve as building blocks for proteins(Table 1) [49]. Amino acids such as ornithine, citrulline, homocysteine, taurine, and β-alanine have major roles in cell metabolism [50,51,52,53]. Important functions of AA catabolism leads to metabolites with important biologic functions such as ammonia, carbon dioxide, long and short-chain fatty acids, glucose, ketone bodies, nitric oxide, urea, uric acid, polyamines, and nitrogenous substances[49]. In addition AA can regulate gene expression and proteins signaling, synthesize hormones and low-molecular weight nitrogenous substances, and regulate metabolic pathways for growth and survival.

**Table 1. Twenty protein building amino acids**

| Essential amino acids | Non-essential amino acids |
|---|---|
| Arginine | Alanine |
| Histidine | Asparagine |
| Isoleucine | Aspartate |
| Leucine | Cysteine |
| Lysine | Glutamate |
| Methionine | Glutamine |
| Phenylalanine | Glycine |
| Threonine | Proline |
| Tryptophan | Serine |
| Valine | Tyrosine |

AA can regulate gene expression at transcription, translation, and post-translational protein modifications [49]. For example, methionine, glycine, serine and histidine can methylate proteins and DNA, thus regulating gene and protein signaling [49]. Glutamine, arginine, and leucine can stimulate mTOR1 in a cell specific manner therefore increasing its anabolic activity of protein synthesis and inhibiting autophagy [54,55].

AA can be precursors for low-molecular weight hormones and neurotransmitters. Tyrosine or phenylalanine can be synthesized into epinephrine, norepinephrine, dopamine, and thyroid hormones [49]. Tryptophan is a precursor for serotonin and

melatonin. Glutamate is the precursor for GABA [49]. Furthermore, high doses of oral of intravenous AA can stimulate hormones from endocrine cells. Arginine, glutamine, and leucine can stimulate insulin, growth hormone, prolactin, glucagon, progesterone, and placental lactogen [56,57].

Another important function of AA is regulating key metabolic pathways in cells. For example, glutamate and aspartate mediate transfer of reducing equivalents across the mitochondrial membrane via the malate-aspartate shuttle which affects glycolysis and cell redox status. The net result of the malate-aspartate shuttle is that NADH is transported from the cytosol into the mitochondria generating 3 ATP molecules [58]. Another example of metabolic regulation by AA is with arginine. Arginine increases expression of AMPK and peroxisome proliferator-activated receptor γ co-activator 1-α (PPAR) proteins which has been shown to affect mitochondrial energy status and rat fat mass [59].

Glutamine is one of the highest nutrients to be consumed by cancer cells. Glutamine is a non-essential amino acid because humans are able to synthesize it from glutamate and ammonia via the enzyme glutamine synthetase(GS)[13]. However, not all human tissues have GS therefore these tissues rely on glutamine uptake from tissues that are able to synthesize glutamine. Glutamine can be used in cells for protein synthesis, nucleotide synthesis, and glucosamine production[60]. Cells that are driven to growth by the oncogene MYC are particularly sensitive to glutamine availability. MYC driven cells will undergo apoptosis by failing anaplerosis from glutamine derived substrates [61].

Glutamine together with glucose provides most of the carbon and nitrogen needed for cell replication [62]. In glioblastoma cells, approximately 60% of glutamine and 90% of glucose can produce lactate and alanine waste. Glutamine provides TCA intermediate alpha-ketoglutarate for anaplerosis which promotes NADPH production via malic enzyme. Pyruvate is synthesized in this reaction which is then converted to lactate by lactate dehydrogenase [62]. Therefore, the excess lactate production seen in the "Warburg effect" is not only a consequence of glucose/glycolysis, but also of the glutatmine/glutaminolysis pathway.

Although glucose is the major lipogenic precursor in cancer cells, glutamine can also provide carbons for lipid synthesis. $^{14}C$ labeling of glutamine showed that 25% fatty acyl molecules in glioblastoma cells were derived from glutamine. Furthermore, glutamine analplerosis provides oxaloacetate substrate that combines with glucose derived acetyl-coA for citrate production via citrate synthetatase[62]. However, some cancer cells with mutations in TCA cycle enzymes or electron transport chain have defective mitochondrial functioning for lipid synthesis. These cancer cells rely on glutamine dependent reductive carboxylation for citrate formation. This pathway relies on cytoplasmic and mitochondria isocitrate dehydrogenase enzyme (IDH), therefore rendering glutamine as the major source for acetyl-coA production in lipid synthesis [63].

There is emerging evidence for the role of other amino acids and their role in cancer progression. For example, inhibiting glycine uptake and its mitochondrial biosynthesis impairs proliferation in cancer cells [64]. Prostate cancer cells have high levels of the amino acid sarcosine (a glycine derivative), and high levels of

sarcosine lead to cancer progression and metastases [65]. Functional genomics has shown that serine synthesis is essential for breast cancer carcinogenesis [66]. Inhibition of the isoform M2 pyruvate kinase (PKM2) leads to accumulation of glycolytic intermediates into the serine synthesis pathway therefore maintains mTOR1 activity [67]. Furthermore, serine starvation in p53 deficient cells resulted in oxidative stress, reduced cell viability and increased cell proliferation [68].

Besides glucose, glutamine is also another nutrient heavily consumed by cancer cells. Glutamine is a non-essential amino acid because humans are able to synthesize it from glutamate and ammonia via the enzyme glutamine synthetase(GS)[13]. However, not all human tissues have GS therefore these tissues rely on glutamine uptake from tissues that are able to synthesize glutamine. Glutamine can be used in cells for protein synthesis, nucleotide synthesis, and glucosamine production[60]. Cells that are driven to growth by the oncogene MYC are particularly sensitive to glutamine availability. MYC driven cells will undergo apoptosis by failing anaplerosis from glutamine derived substrates [61].

Glutamine together with glucose provides most of the carbon and nitrogen needed for cell replication [62]. In glioblastoma cells, approximately 60% of glutamine and 90% of glucose can produce lactate and alanine waste. Glutamine provides TCA intermediate alpha-ketoglutarate for anaplerosis which promotes NADPH production via malic enzyme. Pyruvate is synthesized in this reaction which is then converted to lactate by lactate dehydrogenase [62]. Therefore, the excess lactate production seen in the “Warburg effect” is not only a consequence of glucose/glycolysis, but also of the glutatmine/glutaminolysis pathway.

Although glucose is the major lipogenic precursor in cancer cells, glutamine can also provide carbons for lipid synthesis. $^{14}C$ labeling of glutamine showed that 25% fatty acyl molecules in glioblastoma cells were derived from glutamine. Furthermore, glutamine analplerosis provides oxaloacetate substrate that combines with glucose derived acetyl-coA for citrate production via citrate synthase [62]. However, some cancer cells with mutations in TCA cycle enzymes or electron transport chain have defective mitochondrial functioning for lipid synthesis. These cancer cells rely on glutamine dependent reductive carboxylation for citrate formation. This pathway relies on cytoplasmic and mitochondria isocitrate dehydrogenase enzyme (IDH), therefore rendering glutamine as the major source for acetyl-coA production in lipid synthesis [63].

AMPK and cell metabolism

One of the key metabolic regulators in eukaryotic cells is AMP-activated protein kinase (AMPK)[69]. Ultimately, the role of AMPK is to balance the ratio of ATP consumption and ATP generation. AMPK promotes cell catabolism to generate more ATP, and inhibits anabolic pathways[69]. AMPK can be activated by lowering of intracellular ATP; AMP or ADP can directly bind to its regulatory subunit causing a conformational change that protects its activating phosphorylation [70,71]. The major phosphorylation mechanism of AMPK is by the threonine/serine kinase Liver Kinase B1 (LKB1) at Thr172 [72,73]. AMPK can also be phosphorylated at Thr 172 by calcium flux, independent of LKB1, by CAMKK2 (CAMKKβ) kinase [74]. The majority of AMPK regulation in cell are by LKB1, however, CAMKK2 appears to be major AMPK regulators in T-cells and neurons

[75,76]. TAK1of the MAPKKK family can also activate AMPK by phosphorylating Thr172 [77]. Additional controls of AMPK regulation are currently unknown.

In mammalian cells, AMPK can be activated by a variety of cell stresses and variety of drugs which increase cellular levels of AMP, ADP, or calcium [78]. Metformin, the type 2 diabetes drug, can activate AMPK in a LKB1 dependent manner[79]. Metformin indirectly causes AMPK activation by inhibiting Complex I of the respiratory chain leading to lower ATP levels[80,81]. The AMPK agonist AICAR is a precursor to ZMP which mimics AMP, and also indirectly activates AMPK[82]. The chemotherapy drug pemetrexed can also result in elevated ZMP therefore activating AMPK [83].

There is emerging evidence that AMPK can be activated independent of AMP, ADP, or calcium. In cultured cells, AMPK is activated by reactive oxygen species (ROS). The mechanism of action is unclear, but it has been proposed to involve inhibition of mitochondrial ATP synthesis[80], oxidation of two conserved cysteine residues in the AMPK alpha subunit[84], or by the protein ataxia telangiectasia (ATM) which can phosphorylate LKB1[85]. Genotoxic agents such as etoposide, doxorubicin, and ionizing radiation can also activate AMPK, although the mechanism is not clear [86,87,88].

AMPK coordinates PI3K/AKT/mTOR pathway to control cell growth and autophagy. For example, mTORC1 is tightly regulated by AMPK. AMPK can either phosphorylated the tumor suppressor TSC2 on serine 1387 or directly phosphorylate Raptor (regulator associated protein of mTOR) blocking the ability of

mTORC1 kinase to phosphorylate its substrates [89,90]. The autophagy components ULK1 can be directly activated by AMPK or by mTORC1[91,92] . Autophagy is activated to replenish metabolites and nutrients in times of low energy state. AMPK can trigger destruction of defective mitochondria though ULK1 dependent mitophagy and trigger mitochondrial biogenesis though PGC-1-alpha transcription[69]. In hematopoietic stem cells, genetic knockout of LKB1 or AMPK catalytic subunits caused a significant rise in defective mitochondria[93]. Therefore, AMPK is a key regulator of mitochondrial homeostasis.

AMPK can alter cellular metabolism by directly regulating metabolic enzymes or by altering transcription. AMPK is a key regulator of acetyl-coA carboxylase (ACC) and HMG-coA reductase which are rate limiting steps for fatty acid and sterol synthesis, respectively[94,95]. In fat cells, AMPK directly phosphorylates lipases such as hormone sensitive lipase and adipocyte triglyceride lipase (ATGL)[96,97]. AMPK can regulate glucose uptake of cells by playing a key role in GLUT4 endocytic trafficking [98]. AMPK can phosphorylate a number of transcription factors, coactivators, acetyltransferase p300, histone deacetylases, and histones that can alter cell metabolism[69]. One example is the lipogenic transcription factor (SREBP1) by phosphorylating a conserved serine site suppressing its activation. SREBP1 induces expression of ACC and FASN to promote de novo lipogenesis, and tumor growth [99,100]. AMPK can negatively regulate cAMP-regulated transcriptional co-activators (CRTCs) and histone deacetylates(HDACs) [101,102]. Negative regulations of CRTCs have recently been shown to prolong lifespan in *C. elegans* opening up a new potential of biological functions for these co-activators

[101]. AMPK phosphorylation of HDACs in the liver can translocate to the nucleus to deaceytlate FOXO family transcription factors and regulate glucose homeostasis in the liver[103]. Increased expression of CRTCs and HDACs can promote tumor progression and growth [104,105,106].

P53 and tumor metabolism

Findings from The Cancer Genome Atlas (TCGA) showed that many high grade epithelial ovarian cancers have p53 mutations (96%), a high rate of somatic mutations with few recurrent mutations, and high copy number alterations[107]. P53 is a tumor suppressor by two mechanisms: 1.) regulating repair and survival of damaged cells 2.) Discarding damaged cells that cannot be repaired through apoptosis or autophagy. Activation of p53 from DNA damage leads to G1 cell cycle arrest and DNA repair activation. This mechanism allows to cells to resume normal cell cycle functioning and the genomic integrity is maintained. To remove damaged cells that can't be repaired, p53 can activate pro-apoptotic genes such as Bax, Noxa, and Puma. In addition to cell survival and death, p53 can also influence cellular metabolism.

The evidence of p53 regulation of glycolysis is complex and unclear. Emerging evidence is revealing p53 a major negative regulator of glycolysis mediated by p53 transcriptional activation of TP53-induced glycolysis and apoptosis regulator (TIGAR). TIGAR dephosphorylates fructose-2, 6-bisphosphate (F2-6P) and lowers its cellular levels. F2-6p is a potent activator of the glycolytic rate limiting enzyme 6-phosphofructo-1-kinase (PFK-1), therefore p53 inhibits glycolysis through this mechanism [108]. Also, p53 can down-regulate phosphoglycerate

mutase (PGM) which converts 3-phosphoglycerate to 2-phosphoglycerate in glycolysis, thus inhibiting glycolytic flux. On the other hand, some studies are showing that p53 can activate glycolysis by stimulating type II hexokinase promoter gene expression, and this activation leads to increased tumor survival[109,110]. Clearly, further studies are needed to clarify p53's role in glycolysis.

P53 can stimulate mitochondrial oxidative respiration by activating several key components of the electron transport chain in cancer cell. Furthermore, p53 can increase the TCA cycle rate by activating glutaminase 2 (GLS2)[111,112]. GLS2 is a mitochondrial protein that hydrolyzes glutamine to glutamate, and deamination of glutamate leads to alpha-ketoglutarate synthesis. Furthermore, p53 knock-out mice display impaired mitochondria respiration [112].

De novo lipogenesis has also been shown to be regulated by p53. AMPK expression is up-regulated by p53 and this result in increased inactivation of the lipid rate limiting enzyme ACC [102]. P53 also regulated biomass production by inactivating glucose-6-phosphate dehydrogenase resulting in suppression of pentose phosphate pathway and decreased NADPH production [113]. As stated before, NADPH is critical for lipogenesis in proliferating cells. On the other hand, emerging evidence is developing that in times of energy stress, p53 can up-regulate fatty acid oxidation to produce ATP and NADPH further promoting cell survival and resistance to the metabolic stress[114]. For example, a new p53 target GAMT has been identified which is involved in the creatine pathway. GAMT is involved in p53 induced apoptosis under genotoxic stress. However, under glucose deprivation and energy stress, p53 dependent up-regulation of GAMT induces fatty acid oxidation

increasing cell survival [115]. This complicated dual role of p53 in cancer metabolism suggests that its role may be tissue and/or cancer specific. Further understanding of various cancer types and the role of p53 in regulating its mechanism are needed.

Targeting Cancer Metabolism

It is important to note that targeting cancer metabolism is not a new approach in cancer therapy history. Sidney Farber noticed that adding folic acid to leukemic cells caused an increase in cancer growth[116]. This discovery lead to the development of the first folate analogue drug aminopterin which lead to the first remission of Acute Lymphoblastic Leukemia[117]. Another folate analogue, methotrexate lead to the first cure of solid tumors when administered to choriocarcinoma patients[118].

The emerging studies of altered cancer metabolism have revealed the high consumption of various nutrients, the increased biosynthetic pathways, and the oncogenic signaling driving these changes are paving the way for novel approaches to anti-cancer therapy development. For example, circulating levels of insulin and insulin growth factor (IGF) seen in obesity and diabetes promote cancer progression by activating cancer growth signaling [119,120,121]. Lowering blood glucose levels is associated with improving cancer outcomes [121]. The diabetic drug Metformin is being explored as an agent that can improve cancer outcomes. Metformin lowers blood glucose by inhibiting mitochondrial complex I in liver which decreases ATP production [79,119]. This up-regulates AMPK signaling, which inhibits

gluconeogenesis, effectively lowering blood glucose levels and increasing insulin sensitivity to lower circulating levels of insulin [79].

Despite driver mutations causing cancer growth and progression, there are no effective treatments against these mutations. Targeting metabolic enzymes seems a promising approach to disrupt these driver mutation effects. For example k-RAS and MYC rely on glucose and glutamine uptake for cell growth and survival, respectively [61,122]. Disrupting glucose or glutamine uptake or their pathway molecules in these cells can be an important approach to stopping its growth mechanism. Cytoxic chemotherapy can also disrupt glucose uptake, therefore synthetic lethality approaches by combining chemotherapy and metabolic enzyme drug targets would seem like a promising approach[119].

Ovarian cancer metabolism

Recent investigation of ovarian cancer revealed a shift in cancer metabolism paradigm, Nieman et al. showed that ovarian cancer cells behave like parasites to the surrounding host cells by inducing catabolic processes in the adipocytes and tumor stroma. Ovarian cancer cells were homed to the host cells by cytokines such as IL-8, and would increase catabolic processes such as aerobic glycolysis; mitophagy, autophagy, and lipolysis in the host cells. Because of this processes, cancer cells were able to extract nutrients such as lactate, fatty acids, glutamine, and ketones to fuel the mitochondria and promote growth and metastasis [123]. Therefore, ovarian cancer cells up-regulated their oxidative phosphorylation and beta-oxidation to use these substrates for ATP production. Interestingly, the

authors saw that SKOV3ip1 cells co-cultured with adipocytes had up-regulated AMPK, inhibition of ACC, and up-regulation of beta-oxidation in cancer cells. RPPA analysis of primary ovarian tumors compared to omental metastasis tumor revealed that the metastatic tumors had greater ACC phosphorylation. This was a surprising finding given the many other results show that show up-regulation of AMPK and inhibition of ACC to lead to decreased tumor growth[33,124,125,126,127].

Along with fatty acid metabolism, ovarian cancers have increased choline-containing metabolites [35]. These include phosphotidylcholine, phosphocholine, glycerophosphocholine, and choline is important for many cell functions including proliferation and cell membrane synthesis. Mechanisms behind these elevations include choline transport, choline mediated choline kinase phosphorylation, and activation of phosphotidylcholine phospholipases. Inhibition of these phosphotidycholine metabolic pathways can inhibit tumor growth, and a novel choline kinase inhibitor Mn58b, has shown to inhibit growth in carcinoma models [128].

There has been one attempt at a large scale metabolic profile in ovarian cancer, Denkert C. et al. profiled 66 ovarian cancer tissues and 9 borderline tissues using GC/mass spectrometry. They detected 291 metabolites, but were only able to identify 114 (39%) of these metabolites. Using a threshold of $p<0.01$, they were able to identify 51 metabolites that differed from ovarian cancer and borderline tumors. An increase in glycerolipid, purine and pyrimidine, and energy metabolism were noted to be higher in ovarian cancer. Interestingly, several fatty acids and

lactate were higher in borderline tumors. A major limitation of the study was that the ovarian cancer samples included 25% non-serous tumors, and 43% of the ovarian cancer tumors were not high grade tumors.

Oncometabolites

The recent resurgence of cancer metabolism studies has identified dysregulated metabolic pathways that produce novel oncometabolites in cancer. Genome-wide sequencing of glioblastoma multiforme (GBM) or WHO III and III astrocytoma and oligodendroglioma revealed that the majority of these tumors harbor an IDH1 or IDH2 mutation[129,130]. The two initial studies showed that IDH1 and IDH2 mutation in these patients doubled the median overall survival compared to the wild type IDH1/2 patients [129,130]. These mutations are not only prevalent in high grade gliomas, but also in acute myeloid leukemia [131]. These mutations cause the loss of the cell's ability to convert α-ketoglutarate to isocitrate when the mutant IDH protein forms a heterodimer with the wild type IDH protein therefore inactivating the physiologic IDH enzyme function. When the IDH mutant protein forms a homodimer protein, these mutations gain the ability to create the metabolite called (R)-2-hydroxyglutarate (2HG) [21,131] from α-ketoglutarate and glutamate which can lead to DNA hyper methylation [132,133,134]. Furthermore, studies of 2HG are identifying that 2HG has tumorigenic properties instead of the tumor suppressive role. Recently, high serum levels of 2HG are associated with worse overall survival in AML [135].

In a metabolic profile of human oligodendroglioma cells (HOG), Reitman et al evaluated the effects of isocitrate dehydrogenase 1(IDH1-R132) and 2 (IDH2-R172) mutations. One of the most striking findings in their study was that the levels of N-acetylaspartate (NAA) and N-acetylaspartylglutamate (NAAG) in IDH1-R132 and IDH2-R172 cells compared with wild type IDH1 and IDH2 cells were significantly decreased. No pathogenesis as result of low NAA or NAAG was investigated in this study; therefore the role of NAA and NAAG is unclear in this setting. The authors speculated that since acetyl CoA or free amino acid levels were not decreased between the wild type and IDH mutated cells in this the HOG cells, the decreased NAA can be a result of low NAT8L expression or high ASPA expression. In a separate study of non-invasive detection of 2HG in WHO grade 2 and 3 glioma patients using proton magnetic resonance spectroscopy (MRS) showed with high sensitivity and specificity in IDH1 and IDH2 mutated gliomas had higher 2HG and lower NAA peaks compared to wild type IDHI/2 gliomas. Therefore, both IDH mutation metabolic studies show that the wild type IDH1/2 gliomas lead to low 2HG and higher NAA levels compared to the mutant IDH1/2 gliomas. With that said, the mechanism of IDH mutation decreasing NAA levels is currently unclear and further work is needed to provide insight into the function of NAA and 2HG in gliomas.

The neuron specific metabolite NAA

NAA is the N-acetylated amino acid aspartic acid via the amine nitrogen group. Acetylation is the transfer of an acetyl group from acetyl-coA to another molecule; in this case the amino acid aspartic acid accepts the acetyl group to form NAA. The molecular weight of this compound is 175 Daltons in its ionic form. NAA

biosynthesis occurs in neurons by the catalysis of the enzyme N-acetylaspartate synthetase (NAT8L)[136,137]. The NAA metabolic pathway in the neuron illustrated is discussed below (Figure 1)[138].

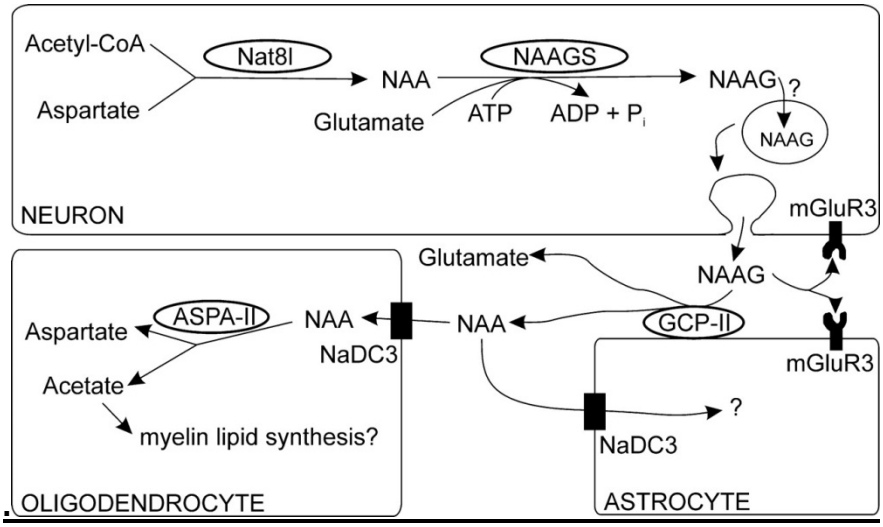


**Figure 1. Schematic presentation of NAA metabolism [138].** NAA is synthesized in the neuron via the enzyme NAT8L by acetyl-coA and aspartate. NAA and glutamate form NAAG in an ATP dependent manner via the enzyme NAAGS. NAAG is transported out of the neuron by an uknown mechanism to the extra-neuronal space (ECF). NAAG is hydrolyzed into NAA and glutamate in the ECF. Glutamate binds to the metabotropic glutamate receptor 3 (mGLuR3) to activate the glutamatergic neurotransmission process. NAA is taken up by oligodendrocytes by sodium-dependent dicarboxylate transporter (NaDC3). Inside oligodendrocytes, NAA is metabolized by aspartoacyclase (ASPA) into aspartate and acetate. Acetate is proposed to be used for the myelin lipid synthesis.

The sources for acetyl-coA for NAA in the brain of developing rats are pyruvate from glycolysis and 3-hydroxybutyrate (a ketone body). The aspartate arises from aspartate transamination (AST) by using the substrates glutamate and oxaloacetate forming aspartate and alpha-ketoglutarate [139]. The NAT8L enzyme has only been localized in the neuronal mitochondria and microsomes (likely endoplasmic

reticulum) [136,140,141]. NAA production is faster under high respiration energy state than in low respiration energy state[139]. NAA production can be stimulated by ADP, and inhibited by ATP production [142].

NAA is a major form of aspartic acid in the brain, and NAA concentrations in the brain are on average 3-8 mM [143], making it one of the most distinct signals that is prominent by brain magnetic resonance spectroscopy (MRS)[144,145,146] [147].

After its synthesis, NAA can bind with glutamate to form NAAG by the ATP dependent enzyme NAAG synthetase [138]. NAAG is transported out of neuron into the ECF where it can be hydrolyzed back into NAA and glutamate by the membrane bound enzyme Glutamate Carboxypeptidase II (GCP-II) or CGP-III. Genes encoding for these proteins are FOLH1 and NAALAD2, respectively. The glutamate binds to astrocyte Glu metabotropic receptor 3 (GRM3), and is taken up to form glutamine[147]. Furthermore, GRM3 activation can signal endothelial cells to form new capillaries allowing for transport of glucose and oxygen to neurons[147]. NAA is targeted towards oligodendrocytes [140], where it is taken up by the sodium ion transporter NaDC3.

Uptake of NAA allows for its degradation into acetate and aspartate by the enzyme aspartoacyclase (ASPA) [148]. ASPA is zinc containing carboxypeptidase enzyme, which deacetylates NAA [149]. ASPA is present in several tissues such as CNS, liver, and kidney in the developing rat [150]. The mammalian neurons do not contain ASPA, therefore oligodendrocyte are where the NAA are transported to be metabolized in the CNS [151].

The primary function of NAA remains elusive as most studies have focused on MRS studies compared to the biochemistry of NAA. Furthermore, almost all studies are based on the mammalian brain. It is proposed that NAA can function as alternative source of acetate for lipid synthesis by transporting into oligodendrocytes where it is broken down into acetate by ASPA for lipid synthesis [152,153,154,155]. Alternatively, NAA has been proposed to act as an osmotic regulator by transporting water bound to NAA into ECF [156].

NAA has also been linked to ATP production, and proposed to be involved in analplerosis [38,139,142]. This is based on the theory that depletion of aspartate from the mitochondria would promote the kinetics of aspartate transaminase (AST) towards aspartic acid and alpha-ketoglutarate production [148,157]. It is reasonable to assume that all of these functions can co-exist as the consequences of NAA biosynthesis and metabolism, and further research would help clarify NAA's biologic role.

More evidence of its biological role are highlighted by two inborn errors of metabolism diseases which involve disruption of the NAA metabolic pathway. The first is called hypoacetylaspartia characterized by the inability to biosynthesize NAA by NAT8L. There has been one documented case in history of a patient with hypoacetylaspartia. This patient suffered from severe mental retardation, ataxia, microcephaly, and seizures[158]. This patient was found to have homozygous mutation of NAT8L [137]. In a single reported study of NAT8L knockout mice study the focus was mainly on the social behavior of mice which showed decreased social interaction and greater anxiety like behaviors in homozygous deleted NAT8L [159];

no other histological or MRS detection of NAA was reported in this study limiting any generalizability to the human condition.

The second inborn error of metabolism disease with abnormal NAA levels is Canavan disease. Canavan disease is characterized by a lack of ASPA activity which leads to NAA accumulation. Clinically, patients with this disease display macrocephaly, severe cognitive and motor delay, seizures, and death by the third decade of life [160]. The pathologic hallmark of Canavan disease is dysmyleination, intramyelinic edema , and central white matter vacuoles[160]. The knockout mice studies for ASPA have recapitulated the biologic effects seen in human Canavan disease. Homozygous (-/-) ASPA mice display failure to thrive, macrocephaly, neurologic impairments such as tremors, abnormal gait, lethargy, pain insensitivity, and some developed seizures by 6 months of age. MRS of the -/- ASPA mice showed abnormally high levels of NAA compared to the wild type mice, and histopathologic evaluation of the brain showed features similar to those seen in Canavan disease [161].

NAA has recently been detected outside of the CNS [65,162,163,164]. Aspiration from ovarian tumor cysts (OTC) has been linked to be significantly higher in the serous histology type benign, borderline, and malignant tumors [163,164], and there was no difference between NAA levels in OTC between the malignant, borderline, or benign serous tumors. The range of OTC NAA concentrations in serous tumors have been reported between 5-187 μM [163,164,165]. However, higher NAA concentrations in ovarian cyst fluid of malignant serous ovarian cancers have been found to be associated with advanced stage disease (Stage III

and IV)[163]. The concentrations of NAA levels in OTC have also been found to be relatively similar to the concentration present in malignant ascites[163]. These findings suggest that NAA in cyst and ascites fluid are associated with higher stage disease, and that NAA levels may be associated with worsening outcomes.

In a small study, the metabolome of normal human ovaries, primary ovarian adenocarcinomas (POC) and metastatic omental ovarian cancer (MOC) tumors were profiled by LC and GC mass spectrometry. NAA and NAAG levels were elevated by 3.5 and 2.2 fold, respectively, in POC compared to the normal ovary. NAA and NAAG were further elevated by 85.6 and 8.5 fold, respectively, in MOC compared to the normal ovary[162]. This indicates that NAA levels are even much higher in the metastatic tumors compared to the primary ovarian cancer site, and suggests that its accumulation may have a role in ovarian cancer pathogenesis.

**Hypothesis and specific aims:**

Hypothesis #1: Metabolic profiling of ovarian cancer compared to the normal ovary will identify tumor promoting metabolites

Specific Aim: Identify the most up-regulated metabolite in ovarian cancer compared to the normal ovary in human patients and determine the consequences to tumor growth when its production is inhibited

Hypothesis #2: High levels of NAA are associated with worse outcomes in ovarian cancer

- Specific Aim: Determine the clinical consequences of alterations in the NAA pathway in ovarian cancer

Hypothesis #3: Decreasing NAA production will decrease tumor growth and progression

- Specific Aim: Examine the biological effects of inhibiting NAA production by siRNA NAT8L in ovarian cancer cell proliferation, survival, and invasion using *in vitro* and *in vivo* assays

## Methods

### Clinical Analysis

After IRB approval was obtained, patients were identified at the University of Texas at M.D. Anderson Cancer Center (MDACC) and the University of Iowa who were diagnosed with ovarian, primary peritoneal, or fallopian tube carcinoma. Patients were excluded if they did not receive primary therapy at the institution of record or did not have routine follow-up at that institution. All patients were treated by surgical cytoreduction performed by a gynecologic oncologist in addition to adjuvant or neoadjuvant taxane- and/or platinum-based chemotherapy. Surgical staging was performed according to International Federation of Gynecology and Obstetrics guidelines. All treatments were administered at the institution of record. Specimens were reviewed by a gynecological pathologist at the institution of record. Clinical data collected included patient demographics, tumor characteristics, details of treatment, as well as outcomes data such as progression-free interval and overall survival. Optimal cytoreduction was defined by convention as residual disease less than 1 cm as reported by the surgeon of record. Tissue samples were obtained at the time of primary evaluation surgery. Patients who were known to be alive and/or progression-free at the time of last contact were censored accordingly. Kaplan-Meier survival curves were generated and compared using a 2-sided log-rank statistic.

Metabolic profiling

Sample Preparation: Ovarian cancer tissue and normal ovary samples were stored at -80°C. At the time of analysis, samples were extracted and prepared for analysis using a standard solvent extraction method. The sample preparation process was carried out using the automated MicroLab STAR® system from Hamilton Company. Recovery standards were added prior to the first step in the extraction process for QC purposes. Sample preparation was conducted using a proprietary series of organic and aqueous extractions to remove the protein fraction while allowing maximum recovery of small molecules. The resulting extract was divided into two fractions; one for analysis by LC and one for analysis by GC. Samples were placed briefly on a TurboVap® (Zymark) to remove the organic solvent. Each sample was then frozen and dried under vacuum. Samples were then prepared for the appropriate instrument, either LC/MS or GC/MS.

Liquid chromatography/Mass Spectrometry (LC/MS): The LC/MS portion of the platform was based on a Waters ACQUITY UPLC and a Thermo-Finnigan LTQ mass spectrometer, which consisted of an electrospray ionization (ESI) source and linear ion-trap (LIT) mass analyzer. The sample extract was split into two aliquots, dried, then reconstituted in acidic or basic LC-compatible solvents, each of which contained 11 or more injection standards at fixed concentrations. One aliquot was analyzed using acidic positive ion optimized conditions and the other using basic negative ion optimized conditions in two independent injections using separate dedicated columns. Extracts reconstituted in acidic conditions were gradient eluted using water and methanol both containing 0.1% Formic acid, while the basic

extracts, which also used water/methanol, contained 6.5mM Ammonium Bicarbonate. The MS analysis alternated between MS and data-dependent MS scans using dynamic exclusion.

Gas chromatography/Mass Spectrometry (GC/MS): The samples destined for GC/MS analysis were re-dried under vacuum desiccation for a minimum of 24 hours prior to being derivatized under dried nitrogen using bistrimethyl-silyl-triflouroacetamide (BSTFA). The GC column was 5% phenyl and the temperature ramp is from 40° to 300° C in a 16 minute period. Samples were analyzed on a Thermo-Finnigan Trace DSQ fast-scanning single-quadrupole mass spectrometer using electron impact ionization. The instrument was tuned and calibrated for mass resolution and mass accuracy on a daily basis. The information output from the raw data files was automatically extracted as discussed below.

Accurate Mass Determination and MS/MS fragmentation (LC/MS), (LC/MS/MS): The LC/MS portion of the platform was based on a Waters ACQUITY UPLC and a Thermo-Finnigan LTQ-FT mass spectrometer, which had a linear ion-trap (LIT) front end and a Fourier transform ion cyclotron resonance (FT-ICR) mass spectrometer backend. For ions with counts greater than 2 million, an accurate mass measurement could be performed. Accurate mass measurements could be made on the parent ion as well as fragments. The typical mass error was less than 5 ppm. Ions with less than two million counts require a greater amount of effort to characterize. Fragmentation spectra (MS/MS) were typically generated in data

dependent manner, but if necessary, targeted MS/MS could be employed, such as in the case of lower level signals.

Bioinformatics: The informatics system consisted of four major components, the Laboratory Information Management System (LIMS), the data extraction and peak-identification software, data processing tools for QC and compound identification, and a collection of information interpretation and visualization tools for use by data analysts. The hardware and software foundations for these informatics components were the LAN backbone, and a database server running Oracle 10.2.0.1 Enterprise Edition.

Compound identification: Compounds were identified by comparison to library entries of purified standards or recurrent unknown entities. Identification of known chemical entities was based on comparison to metabolomics library entries of purified standards. As of this writing, more than 1000 commercially available purified standard compounds had been acquired registered into LIMS for distribution to both the LC and GC platforms for determination of their analytical characteristics. The combination of chromatographic properties and mass spectra gave an indication of a match to the specific compound or an isobaric entity. Additional entities could be identified by virtue of their recurrent nature (both chromatographic and mass spectral). These compounds have the potential to be identified by future acquisition of a matching purified standard or by classical structural analysis.

Normalization: For studies spanning multiple days, a data normalization step was performed to correct variation resulting from instrument inter-day tuning differences. Essentially, each compound was corrected in run-day blocks by registering the medians to equal one (1.00) and normalizing each data point proportionately. For studies that did not require more than one day of analysis, no normalization is necessary, other than for purposes of data visualization.

Metabolite statistics: All Wilcoxon rank-sum tests and *t*-tests are two-sided using a threshold of $P < 0.05$ for significance. Class-specific metabolomics patterns were visualized using heat maps. Unsupervised clustering of samples using metabolomics signatures was performed using Cluster and TreeView, and visualized using heat maps.

NAT8L gene expression:

To determine NAT8L gene expression across different cancer types, RNA expression of 20 cancer types were analyzed by RNASeqV2 data available from the open access TCGA web page as of Jan 18, 2013 were accessed. The normalized counts were log2 transformed (after adding 1) to emphasize differences on a multiplicative scale. The copy number data was analyzed as well using all of the public level 3 data available as of Oct 30, 2012.

To determine gene expression of NAT8L's association with clinical outcomes, RNA expression data was analyzed by RNASeqV2 data available from the open access TCGA web site www.cbioportal.org as of April 2013 were

accessed. Overall survival was analyzed by best cut-off method on provisional databases, and based on all tumors from each query.

To validate gene expression data from non-TCGA cohorts, clinical information CEL (Affymetrix U133Plus2)) arrays files from the publication by Tinker et al. [166] were analyzed to validate ovarian cancer NAT8L outcomes. To determine NAT8L gene expression's association with melanoma outcomes, clinical information CEL (Affymetrix U133Plus2)) arrays files from the publication Bogunovic et al.[167] was accessed for analysis. Also, clinical information and expression values from melanoma samples profiled with Illumina arrays by Jonsson G et al.[168] were analyzed. All analyses were performed in R (version 2.14.2) (http:///www.r-project.org/). The RMA gene expression values were analyzed, and best cut off method to identify clinical outcomes. For survival analysis the patients were grouped into percentiles according to NAT8L expression. Gene expression by best cut-off was done to optimally split the samples into two groups. The Log-rank test was employed to determine the significance of the association between NAT8L expression and overall survival. The Kaplan-Meyer method was used to generate survival curves.

Immunohistochemistry

Immunohistochemical (IHC) analysis was done on formalin-fixed, paraffin-embedded samples, using standard techniques. For NAT8L, antigen retrieval was in citrate buffer for 45 minutes in an atmospheric pressure steamer, using anti-NAT8L antibody (Sigma-Aldrich) at 1:100 dilution was incubated overnight at 4°C. Primary

antibody detection was with Biotenelatled HRP polymer for 6 minutes at room temperature, followed by diaminobenzidine incubation. After IHC staining, a semi-quantitative H-score was done. Briefly, the intensity of tumor cells positive for NAT8L was 1= weak, 2 = moderate, or 3= strong intensity. NAT8L counted and expressed as a percentage of all tumor cells by an examiner blinded to clinical outcome. Patient samples were categorized as having low (<25%) =1, intermediate (25 %< x<75%) =2 or high (>75%) =3. The product of percentage of cell score and intensity score equaled the H-Score. The IHC analysis was done on samples collected at primary debulking surgery on 209 untreated patients with stage III–IV, high-grade papillary serous adenocarcinoma; with institutional review board approval, clinical information was collected. Progression-free and overall survival were plotted with the Kaplan–Meier method for patients in each group of NAT8L expression and compared with the log-rank statistic.

Gene Array

Gene array data from HeyA8 ovarian cancer cells double transfected with NAT8L siRNA and NT siRNA were deposited into the GEO database. Array data processing was performed on Illumina BeadStudio software. We normalized gene expression data using Quantile normalization and $\log_2$ transformation. To export to a data matrix, Sample Gene Profile option of this software was used. BRB-ArrayTools were primarily used to identify genes differentially expressed between the 2 subgroups [169], and all other statistical analyses were performed in the R language environment. Gene expression differences were considered significant if *P* values were less than 0.001. A random-walk based network scoring method,

NetWalker, for genomic data analysis was employed (Komurov, White et al 2010). The replicates in gene expression array (siRNA NAT8L in HeyA8) were averaged and the ratio of average siRNA NATBL/average Control in HeyA8 was considered. The gene names were converted into HUGO formats. Unbiased network of the top down and up regulating genes (considered around top 100 interactions) is displayed by running NetWalker on the entire gene set.

Reverse Phase Protein Array

HeyA8 cell lines were double transfected with NAT8L siRNA and NT siRNA. Cellular proteins were denatured by 1% SDS (with beta-mercaptoethanol) and diluted in five 2-fold serial dilutions in dilution buffer (lysis buffer containing 1% SDS). Serial diluted lysates were arrayed on nitrocellulose-coated slides (Grace Biolab) by Aushon 2470 Arrayer (Aushon BioSystems). Total 5808 array spots were arranged on each slide including the spots corresponding to positive and negative controls prepared from mixed cell lysates or dilution buffer, respectively.

Each slide was probed with a validated primary antibody plus a biotin-conjugated secondary antibody. Only antibodies with a Pearson correlation coefficient between RPPA and western blotting of greater than 0.8 were used in reverse phase protein array study. Antibodies with a single or dominant band on western blotting were further assessed by direct comparison to RPPA using cell lines with differential protein expression or modulated with ligands/inhibitors or siRNA for phospho- or structural proteins, respectively.

The signal obtained was amplified using a Dako Cytomation–catalyzed system (Dako) and visualized by DAB colorimetric reaction. The slides were

scanned, analyzed, and quantified using a customerized-software Microvigene (VigeneTech Inc.) to generate spot intensity.

Each dilution curve was fitted with a logistic model ("Supercurve Fitting" developed by the Department of Bioinformatics and Computational Biology in MD Anderson Cancer Center, "http://bioinformatics.mdanderson.org/OOMPA"). This fits a single curve using all the samples (i.e., dilution series) on a slide with the signal intensity as the response variable and the dilution steps are independent variable. The fitted curve is plotted with the signal intensities – both observed and fitted - on the y-axis and the log2-concentration of proteins on the x-axis for diagnostic purposes. The protein concentrations of each set of slides were then normalized by median polish, which was corrected across samples by the linear expression values using the median expression levels of all antibody experiments to calculate a loading correction factor for each sample. "Linear after normalization" values were transformed to Log2 values and median centered for hierarchical clustering analysis. Heatmaps for unsupervised hierarchical clustering (antibody unsupervised but samples in order for reference). The heatmap was generated in Cluster 3.0 (http://bonsai.hgc.jp/~mdehoon/software/cluster/software.htm) as a hierarchical cluster using Pearson correlation and a centered metric. The resulting heat map was visualized in Treeview (http://www.eisenlab.org/eisen).

Network of the top up and down regulating proteins and phosphorylated proteins was displayed. The protein names were converted into HUGO formats. NetWalker was used to display the network of the proteins in red-green colormap and the phosphor-proteins in the yellow-blue colormap. Note that if for some

protein the total and phosphor both were down (or up, respectively) then the color is dominated by the level of the total protein. The RPPA data was median centered and the ratio of the NAT8L/Control was considered to draw these networks.

Cell lines and culture conditions

The derivation of the human ovarian cancer cell lines A2780, HeyA8, SKOV3-IP1, are previously reported [170,171,172,173,174]. The cell lines A2780, HeyA8, and SKOV3-IP1 were maintained in RPMI-1640 medium with 15% Fetal Bovine Serum (FBS). HeyA8-MDR and SKOV3-TR are taxane-resistant derivations of HeyA8 and SKOV3ip1 (Dr. Isaiah J. Fidler, MDACC, Houston, TX). The taxane-resistant phenotype was maintained by adding 300 ng/mL (HeyA8-MDR) and 100 ng/mL (SKOV3-TR) of paclitaxel to the media used for HeyA8 and SKOV3-ip1. The human melanoma cell line A375SM was established from pooled lung metastases produced by A375-P cells injected intravenously into nude mice [175]. These cells were maintained in Eagle's minimal essential medium supplemented with 10% fetal bovine serum (FBS)[176]. The melanoma cell lines UACC 62, UACC 257, and M14 were obtained from Dr. Suhendan Ekmekcioglu (The University of Texas-MD Anderson Cancer Center; Houston, Texas), and were maintained in MEM supplemented with 10% fetal bovine serum, 100 µg/ml glutamine, penicillin (100 units/mL), and streptomycin (100 µg/mL) (Invitrogen, Carlsbad, CA). The Ishikawa human endometrial cancer cell line was maintained in MEM supplemented with 10% FBS and 0.1% gentamicin sulfate (gift from Dr. Russell Broaddus, MDACC, Houston, TX) [177]. Cell lines were also routinely tested to confirm absence of Mycoplasma. Cells were maintained at 37°C in a humidified incubator infused with

20% $O_2$ and 5% $CO_2$.

Orthotopic model of ovarian cancer and melanoma in nude mice

Female athymic nude (NCr-*nu*) were purchased from Taconic Farms, Inc. (Rockville, MD). The development and characterization of the orthotopic mouse model of ovarian cancer has been previously described [178,179,180]. Briefly, SKOV3-IP1 ($1 \times 10^6$), A2780 ($1 \times 10^6$), HeyA8 ($0.25 \times 10^6$) human ovarian cancer cells were lifted with trypsin/edta, washed with PBS, and resuspended in 200 µL of Hank's balanced salt solution (HBSS, Mediatech, Inc. Manassas, VA) and were injected into the peritoneal cavity of female nude mice. A375-SM subcutaneous tumors were produced by injecting $1 \times 10^6$ cells/0.2 ml HBSS over the right hip region of the mice. Growth of subcutaneous tumors was monitored by weekly examination of the mice and measurement of tumors with calipers. All cell lines have been shown to reliably form macroscopic tumor implants on peritoneal surfaces throughout the pelvis and abdominal cavity.

Tumor weight was recorded at the time of necropsy and tumor tissue was harvested for histopatholoigcal analysis. Proliferation index and apoptosis were evaluated in tumor sections with immunohistochemical staining for Ki67 and cleaved caspase-3 antigens, respectively. Frozen sections were fixed in acetone + chloroform 1:1 for 5 minutes between two 5 minute incubations in cold acetone alone. Endogenous peroxidases and non-specific epitopes were blocked with 3% $H_2O_2$ in PBS and 5% normal horse serum + 1% normal goat serum in PBS, respectively. Sections were then incubated with primary antibody directed against

either Ki-67 (1:200, Neomarker, Fremont, CA) or CD31 (1:800, Cell Signaling, Danvers, MA) at 4°C overnight. After washing with PBS, the appropriate HRP-conjugated secondary antibody in blocking solution was added for 1 hour at room temperature. Slides were developed with 3, 3'-diaminobenzidine (DAB) chromogen (Invitrogen, Carlsbad, CA) and counterstained with Gil No.3 hematoxylin (Sigma-Aldrich, St. Louis, MO). Proliferative index and cleaved caspase 3 index was calculated by dividing the number of positive nuclei (brown) or by the total number of cells for each of 5 randomly selected 200x high power fields per tumor specimen for each treatment group.

Forward transfection

In the case of forward transfection, 6-well plates were inoculated with 150,000 cancer cells per well with a goal of transfection at 50% confluence within 12-24 hours of plating. Based on validation experiments, the appropriate amount of the siRNA of choice was incubated for 20 minutes at room temperature in serum-free culture medium (1 mL/well) with Lipofectamine 2000 (Invitrogen, Carlsbad, CA) at a 3:1 ratio of volume (μL) Lipofectamine 2000 to microgram siRNA. After incubation, siRNA/Lipofectamine-containing medium were added to cells and media to achieve a siRNA concentration of 50 nM. Cells and transfection media were incubated at 37°C for 4 hours, and then transfection medium was changed to serum-containing medium.

Reverse transfection

In the case of reverse transfection, and based on previously performed validation experiments, the appropriate amount of the siRNA of choice was incubated for 20 minutes at room temperature in serum-free culture medium (500 mcL/well) with Lipofectamine RNAiMAX (Invitrogen, Carlsbad, CA) at a 5:1 ratio of volume of Lipofectamine RNAiMAX to mcL siRNA. After incubation, 500 mcL of the solution was placed in each well, and then 75,000 cancer cells in 2.5 mL of serum-free media were added to each well to achieve a final siRNA concentration of 50 nM. Cells were incubated with the transfection medium for 4-6 hours at 37$^{o}$C, and then medium was changed to serum-containing medium.

Double transfection

If a longer duration of mRNA knockdown was needed than was offered by single forward or reverse transfection, then sequential double transfection was used. In this case, forward transfection was initially performed, and 72 hours later, a reverse transfection was performed.

RNA Extraction

Total RNA was extracted from cells growing *in vitro* using RNeasy Kit (Quiagen, Venlo, Netherlands). Cells were lifted with trypsin/edta, washed with PBS, and centrifuged at 10,000 rpm for 5 minutes to form the pellet. The supernatant was discarded, and RNA was extracted according to the company protocol. RNA was quantified using a spectrophotometer and 1 µg was transcribed into complementary DNA (cDNA) using the Verso cDNA kit (Thermo Fisher Scientific), closely following

the manufacturer's protocol. Quantitative RT PCR was then used to assess levels of expression.

*In vitro* apoptosis

Cells were plated in 6-well plates at 150,000 cells per plate, targeting approximately 50% confluence in serum-containing medium. After two rounds of transfection with siRNA (144 hours), cell viability was assessed using Annexin V and 7-amino-actinomycin-D (7AAD) staining (BD Pharmingen™, Franklin Lakes, NJ) by flow cytometry. Briefly, cells were harvested, washed in PBS, and incubated with PE-Annexin V and 7AAD according to package insert instructions for 20 minutes prior to flow cytometric analysis.

*In vitro* proliferation

Cells were plated in 6-well plates at 150,000 cells per plate, targeting approximately 50% confluence in serum-containing medium. After two rounds of siRNA transfection at time point 96 hours, the percentages of cells proliferating (defined as S-phase) were determined using the Click-iT EdU flow cytometry kit (Invitrogen, Carlsbad, CA). Cells were incubated with 10 mcM 5-ethynyl-2-deoxyuridine (EdU) for 2 hours, lifted, and washed with 1% bovine serum antigen in d-PBS. Cells were fixed with 4% paraformaldehyde in d-PBS for 15 minutes at room temperature and then maintained at 4°C protected from light until the time of flow cytometric analysis, duration not to exceed 7 days. On the day of analysis, cells were washed in 1% BSA in d-PBS and then permeabilized with 1x saponin-based reagent for 15 minutes at room temperature. The cells were then incubated with a

solution of 1x reaction buffer, CuSO4, Alexa-Fluor 488 azide dye, and proprietary reaction buffer additive for 30 minutes at room temperature prior to flow cytometric analysis.

In vitro cell cycle

For cell-cycle analysis, cells were transfected with siRNA as described for 48 hours, trypsinized, washed in PBS, and fixed in 75% ethanol overnight. Cells were then centrifuged, washed twice in PBS, and reconstituted in PBS with 50 µg/mL of propidium iodide. Propidium iodide fluorescence was assessed by flow cytometry.

*In vitro* invasion and migration

A polycarbonate membrane with 10-µm pores (Osmonics, Livermore, CA) was uniformly coated with a defined basement membrane matrix consisting of human laminin/type IV collagen/gelatin and used as the intervening barrier to invasion. The bottom well contained 500 µl of 5% FBS media. Cancer cells were added to the top wells with approximately 100,000 cells/well in serum free media. After 24-hour incubation in a humidified incubator at 37°C with 5% $CO_2$, cells that had invaded through the basement membrane were collected, stained, and counted by light microscopy[181]. Motility (migration) was determined in membrane invasion culture system chambers containing polycarbonate filter (with 10 µm pores) that had been soaked in 0.1% gelatin. Tumor cells ($5 \times 10^4$) were seeded in each upper well, allowed to incubate at 37°C for 6 hours in complete media, and subsequently processed as described for the invasion assay.

## Results

### Metabolic Profile of high grade serous epithelial ovarian cancer

To evaluate the global metabolic profile of human epithelial ovarian cancer (n=71) tissues and normal non-cancerous ovarian tissue (n=15), we used both liquid and gas chromatography coupled with mass spectrometry to identify relative metabolite levels. A total of 313 metabolites were identified between these two groups (Figure 2), of which 172 were significantly altered ($p<0.05$) between ovarian cancer tissues and normal ovary tissues. Of those 172 significantly altered metabolites, 142 were elevated and 30 were decreased in ovarian cancer. For visualizing the relationship between the 172 altered metabolites, hierarchical clustering was used to arrange the metabolites on the basis of their relative abundance levels across samples (Figure 3).

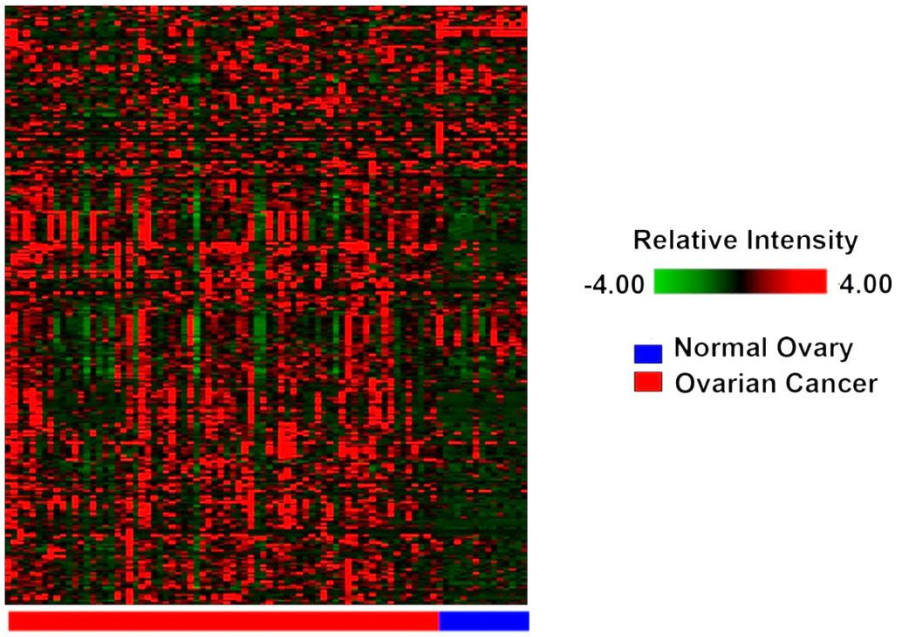


**Figure 2. Global metabolic profile of ovarian cancer and normal ovary.** Hierarchical clustering of 313 metabolites identified in LC/MS and GC/ MS metabolic progiling of ovarian cancer (n=72) and normal ovarian sample (n=15). Analysis reported with relative intensity to the median value for each metabolite set to 1.

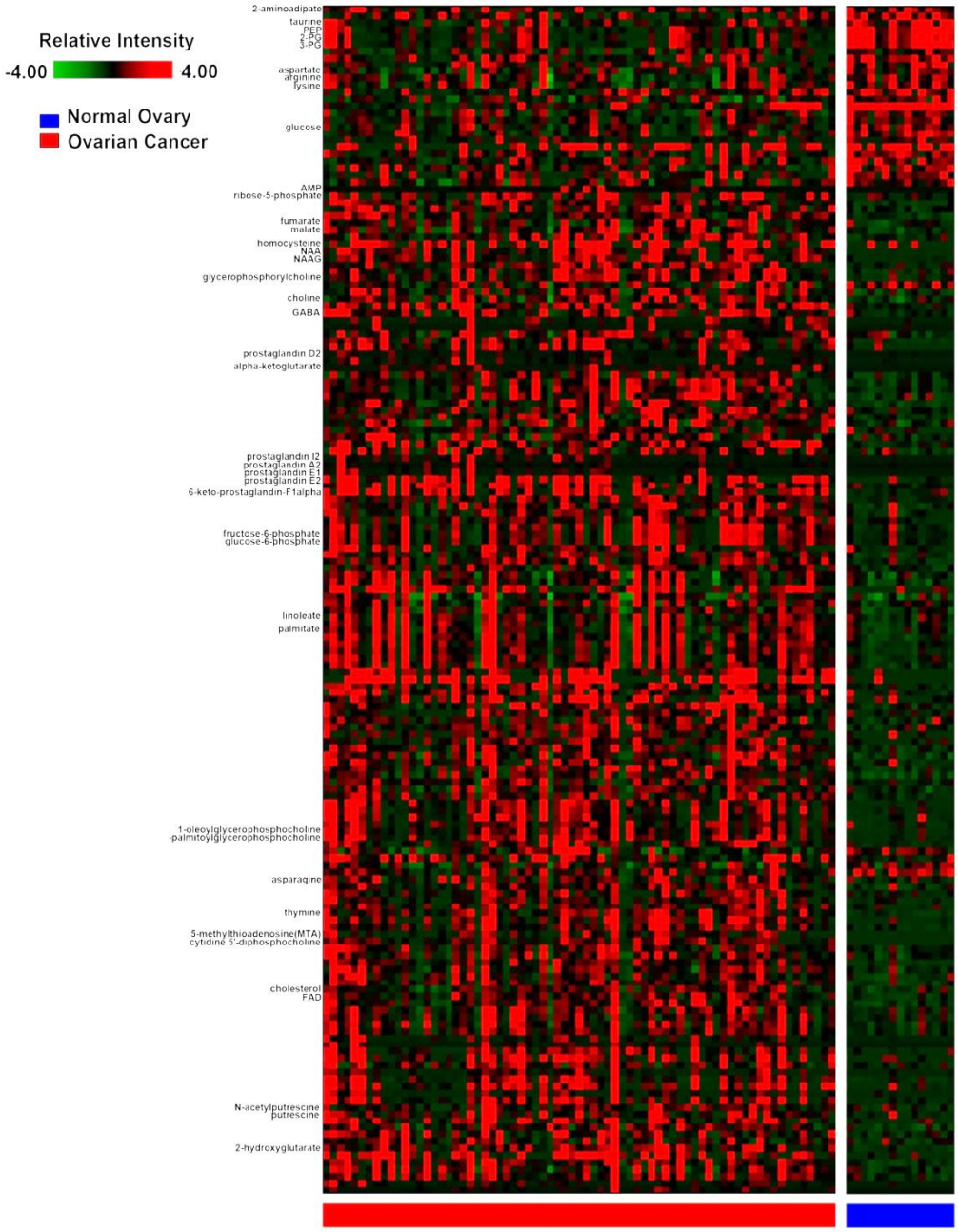


**Figure 3. Significantly altered metabolites in ovarian cancer.**
Hierarchical clustering of 172 significantly altered metabolites ($p<0.05$).

Of the 142 metabolites that were significantly up-regulated, the majority involved the lipid pathway (53.5%); this was followed by amino acid (19.0%), carbohydrate (9.9%), and nucleotide metabolic pathways (9.2%) (Figure 4).

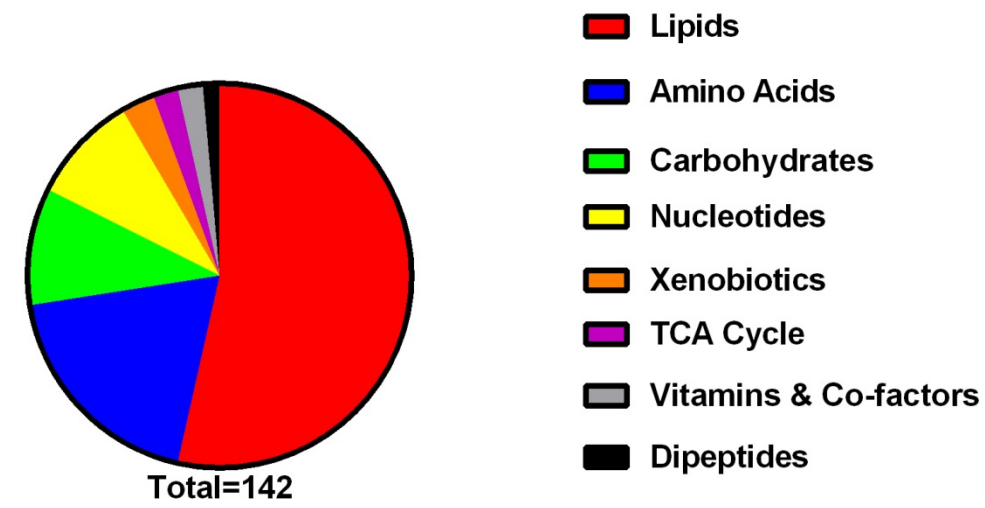


**Figure 4. Pathways affected by altered metabolism in ovarian cancer.**

Although lactate levels were not significantly elevated in ovarian cancer as compared to the normal ovary, the changes observed in the glycolytic intermediates was consistent with increased glucose metabolism in ovarian cancer. Increased levels of 6-carbon glycolytic intermediates glucose-6-phosphate (G6P) and fructose-6-phosphate (F6P) reflect increased utilization of intracellular glucose, while decreased levels of glucose, 3-phosphoglycerate (3-PG), 2-phosphoglycerate (2-PG) and phosphoenolpyruvate (PEP) suggest increased glycolytic activity with

contributions to lipid, amino acid, and nucleotide synthesis through pentose phosphate pathway (Figure 5).

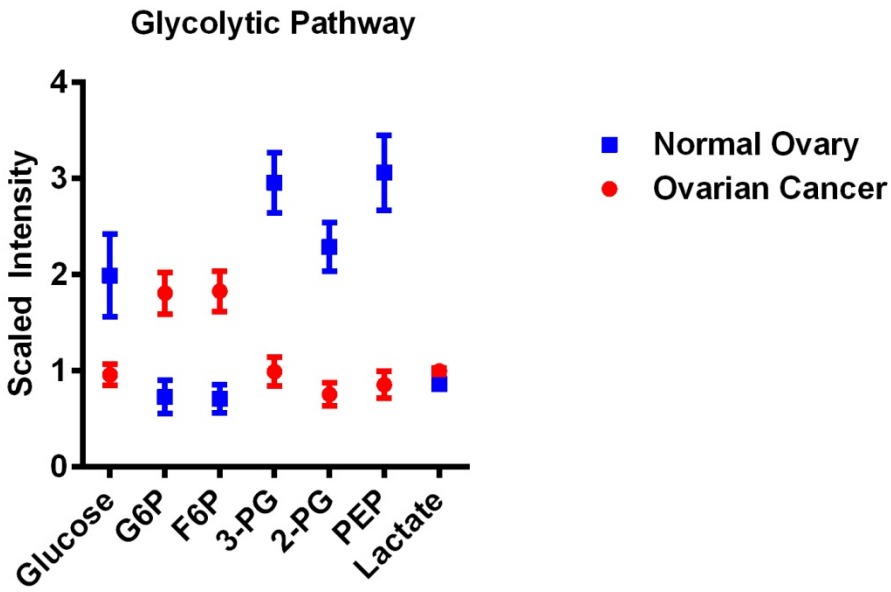


**Figure 5. Increased glucose metabolism in ovarian cancer.** Values are mean values of the relative intensity ± SEM.

Indeed, ovarian cancer revealed low 6-phosphogluconate, and elevated ribose-5-phosphate, and sedoheptulose-7-phosphate further suggesting increased activity of the pentose phosphate pathway (PPP) to promote NADPH production and nucleotide synthesis (Figure 6).

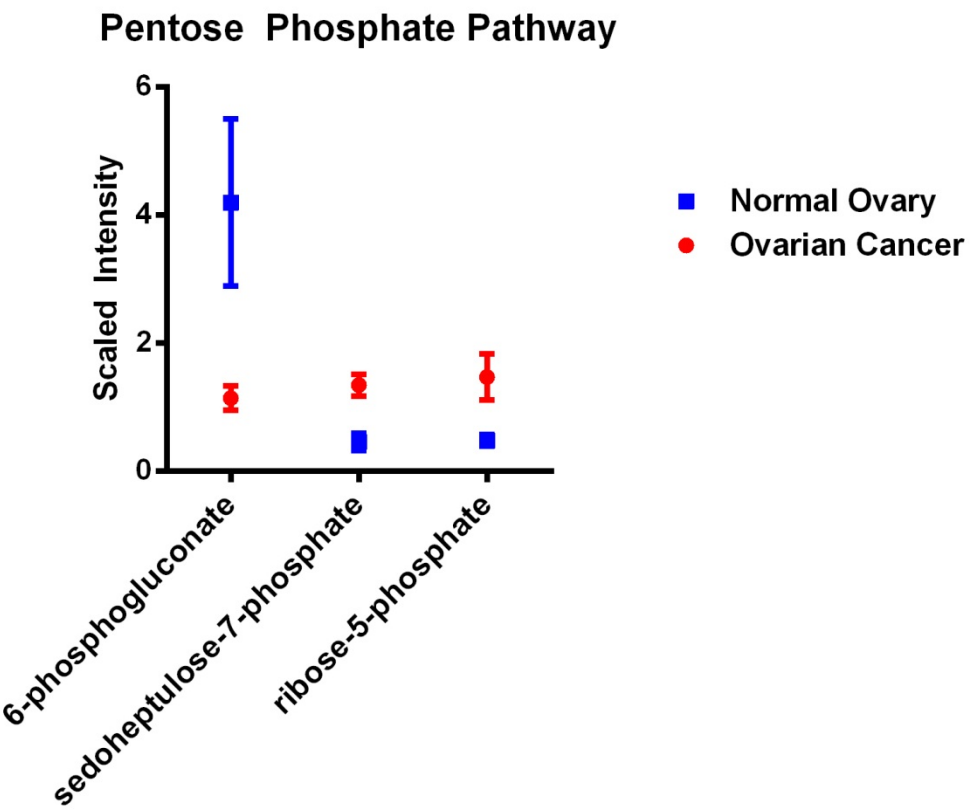


**Figure 6. Increased PPP metabolism in ovarian cancer**. Values are mean values of the relative intensity ± SEM.

The major pathway altered in ovarian cancer from the normal ovary was the lipid pathway. Ovarian cancer showed significantly elevated levels for essentially all long-chain fatty acids, with the notable exception of arachidonate and adrenate (Table 2).

**Table 2. Elevation of long-chain fatty acids in ovarian cancer.** Fold changes are the mean relative values of ovarian cancer over the normal ovary. NS is p>0.05.

| Metabolite | Fold Change | p-value |
|---|---|---|
| conjugated linoleate | 4.19 | 1.86E-05 |
| eicosenoate (20:1n9 or 11) | 3.50 | 1.32E-06 |
| 10-nonadecenoate (19:1n9) | 3.06 | 5.70E-06 |
| behenate (22:0) | 2.81 | 6.10E-05 |
| docosadienoate (22:2n6) | 2.61 | 0.0002 |
| dihomo-linoleate (20:2n6) | 2.33 | 0.0005 |
| palmitoleate (16:1n7) | 2.24 | 2.33E-05 |
| 10-heptadecenoate (17:1n7) | 2.18 | 4.39E-05 |
| docosatrienoate (22:3n3) | 2.10 | 0.0148 |
| oleate (18:1n9) | 1.89 | 0.0004 |
| myristoleate (14:1n5) | 1.73 | 0.0002 |
| nonadecanoate (19:0) | 1.72 | 2.07E-10 |
| stearidonate (18:4n3) | 1.67 | NS |
| margarate (17:0) | 1.66 | 1.80E-06 |
| adrenate (22:4n6) | 1.46 | NS |
| pentadecanoate (15:0) | 1.44 | 0.0306 |
| myristate (14:0) | 1.39 | 0.0053 |
| palmitate (16:0) | 1.38 | 0.0027 |
| arachidonate (20:4n6) | 1.24 | NS |
| stearate (18:0) | 1.20 | 0.0073 |

The most up-regulated long chain fatty acid was the bacterial gut derived conjugated linoleate (Fold change 4.19, p-value 1.86E-05). Also, odd-numbered carbon chain fatty acids such as pentadecanoate and margarate, and both saturated (e.g. palmitate and stearate) and unsaturated (e.g. palmitoleate and oleate) fatty acids were elevated. Interestingly, in ovarian cancer, there are significantly increased levels of the essential fatty acids linoleic acid (n-6), and linolenic acid (n-3) (Figure 7). Importantly, n-6 and n-3 levels are the precursors for prostaglandins, thromboxanes, leukotrienes, hydroxy fatty acids, and lipoxins[182]. Higher levels of these compounds are associated with a pro-inflammatory state in

cancer. Indeed, a significant up-regulation of eicosanoids were seen in the ovarian cancer samples compared to the normal ovarian tissue with prostaglandin E2 being the highest up-regulated eicosanoid (Fold change 15.15, p-value: 4.09E-08) (Table 3).

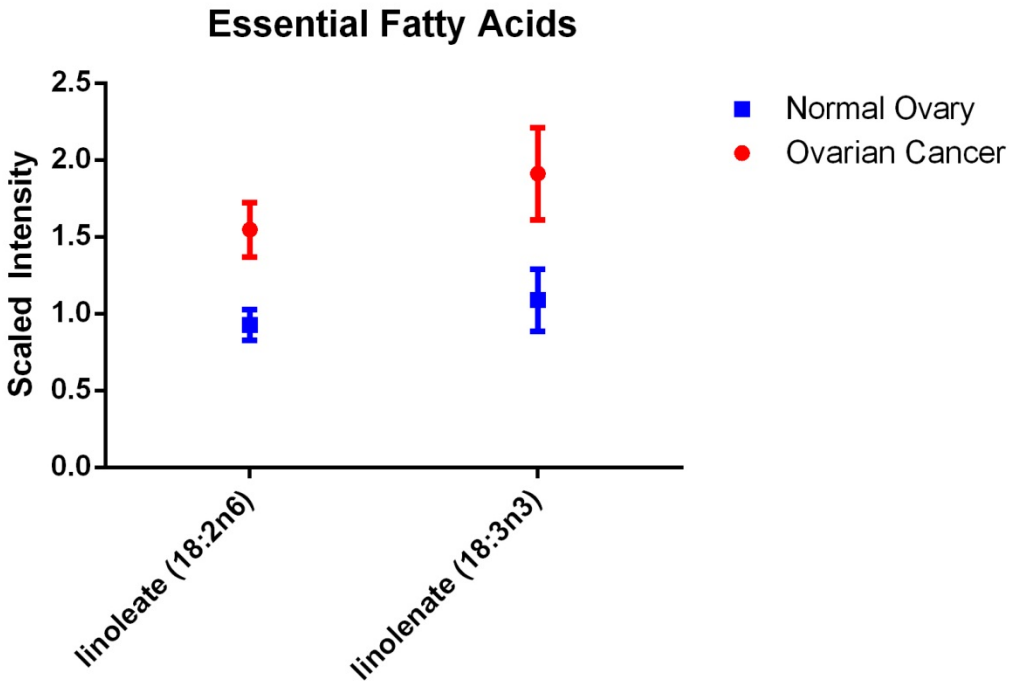


**Figure 7. Elevated levels of the essential fatty acids, linoleic acid (n-6) and linolenic acid (n-3), in ovarian cancer .** Values are relative scaled intensity mean values±SEM.

**Table 3. Up-regulation of eicosanoids in ovarian cancer.** Fold changes are the mean relative values of ovarian cancer over the normal ovary. NS is p>0.05.

| Metabolite | Fold Change | p-value |
|---|---|---|
| prostaglandin E2 | 15.15 | 4.09E-08 |
| 6-keto prostaglandin F1alpha | 11.12 | 1.88E-06 |
| prostaglandin I2 | 8.25 | 8.21E-06 |
| prostaglandin A2 | 6.80 | 5.14E-05 |
| 15-HETE | 6.28 | 8.81E-05 |
| prostaglandin D2 | 5.87 | 1.00E-04 |
| prostaglandin E1 | 5.04 | 1.05E-06 |
| thromboxane B2 | 2.57 | 1.72E-06 |

Along with the up-regulated fatty acids and eicosanoids in the lipid pathway, a similar lipid profile was seen with multiple components of the phospholipid biosynthetic pathways to support elevated membrane demands of cancer. There were significantly elevated levels of the membrane phospholipid precursor compounds such as choline, ethanolamine, and cytidine 5'-diphosphocholine (CDP-choline), and multiple lysophospholipid intermediates in membrane phospholipid biosynthesis (e.g. 2-myristoylglycerophosphocholine, 2-palmitoleoylglycerophosphoethanolamine, and 1-stearoylglycerophosphoinositol). These changes along with changes in cholesterol metabolism together indicate the massively altered membrane phospholipid metabolism in cancer.

**Brain specific N-acetylaspartate (NAA) is one of the highest up-regulated metabolites in ovarian cancer**

For further evaluation of each individual of the 142 metabolites that were significantly up-regulated, we narrowed our list to the 20 highest fold changes of metabolites in ovarian cancer (Table 4).

**Table 4. Twenty highest up-regulated metabolites in ovarian cancer.** Fold changes are the mean relative values of ovarian cancer over the normal ovary.

| Metabolic Pathway | Metabolite | Fold Change | p-value |
|---|---|---|---|
| Nucloetide | adenosine 5'-monophosphate (AMP) | 58.54 | 2.53E-06 |
| Lipids | CDP-choline | 30.38 | 1.00E-16 |
| Amino Acid | N-acetylaspartate (NAA) | 28.38 | 2.30E-11 |
| Lipids | 2-oleoylglycerophosphocholine | 19.4 | 1.13E-10 |
| Lipids | prostaglandin E2 | 15.15 | 4.09E-08 |
| Amino Acid | 5-methylthioadenosine (MTA) | 13.13 | 3.94E-12 |
| Lipids | 6-keto prostaglandin F1alpha | 11.12 | 1.88E-06 |
| Amino Acid | gamma-aminobutyrate (GABA) | 11.07 | 0.001 |
| Lipids | 1-palmitoylglycerophosphocholine | 10.19 | 6.06E-06 |
| Carbohydrates | UDP-glucuronate | 9.27 | 3.10E-09 |
| Amino Acid | N-acetyl-aspartyl-glutamate (NAAG) | 9.14 | 3.51E-10 |
| Lipids | 1-oleoylglycerophosphocholine | 9.07 | 1.39E-07 |
| Lipids | 2-palmitoylglycerophosphocholine | 8.38 | 2.91E-07 |
| Lipids | prostaglandin I2 | 8.25 | 8.21E-06 |
| Nucloetide | thymine | 7.83 | 8.27E-07 |
| Lipids | 2-arachidonoylglycerophosphocholine | 7.72 | 8.93E-05 |
| Lipids | prostaglandin A2 | 6.8 | 5.14E-05 |
| Lipids | 1,2-propanediol | 6.77 | 0.0105 |
| Amino Acid | 4-hydroxyphenylpyruvate | 6.63 | 9.23E-08 |
| Lipids | 15-HETE | 6.28 | 8.81E-05 |

Again, the majority of the highest up-regulated metabolites involved lipid and amino acid pathways. The highest fold change was the nucleotide and energy signaling molecule adenosine 5'-monophosphate (AMP), followed by the lipid

membrane precursor CDP-choline, and NAA. Since these fold changes were based on mean values, and there are skewed distributions across metabolites, we analyzed the median values of the top 8 up-regulated metabolites from table 1 to further determine which metabolites are consistently more abundant in ovarian cancer. Of these 8, NAA had the highest median level in ovarian cancer (Figure 8).

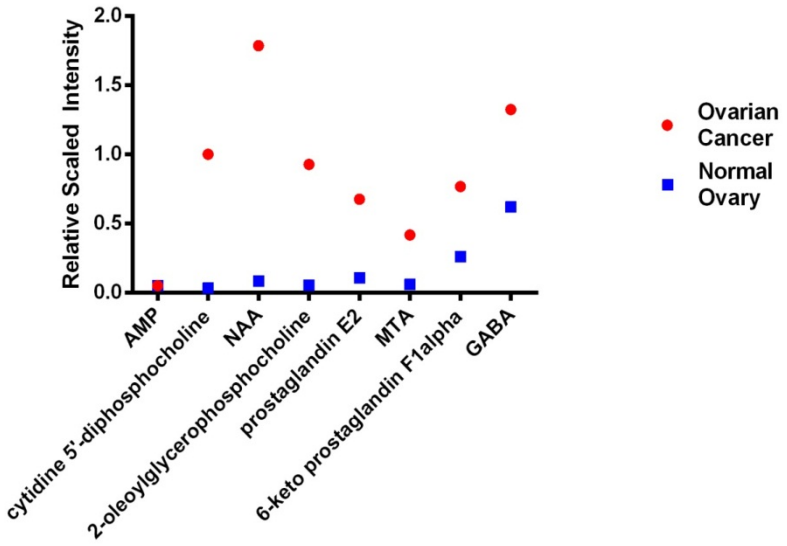


**Figure 8. Median levels of the highest fold-change metabolites in ovarian cancer and in the normal ovary.**

NAA was one of the most significant alterations in ovarian cancer tissues compared to the normal ovary. NAA was greater than 28 fold up-regulated in ovarian cancer compared to the normal ovary (2.30E-11) (Table 4). NAA levels in ovarian cancer tumors were strongly positively correlated with the brain dipeptide N-

acetyl-aspartyl-glutamate (NAAG) (r=0.85, p<0.001), along with several eicosanoids including prostaglandins E1 (r=0.54, p<0.001) and E2 (r=0.50, p<0.001), the TCA cycle substrate malate (r=0.45, p<0.001), and AMP (r=0.40, p<0.001) (Table 5). NAAG was greater than 9 fold elevated in ovarian cancer (p<3.51E-10) (Table 4).

**Table 5. Metabolites associated with NAA levels**. List of metabolites that were strongly significantly associated with NAA levels.

| Metabolite | Super-Pathway | Spearmon's r | p-value |
|---|---|---|---|
| N-acetyl-aspartyl-glutamate (NAAG) | Amino acid | 0.85 | <0.001 |
| prostaglandin E1 | Lipid | 0.54 | <0.001 |
| 6-keto prostaglandin F1-alpha | Lipid | 0.52 | <0.001 |
| homocysteine | Amino acid | 0.51 | <0.001 |
| prostaglandin E2 | Lipid | 0.50 | <0.001 |
| prostaglandin I2 | Lipid | 0.46 | <0.001 |
| malate | Energy | 0.45 | <0.001 |
| thromboxane B2 | Lipid | 0.44 | <0.001 |
| nicotinamide | Cofactors and vitamins | 0.44 | <0.001 |
| gamma-glutamylalanine | Peptide | 0.44 | <0.001 |
| prostaglandin D2 | Lipid | 0.42 | <0.001 |
| inositol 1-phosphate (I1P) | Lipid | 0.42 | <0.001 |
| phenyllactate (PLA) | Amino acid | 0.41 | <0.001 |
| 3-(4-hydroxyphenyl)lactate | Amino acid | 0.41 | <0.001 |
| adenosine 5'-monophosphate (AMP) | Nucleotide | 0.40 | <0.001 |

As mentioned, there are several known biochemical reactions that form and breakdown NAA (Figure 9). The main biosynthetic enzyme for NAA is Aspartate N-acetyltransferase (NAT8L). The substrates for the NAT8L enzyme are acetyl-coA and aspartic acid which form NAA and coA. This hydrolysis of NAAG releases glutamate and NAA. The main breakdown enzyme for NAA is aspartocyclase (ASPA). NAA is hydrolyzed by ASPA into aspartate and a carboxylate, typically acetate. NAA reacts with glutamate to form NAAG by the enzyme NAAG Synthetase encoded by RIMKLB. To determine if the elevation in NAA was associated with its accumulation or its breakdown, we determined patient gene

expression levels of NAT8L, FOLH1, and NAALAD2 as the NAA accumulation genes. ASPA and RIMKLB gene expression levels were evaluated as the NAA breakdown genes (Figure 10). NAA levels was strongly correlated with NAT8L gene expression levels ($r=0.52$, $p<0.0001$), FOLH1 was weakly correlative ($r=0.25$, $p=0.017$), and NAALAD2 was weakly negatively correlative ($r= -0.24$, $p=0.023$). ASPA and RIMKLB had no correlation with NAA levels. This suggests that high NAA levels in ovarian cancer are driven by up-regulation of its biosynthesis NAT8L. Furthermore, the low levels of its substrate aspartate in ovarian cancer further suggest that NAA biosynthesis as the cause of high NAA levels (Figure 11).

One possibility of elevated NAA is due to global up-regulation of N-acetylation across various amino acids. However, our metabolic profile did not show a consistent pattern of elevated N-acetyl amino acids (Table 6). In fact, aspartic acid was disproportionately more N-acetylated than all of the N-acetylated amino acids in ovarian cancer. This suggests that elevated NAA is not a result of global N-acetylation processes of amino acids; rather, there is a significant selection for N-acetylation of aspartic to form NAA in ovarian cancer.

**Table 6. Fold change N-acetylation of amino acids in ovarian cancer.** Fold change is relative intensity of ovarian cancer over the normal ovary.
*[red box= up regulation(p<0.05), green box= down regulation (p<0.05)]*

| Amino Acid | Fold Change | N-acetylated amino acid | Fold change |
|---|---|---|---|
| serine | 1.03 | N-acetylserine | 0.88 |
| threonine | 1.1 | N-acetylthreonine | 1.6 |
| alanine | 1.35 | N-acetylalanine | 0.91 |
| aspartate | 0.71 | N-acetylaspartate (NAA) | 28.38 |
| glutamate | 1.14 | N-acetylglutamate | 4.62 |
| tryptophan | 0.87 | N-acetyltryptophan | 0.65 |
| methionine | 0.97 | N-acetylmethionine | 0.76 |
| ornithine | 0.48 | N-acetylornithine | 0.8 |
| putrescine | 3.72 | N-acetylputrescine | 2 |
| glycine | 1.27 | N-acetylglycine | 0.7 |

To validate that NAA levels were significantly higher in ovarian cancer compared to the normal ovary, we evaluated a separate cohort of ovarian cancer (n=47) and normal ovarian samples (n=3) using NMR spectroscopy. NMR also has the advantage of giving exact quantification of metabolite concentrations. Indeed, the NAA peak at 2.0-2.1 ppm was distinctly seen in ovarian cancer samples, and absent in the normal ovary (Figure 12a). Ovarian cancer samples had significantly higher levels of NAA compared to the normal ovary (Figure 12b) with concentrations on average at 104.2 μM (±14.57 SEM), and NMR could not detect any NAA in normal ovaries ($p<0.0001$).

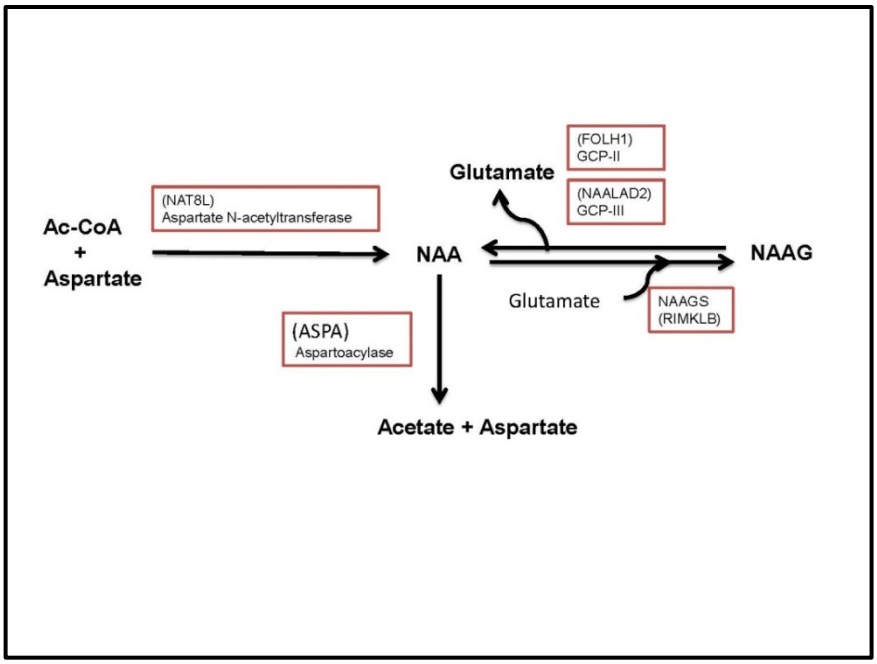


**Figure 9. Schema of the NAA-NAAG pathway.** NAA is biosynthesized by aspartate N-acetyltransferase (NAT8L) from acetyl CoA (Ac-CoA) and aspartate. NAA is metabolized into acetate and aspartate by aspartoacyclase (ASPA). NAA can also form NAAG by reacting with glutamate by the enzyme NAAGS encoded by RIMKLB gene. NAAG can also revert back to NAA and glutamate by the enzymes GCP-II encoded by FOLH1 or by GCP-III encoded by NAALAD2.

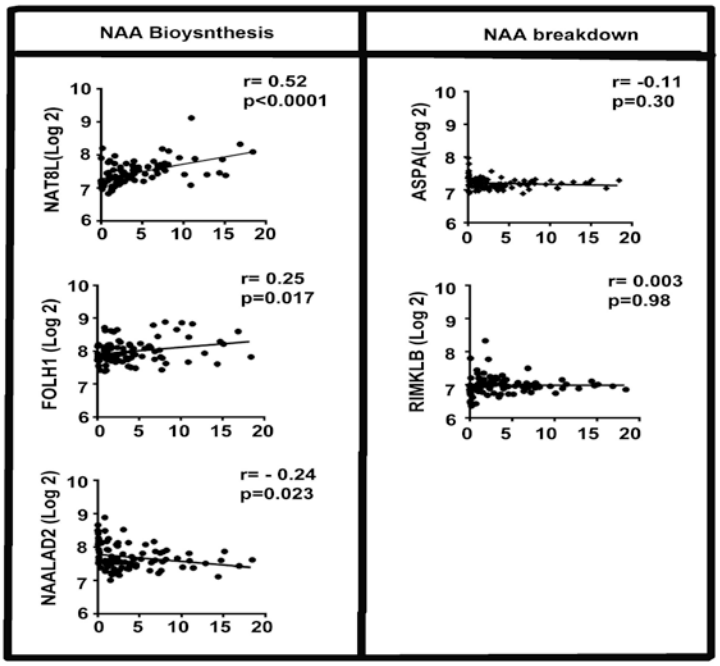


**Figure 10. NAT8L is strongly correlated with NAA levels in ovarian cancer.** Spearmon's correlation (r ) of relative NAA levels in 101 ovarian cancer patients and patient gene expression levels of the NAA pathway.

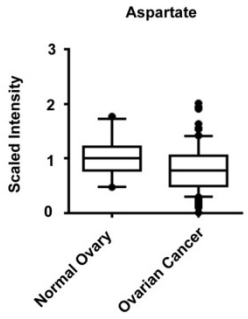


**Figure 11. Low levels of aspartic acid in ovarian cancer.** Aspartate levels of 101 ovarian cancer samples and 15 normal ovary samples shows lower levels of aspartate in ovarian cancer compared to the normal ovary.

a.)

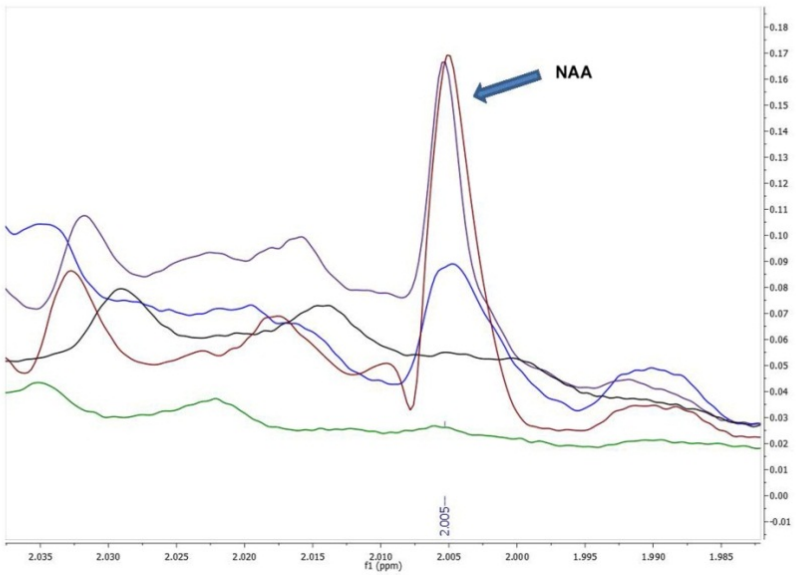


b.)

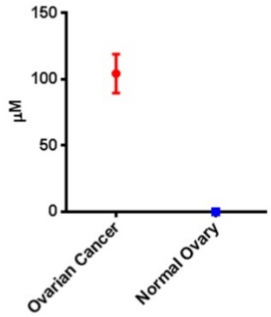


**Figure 12. NMR spectroscopy: higher levels of NAA in ovarian cancer.** a.) NMR spectra of 3 ovarian cancer samples and 2 normal ovary samples shows the distinct NAA peak in ovarian cancer. (blue, purple, red color spectra= 3 ovarian cancer samples; black and green color spectra= 2 normal ovary samples) b.) NMR spectroscopy of NAA samples showing the levels of NAA in 69 ovarian cancer samples and 10 normal ovaries.

**Clinical implications of NAA biosynthesis**

On the basis of substantial elevations in NAA observed in ovarian cancer, we next wondered if there were any clinical implications of these elevations. We investigated the relative NAA levels of 101 ovarian cancer samples using GC/LC mass spectrometry. Patients with higher levels of NAA had worsening overall survival compared to patients with low NAA levels (Figure 13). High NAA overall survival was 1295 days and low NAA survival was not reached (p=0.038).

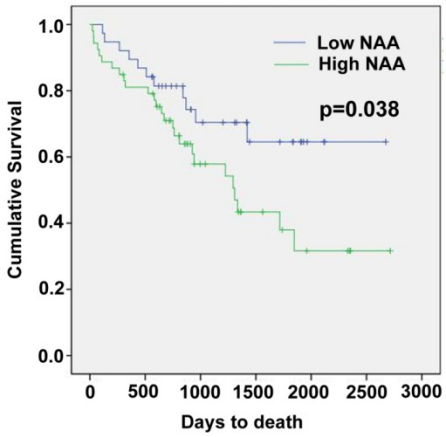


**Figure 13. High NAA levels are associated with worsening overall survival in ovarian cancer.** Kaplan-Meier analysis of relative NAA levels and overall survival in 101 ovarian cancer patients.

On the basis of NAA levels being strongly correlated with NAT8L gene expression, we next examined clinical outcomes of 485 patients based on NAT8L gene expression from the TCGA. Analysis of RNASeq gene expression data revealed that high expression of NAT8L (cut-off > 0.5 z-score) is associated with

worse overall survival in high grade serous ovarian cancer (Figure 14a). The median overall survival of the high NAT8L expression was 35 months compared to 45 months in the low NAT8L group (p=0.031). To validate, we analyzed a second independent cohort of 285 ovarian cancer patients (Figure 14b). Concordantly, high NAT8L (cut-off > 47th percentile) gene expression was associated with worse overall survival compared to the low NAT8L gene expression group. The median overall survival of the high NAT8L expression were 40 months compared to 52 months in the low NAT8L group (p=0.005). Finally, we evaluated mRNA levels of NAT8L in a cohort of ovarian cancer patients from our institution (n= 135) and normal non-cancerous ovaries (n=15). Ovarian cancer patients had over a 3 fold increased levels of NAT8L expression compared to the normal ovary (p<0.001) (Figure 15).

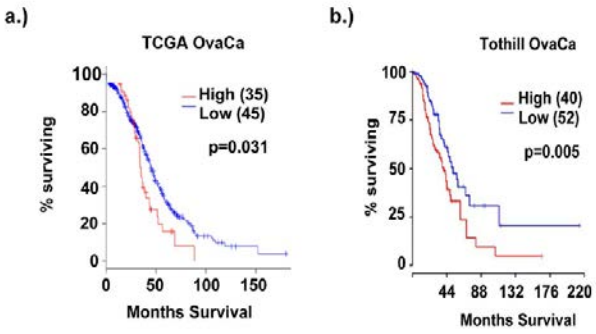


**Figure 14. High NAT8L gene expression is associated with worse overall survival.** a.) Kaplan Meier analysis of NAT8L gene expression and overall survival using RNASeq platform in TCGA. b.) Kaplan Meier analysis of NAT8L gene expression and overall survival from Tothill gene expression database.

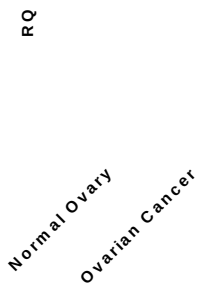


**Figure 15. NAT8L gene expression is significantly higher in ovarian cancer**. RT-PCR of NAT8L gene expression comparing ovarian cancer samples (n=135) to normal ovary samples (n=15). Mean RQ values ± SEM.

To determine if NAT8L protein levels were also significantly elevated in ovarian cancer and the normal ovary, we examined 209 ovarian cancer patients and 10 normal ovary tissues from our institution using immunohistochemistry of anti-NAT8L protein in a tissue microarray. We found significantly higher expression of NAT8L compared to the normal ovary (Figure 16). Based on a semi-quantitative H-score method, ovarian cancer had a 1.92 fold higher levels of NAT8L staining compared to the normal ovary ($p<0.0001$). Furthermore, higher NAT8L staining was associated with poor overall survival in ovarian cancer (Figure 17). High NAT8L expression was associated with 3.86 years overall survival compared to 9.09 years with low NAT8L expression ($p<0.001$).

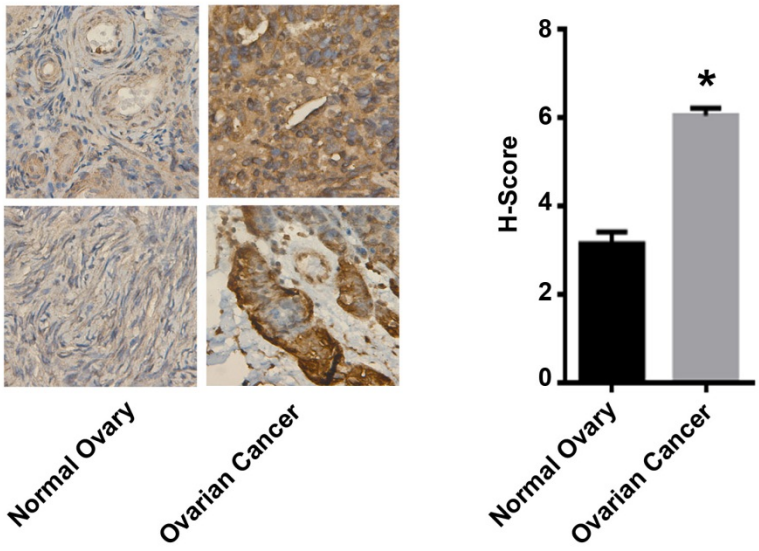


**Figure 16. Ovarian cancer has significantly higher NAT8L protein levels compared to the normal .** Immunohistochemistry of anti-NAT8L in 208 ovarian cancer samples and 10 normal ovarian samples. *=p<0.001.

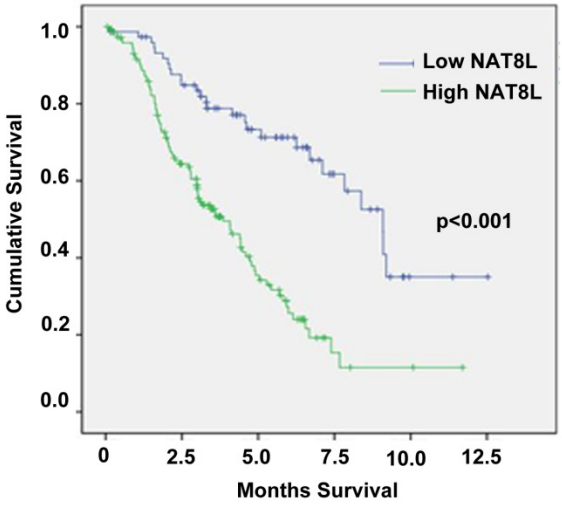


**Figure 17. High NAT8L protein levels are associated with worse overall survival in ovarian cancer.** Kaplan-Meier analysis of NAT8L protein expression and overall survival in 208 ovarian cancer samples.

On the basis that high NAT8L up-regulation is driving NAA accumulation in ovarian cancer; we considered the relative NAT8L gene expression across various cancer types in the TCGA. We evaluated the relative gene expression levels and copy number alterations of NAT8L from across the 20 cancer types. Surprisingly, we found relatively high levels of NAT8L expression in HSOEC, skin cutaneous melanoma; glioblastoma multiforme (GBM), kidney chromophobe, and brain lower grade glioma cancer having the highest expressions of NAT8L in the TCGA (Figure 18) (Table. Breast, uterine endometroid, and thyroid cancer also had relatively high NAT8L expression among the 20 tumors assessed from the TCGA. NAT8L

copy number alterations distinctly showed that ovarian cancer had the greatest degree of copy number alterations among the 20 cancer types (Figure 19).

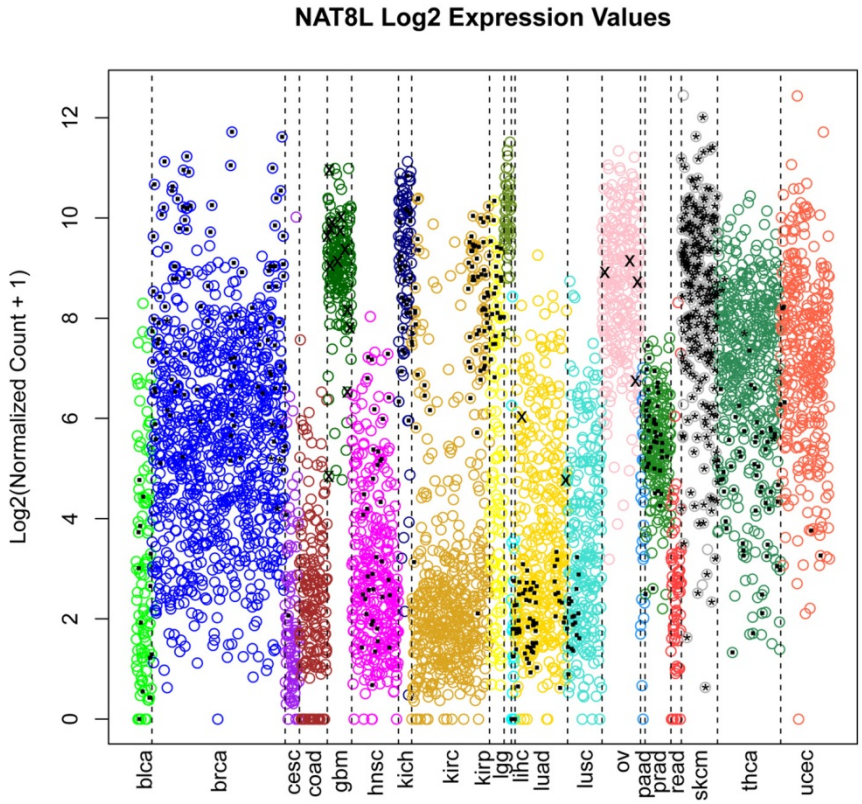


**Figure 18. NAT8L gene expression across 20 different tumor types.** Gene expression data of NAT8L Log2 normalized from TCGA.

**Table 7. TCGA acronymns for figure 18 and 19.**

| Acronymn | Tumor Type |
|---|---|
| BRCA | Breast cancer |
| KIRC | Renal clear cell |
| COAD, READ | Colon and Rectal adenocarcinoma |
| UCEC | Endometrial Cancer |
| GBM | Glioblastoma multiforme |
| LUSC | Lung squamous carcinoma |
| OV | Ovarian |
| LUAD | Lung adenocarcinoma |
| HNSC | Head and neck squamous cell carcinoma |
| THCA | Pappillary thyroid cancer |
| SKCM | Cutaneous melanoma |
| STAD | Stomach adenocarcinoma |
| BLCA | Bladder cancer |
| LGG | Lower grade glioma |
| CESC | Cervical |
| LAML | Acute Myeloid leukemia |
| DLBC | Diffuse large B cell lymphoma |
| ESCA | Esophageal carcinoma |
| KIRP | Papillary kidney |
| LIHC | Liver |
| PAAD | Pancreatic adenomcarcinoma |
| PRAD | Prostate adenocarcinoma |

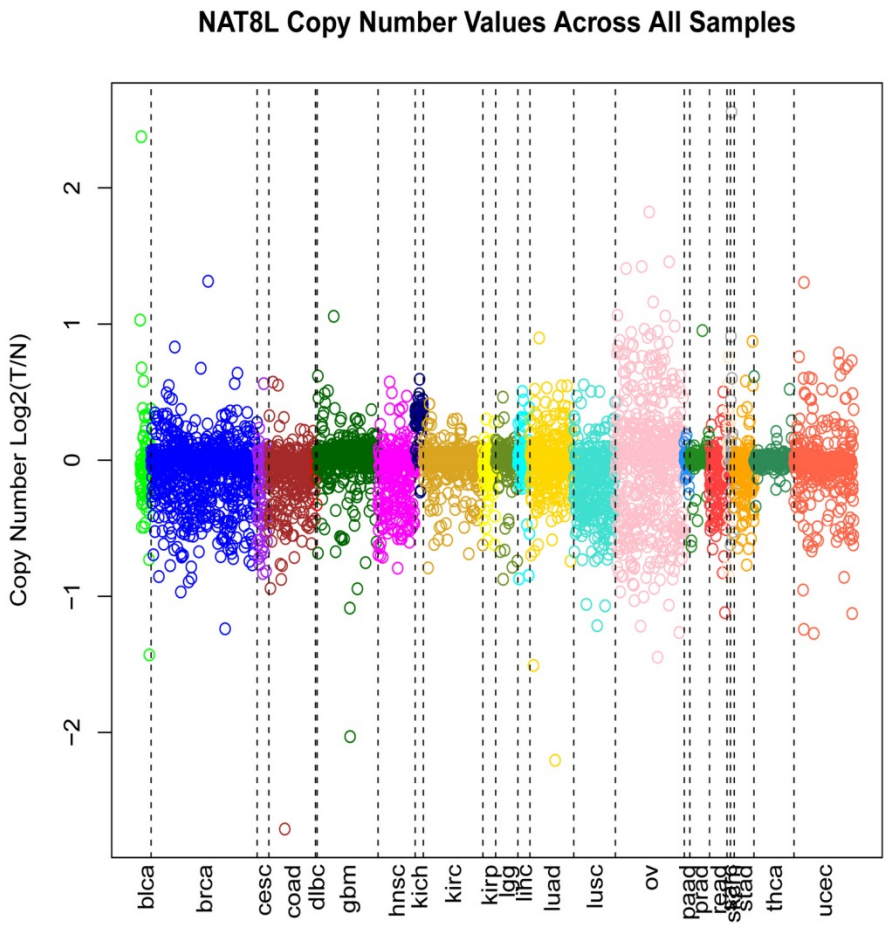


**Figure 19. NAT8L copy number alterations across 20 types.** TCGA Copy number alterations Log2 transforemed.

Based on the fact that NAT8L gene expression levels were comparatively high across several tumor types, we evaluated the TCGA database to determine if high NAT8L affects clinical outcomes in other cancer types. Using the publically available website www.cbioportal.org, TCGA survival data for NAT8L was analyzed. TCGA currently does not have melanoma survival data, therefore we analyzed two different patient cohort gene arrays in melanoma. Profoundly, high NAT8L expression was found to have worse overall survival in invasive breast, lung

squamous, colon, uterine, melanoma and kidney renal cell cancers (Figure 20). Thus suggesting that worsening survival due to elevated NAA biosynthesis is not unique only to ovarian cancer.

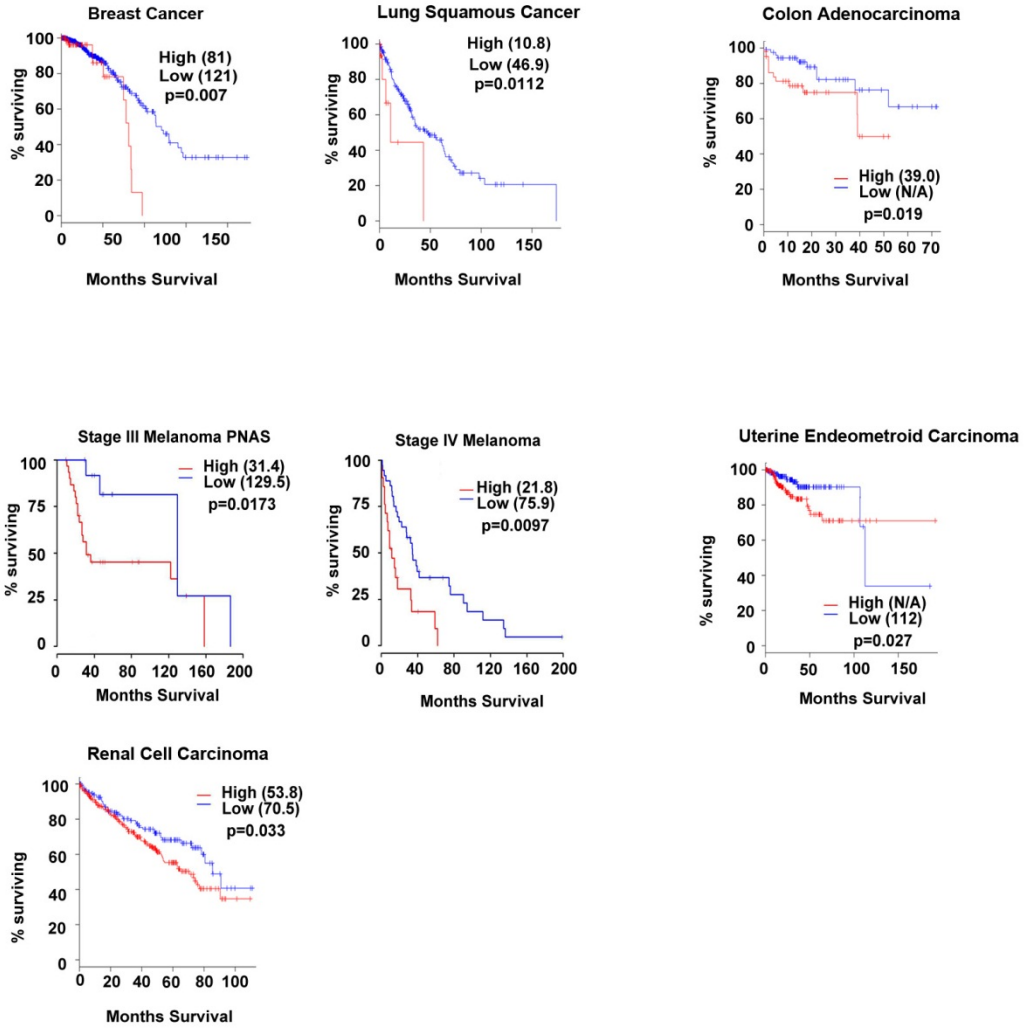


**Figure 20. High NAT8L with worse overall survival in several cancer types.** NAT8L gene expression data from TCGA (breast cancer, lung squamous, colon adenocarcinoma, uterine endometrioid carcinoma, renal cell carcinoma) and melanoma gene expression from previously published database [167-168].

**Biologic significance of NAA synthesis**

To determine the biological significance of NAA biosynthesis in ovarian cancer, we next screened the CCLE and NCI-60 database to identify cell lines and cancer types with high NAT8L expression. Indeed in the CCLE, ovarian cancer cell lines had some of the highest expressions of NAT8L (Figure 21). We also analyzed the NCI-60 cell lines, the median (±S.D.) NAT8L expression level of all 60 cancer lines was 4.45(±0.81) GCRMA. Melanoma, lung, renal, and ovarian cancer cell lines had some of the highest expression of NAT8L (Figure 22).

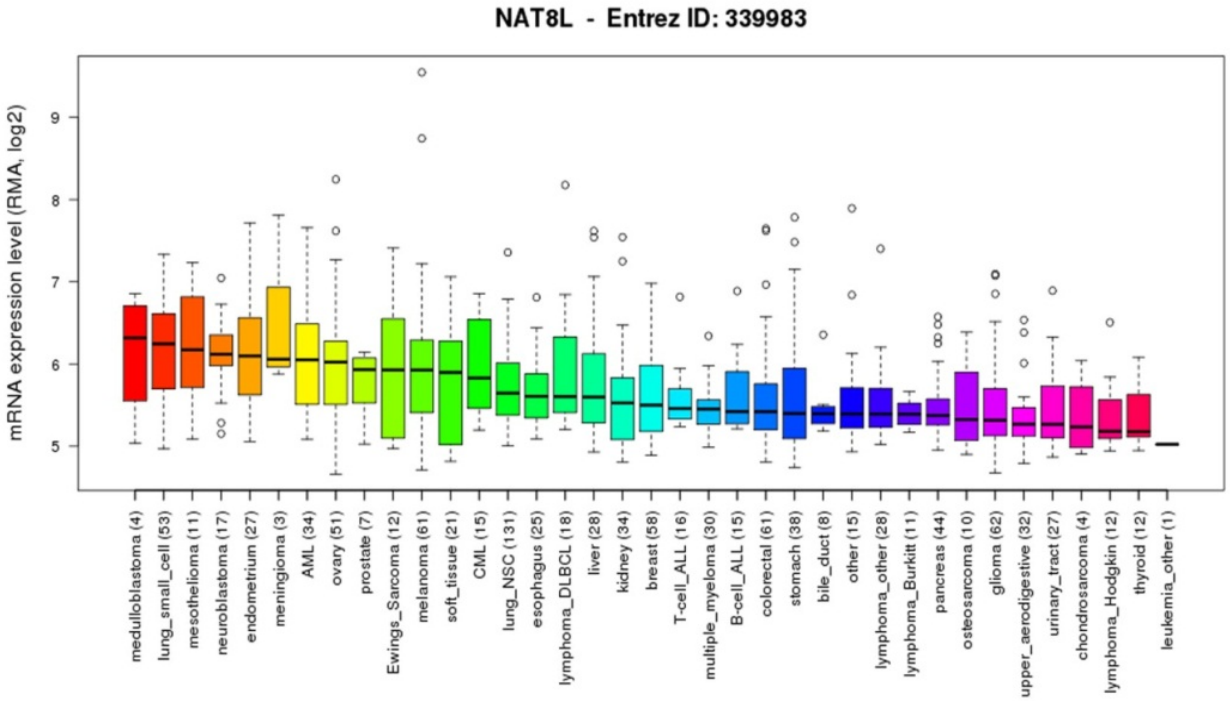


**Figure 21. Gene expression of NAT8L from CCLE.** Gene expression of cell lines clustered by cancer type. Numbers in paraenthesis after each cancer type are the number of cell lines.

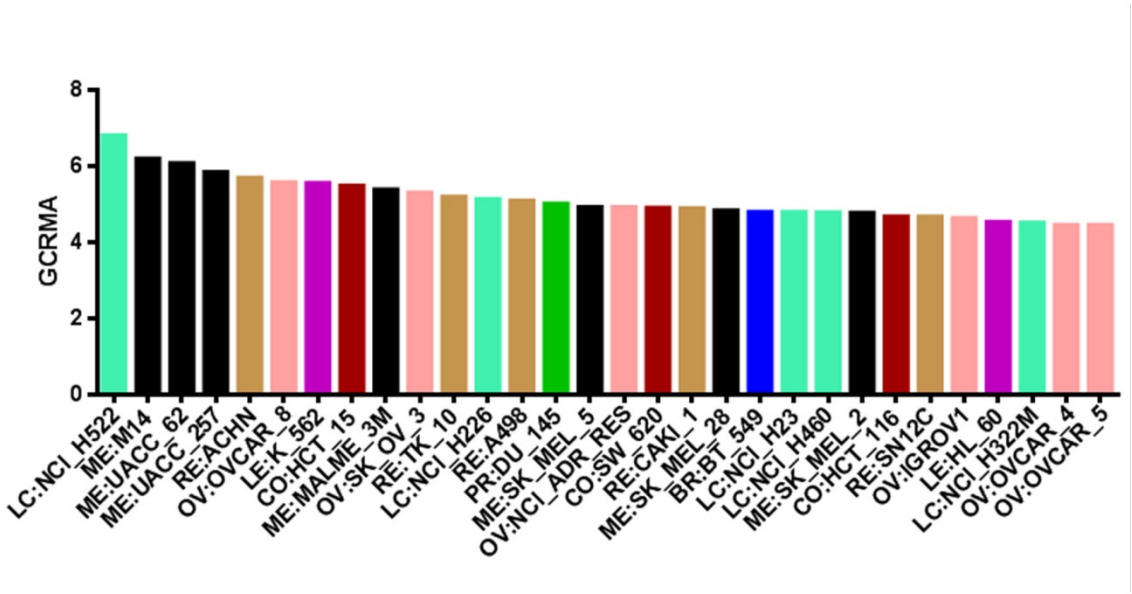


**Figure 22. NCI-60 cell lines with high NAT8L gene expression (sorted by top 50%).** LC=lung cancer, ME=melanoma, RE= renal, OV= ovary, CO=colon cancer, PR=prostate cancer, BR=breast, LE=leukemia.

To determine the effects of NAT8L inhibition in cancer cells, siRNA was used to reduce NAT8L levels in cancer cell lines. To confirm NAT8L knockdown, transient transfection of several ovarian (HEYA8, SKOV3, A2780) and melanoma cell lines

(UACC 257, UACC 62, and M14) caused 60-96% knockdown of NAT8L gene expression at 48 hours (Figure 23).

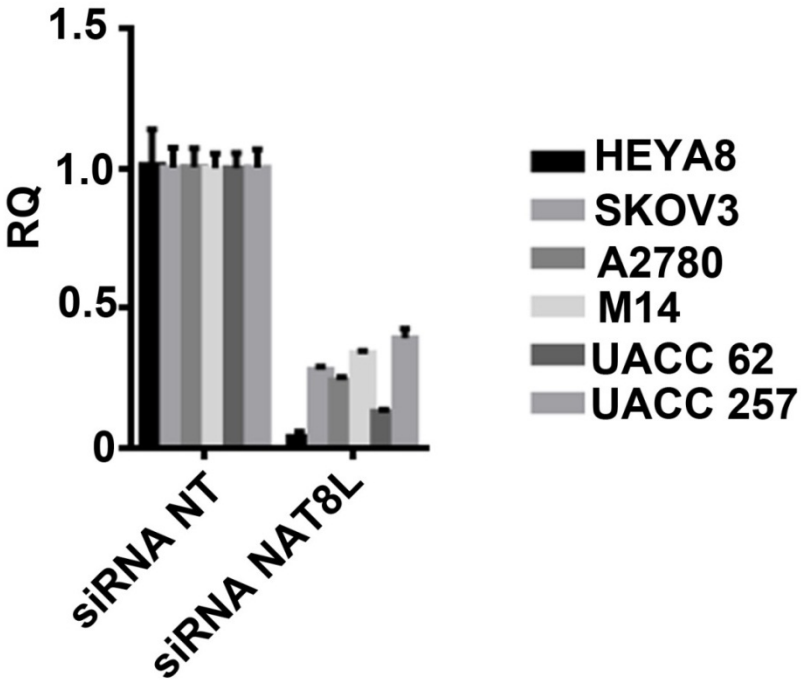


**Figure 23. siRNA NAT8L knockdown of NAT8L gene expression in ovarian and melanoma cancer cell lines.** Gene expression levels of NAT8L detected by RT-PCR. RQ= relative real time quantitation. Values are mean±SEM.

We next evaluated the effect of NAT8L knockdown on cancer cell growth and survival. We selected HEYA8 and A2780 cell lines in ovarian cancer as they had the highest knockdown of NAT8L using siRNA. First, we evaluated the effect of NAT8L knockdown on cell viability (Trypan blue) after one [72 hours(3 days)] and two [144 hours(6 days)] rounds of transfections (Figure 24). After the one round,

cell viability was decreased by 9.4% by siRNA NAT8L compared to the control non-target siRNA (siRNA NT) ($p<0.003$). After two rounds of transfections, cell viability was decreased by 24.0% by siRNA NAT8L compared to siRNA NT ($p<0.01$). We also analyzed a synthetic lethality screen for chemotherapy resistant cell lines A2780-CP, HEYA8-MDR, and SKOV3-TR. Surprisingly, after one round NAT8L knockdown and chemotherapy at 120 hours (Day 5), we saw a significant decrease in cell viability in all three chemo-resistant cell lines (Figure 25). Thus, the effect of NAT8L knockdown in cancer cell viability using siRNA appears to occur after 5 days of treatment. Therefore, we performed the remainder of our in vitro siRNA experiments with two rounds of transfections unless noted otherwise.

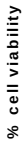


**Figure 24. Effect of siRNA NAT8L on cancer cell viability after one and two rounds of transfections.** Values are mean ±SEM.

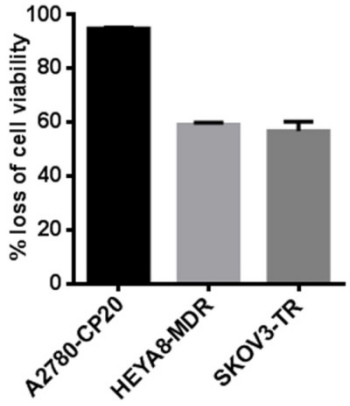


**Figure 25. Cell viability with siRNA NAT8L compared to siRNA NT in chemotherapy resistant cell lines.** Values are mean ±SEM.

Trypan blue stains cells that are either dead or have damaged cell membranes; therefore we investigated if NAT8L knockdown increased cellular apoptosis. Indeed, HEYA8 and A2780 showed that siRNA NAT8L had a significant increase of total apoptosis compared to siRNA NT by 38.53% ($p<0.001$) and 37.85% ($p<0.001$), respectively (Figure 26). To evaluate the *in vitro* generalizability of siRNA NAT8L, melanoma cell lines UACC 257, UACC 62, and M14 similarly showed an increase in apoptosis consistent with findings in ovarian cancer cell lines (Figure 27). Furthermore, knockdown of NAT8L in combination with paclitaxel treatment displayed a synergistic effect on apoptosis (Figure 28). Cells treated with paclitaxel and siRNA NAT8L had a 29.83% increase in apoptosis compared to paclitaxel and siRNA NT treated cells ($p<0.001$).

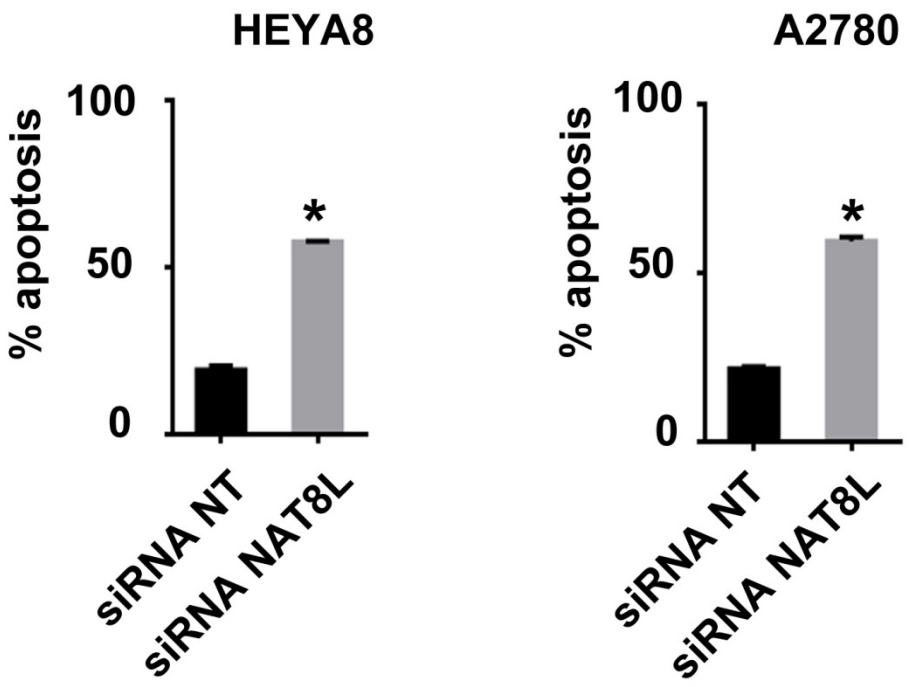


**Figure 26. Knockdown of NAT8L increases apoptosis in ovarian cancer cells.**
Values are mean ±SEM. *= p<0.001.

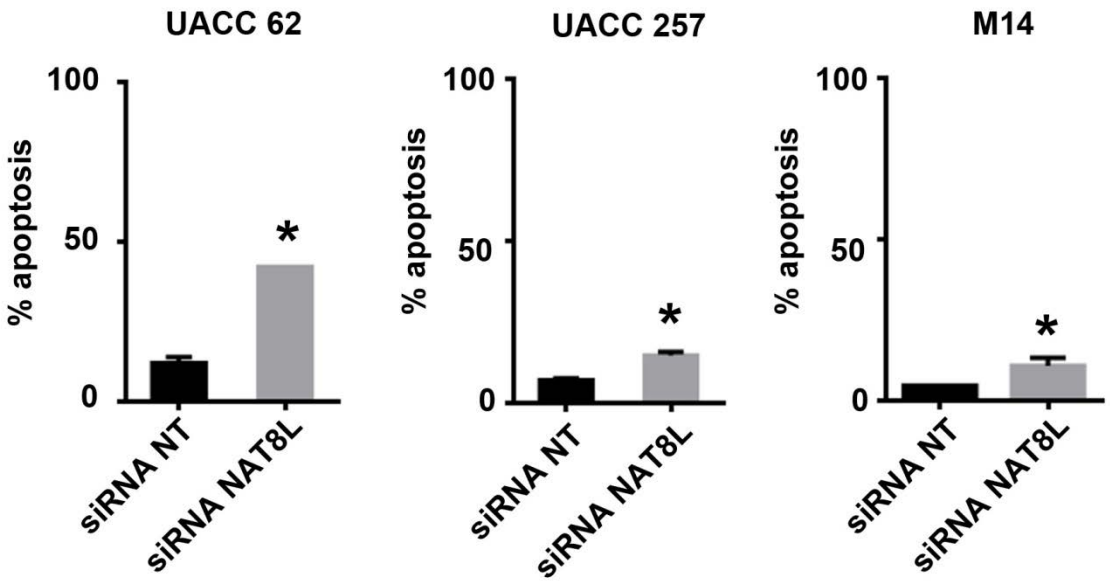


**Figure 27. Knockdown of NAT8L increases apoptosis in melanoma cancer cells.** Values are mean ±SEM. *= p<0.001.

.

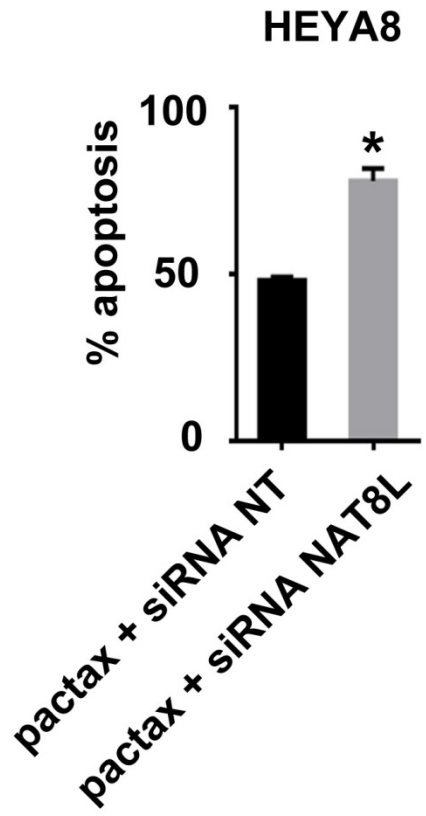


**Figure 28. Knockdown of NAT8L increases sensitivity of paclitaxel's effect on ovarian cancer cell apoptosis.** Values are mean ±SEM. *= p<0.001

On the basis that NAT8L is a putative GCN5 related gene (GCN5 is a ubiquitous histone acetyltransferase that promotes transcriptional activation), we investigated if NAT8L knockdown has an effect in cancer cell proliferation and cell cycle progression. Indeed, ovarian cancer cells treated with siRNA NAT8L had a significantly decreased cell proliferation compared to siRNA NT (Figure 29a).

Proliferation decreased by 23.65% ($p<0.001$) and 19.13% ($p<0.001$) in A2780 and HEYA8 cells, respectively. Furthermore, cells treated with siRNA NAT8L decreased cell cycle progression compared to siRNA NT. HEYA8 cells with down-regulated NAT8L had an 8.4% increase in the number of cells with G1 phase ($p<0.001$), and an 11.65% decrease in the number cells in the S phase ($p<0.001$) (Figure 29b). Thus, knockdown of NAT8L decreased ovarian cancer cell's ability to proliferate and progress through the cell cycle suggesting that NAT8L acetylation may have functions similar to histone acetyltransferases to promote transcriptional activation.

a.)

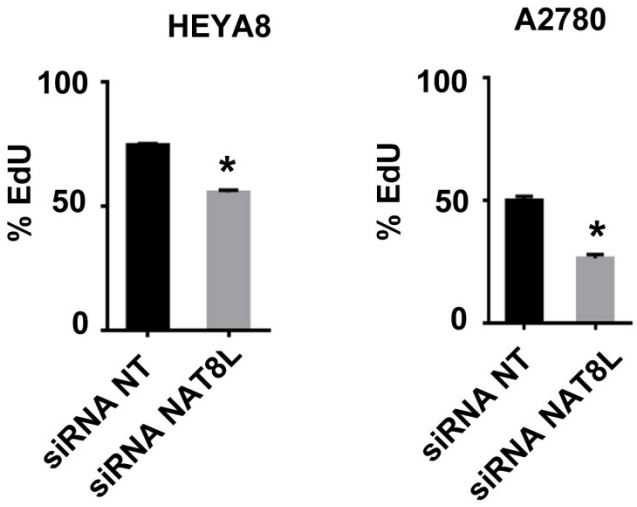


b.)

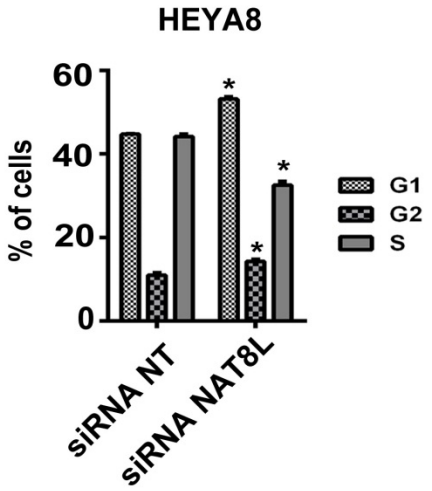


**Figure 29. Knockdown of NAT8L decreases cell proliferation and cell cycle progression.** Values are mean ±SEM. *= p<0.001

On the basis that one of the proposed functions and association of NAA biosynthesis in the human brain is in cell energy production, we hypothesized that knockdown of NAT8L would decrease the levels of ATP in cancers cells. We observed a significant decrease in ATP and ADP levels in HEYA8 cells treated with siRNA NAT8L, and a decrease of ADP in A2780 cells (Figure 30). ATP levels decreased by 20.8% (p=0.03) in HEYA8 cells. In A2780, although ATP levels were decreased by 13%, this was not statistically significant (p=0.17). ADP levels were decreased by 19 %( p<0.001) and 32% (p=0.002) in HEYA8 and A2780 cells, respectively.

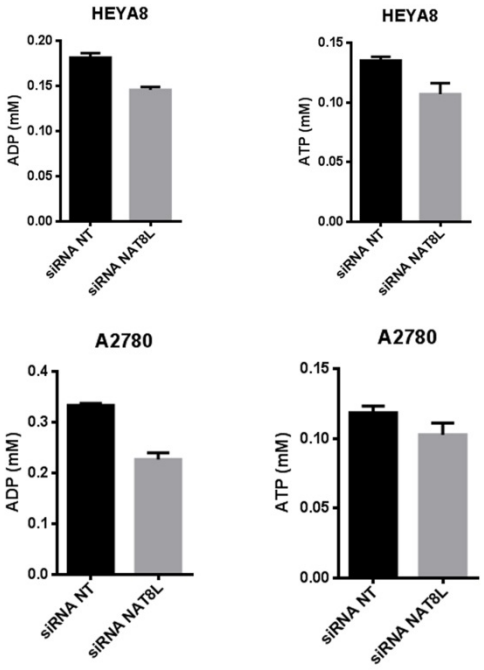


**Figure 30. The effect of siRNA NAT8L on intracellular ATP and ADP.** Values are mean ±SEM.

Due to the decreased ATP and ADP levels in siRNA NAT8L, we hypothesized that this catabolic switch would significantly decrease cancer cell's metastatic potential. Indeed, knockdown of NAT8L in HEYA8 cells significantly decreased migration and invasion by 91% and 92%, respectively ($p<0.001$) (Figure 31).

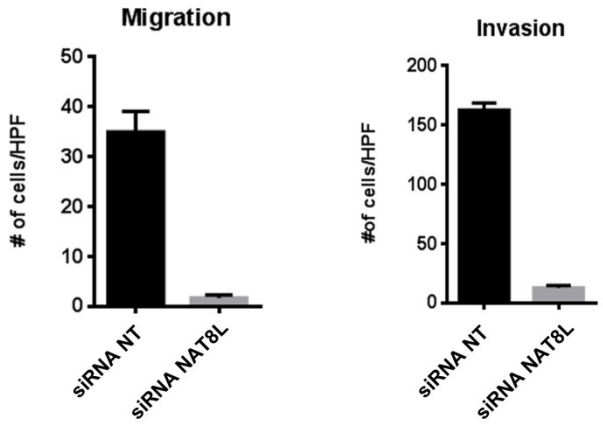


**Figure 31. Knockdown of NAT8L significantly decreased migration and invasion** Values are mean ±SEM.

To better understand the consequences of inhibiting NAA production on cancer cell gene and protein signaling, we evaluated siRNA NAT8L knockdown in HEYA8 cells using a high throughput antibody based reverse phase protein array (RPPA) and high throughput gene expression array. We used HEYA8 cell lines due to the fact that there was 96% knockdown of NAT8L from the siRNA, and its robust therapeutic response. From our RPPA analysis, one of the largest effects of siRNA NAT8L was inhibition of negative cell death regulation, and increase in regulation of

kinase activity (Figure 32A). One of the largest effects was down-regulation of AKT phosphorylation at Serine 479 and Threonine 308 suggesting that the anabolic and tumorigenic effects of this major oncogenic kinase were abrogated (Figure 32A). Furthermore in this network, significant inhibition in regulation of cell localization is predicted with decreases in paxillin, fibronectin, PKC-α, and Src phosphorylation at Y416 and Y527, thus suggesting decreased metastatic potential in cancer cells. In the network of regulation of kinase activity, AMPK (PRKAA1) phosphorylation at Threonine 172 was dramatically higher with NAT8L knockdown. Furthermore, there was high phosphorylation of acetyl-coA carboxylase (ACC) at residue position serine 79 which inhibits its activity (Figure 32A). AKT is a major negative regulator of AMPK. This indicates that knockdown of NAT8L switches HEYA8 cancer cells from an anabolic state to a catabolic state. Since ACC is the major rate limiting enzyme reaction for de novo lipid synthesis, we evaluated the effect NAT8L knockdown on the cell's fatty acid levels. Cells were transfected with siRNA NAT8L lead to a dramatic decrease in cell fatty acids compared to NT siRNA (Figure 32B). NAT8L siRNA caused a 67.7% decrease of fatty acid levels compared to the NT siRNA ($p=0.0004$).

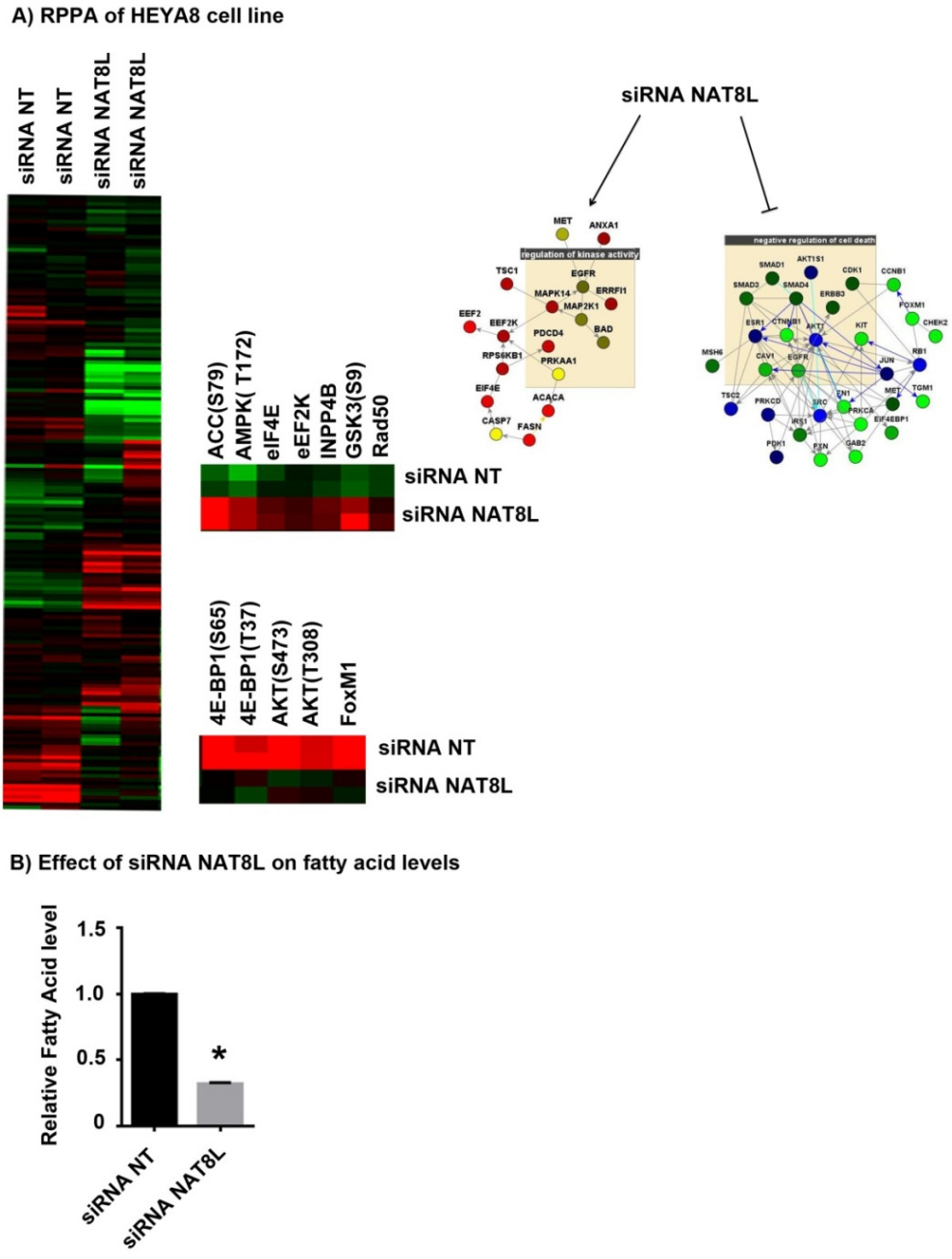


**Figure 32. Knockdown of NAT8L up-regulates switches cell to a catabolic state and decreases de novo lipogenesis.** Red boxes = upregulation, green boxes= down regulation, black boxes = no change. Red circle = upregulation of protein levels, Yellow circle = upregulation of protein phosphorylation, Green ciricle= down regulation of protein levels, blue circle = down regulation of phosphorylation of protein. *=p<0.001.

Hierarchical cluster analysis of integrated gene expression from siRNA NAT8L and siRNA NT had 1961 significantly different gene expression data ($p<0.001$) (Figure 33). Network analysis showed significant decreases in a large number of genes involved in mitosis and the M phase of the cell cycle. On the other hand, a number of genes involved in the catabolic processes were up-regulated with NAT8L knockdown. These gene and protein expression results indicate that one of the major roles of NAA biosynthesis involves regulation of cell division and growth in mitosis, and the absence of NAA biosynthesis confers a catabolic process in cancers cells decreasing its potential for proliferation, metastasis, and survival.

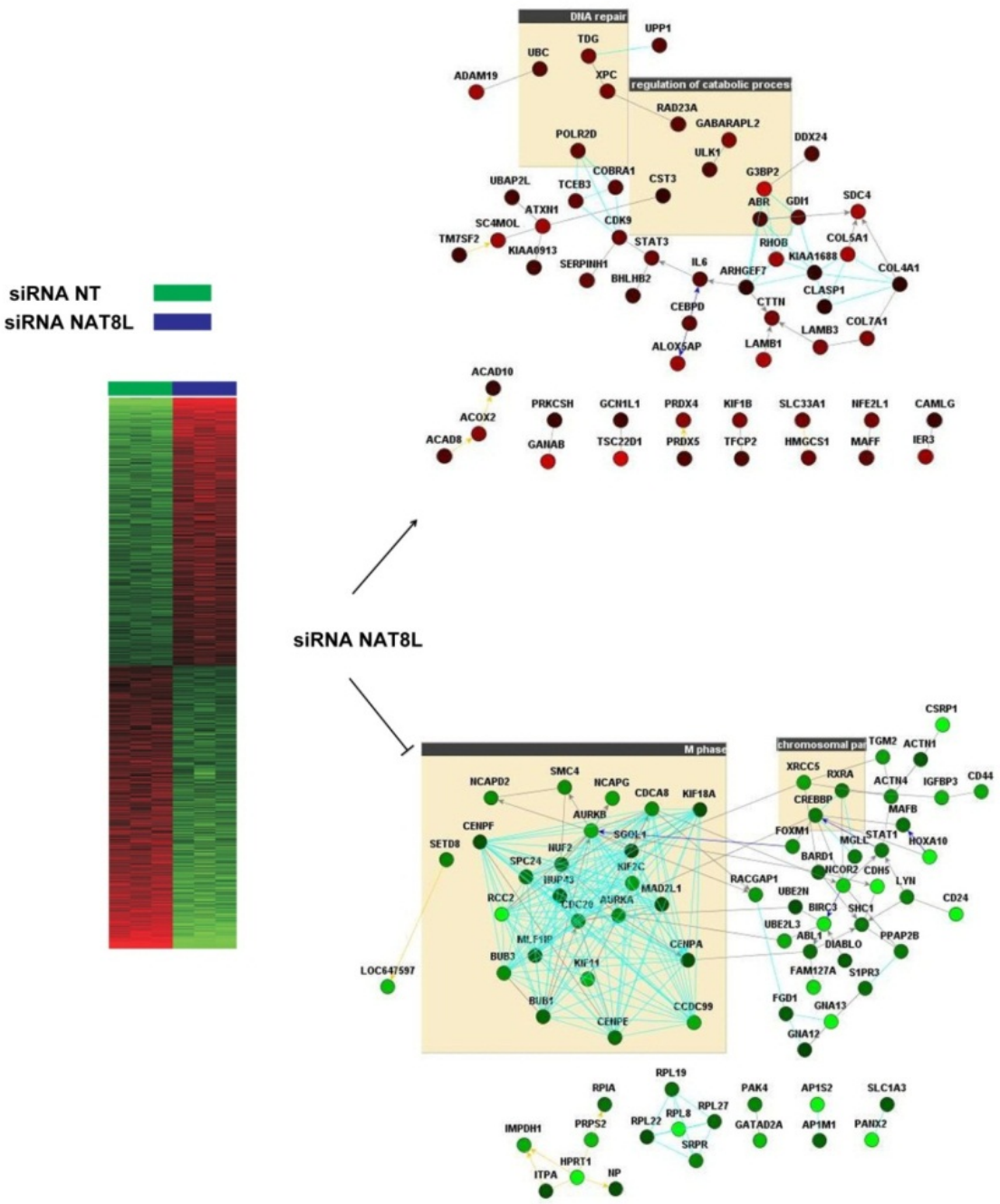


**Figure 33. Knockdown of NAT8L involves the negative regulation of cell division/mitosis and positive regulation of catabolic genes.** Green boxes= down regulation of gene expression, Red boxes= up regulation of gene expression. Red circle = upregulation of gene expression levels, Green ciricle= down regulation of protein levels.

**Effect of NAA biosynthesis in orthotopic ovarian cancer mouse model**

On the basis of the clinical and *in vitro* findings, we evaluated the effect of siRNA NAT8L in orthotopic ovarian cancer models. As compared to mice treated with siRNA NT, those treated with siRNA NAT8L had significantly decreased tumor growth (Figure 34a). A2780 and HEYA8 orthotopic ovarian cancer model had an 84.14% ($p<0.001$) and 69.17% ($p<0.01$) decrease in tumor weight, respectively. A2780 and HEYA8 mouse models also had statistically significant two-three fold reduction in the number of intraperitoneal tumor nodules. We also observed a synergistic effect of siRNA NAT8L and paclitaxel (Figure 34b). Using the HEYA8 orthotopic in vivo model, siRNA NAT8L + paclitaxel had significantly less tumor burden compared to siRNA NT($p<0.001$), paclitaxel + siRNA NT ($p=0.004$), and siRNA NAT8L alone ($p=0.032$). We also observed a decrease in the number of intraperitoneal tumor nodules with siRNA NAT8L + paclitaxel compared to siRNA NT ($p=0.008$), and siRNA NT + paclitaxel ($p=0.020$); however, no difference was observed between siRNA NAT8L alone and siRNA NAT8L + paclitaxel ($p=0.611$). To validate our in vitro data where siRNA NAT8L had significant effect on cell proliferation and apoptosis, we performed immunohistochemistry of ki67 and caspase-3 from our in vivo models. Consistent with the in vitro findings, HEYA8 tissues treated with siRNA NAT8L had significantly less proliferation ($p<0.001$) (Figure 35), and significantly more apoptosis (Figure 36). IHC staining using cleaved-caspase 3 was increased by 2.46 fold in siRNA NAT8L compared to siRNA NT ($p=0.003$) (Figure 36a). Although siRNA NAT8L + paclitaxel had a 1.57 fold

increase in apoptosis compared to paclitaxel treatment alone, this was not statistically significant (p=0.19) (Figure 36b).

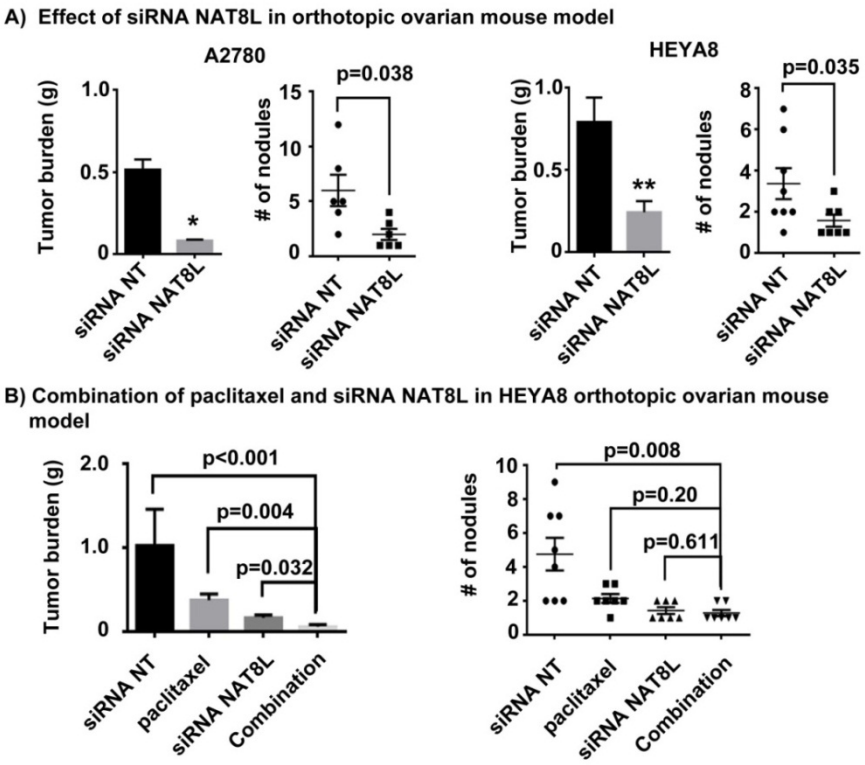


**Figure 34. Effect of siRNA NAT8L treatment in orthotopic ovarian cancer mouse models.** Values are mean ±SEM.

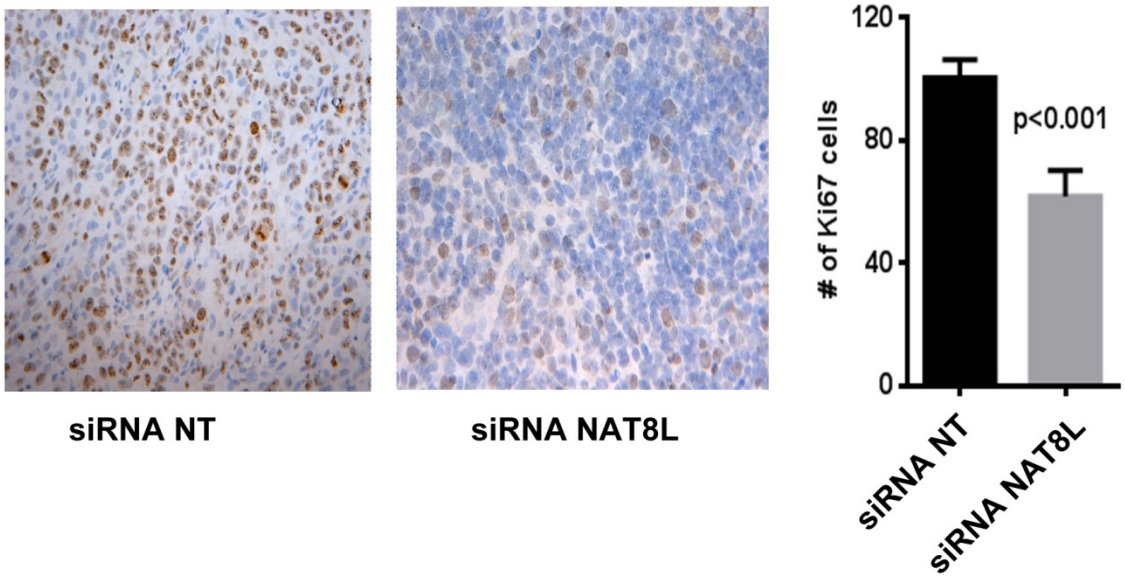


**Figure 35. Effect of siRNA NAT8L on cell proliferation in HEYA8 orthotopic mouse model.** Values are mean ±SEM.

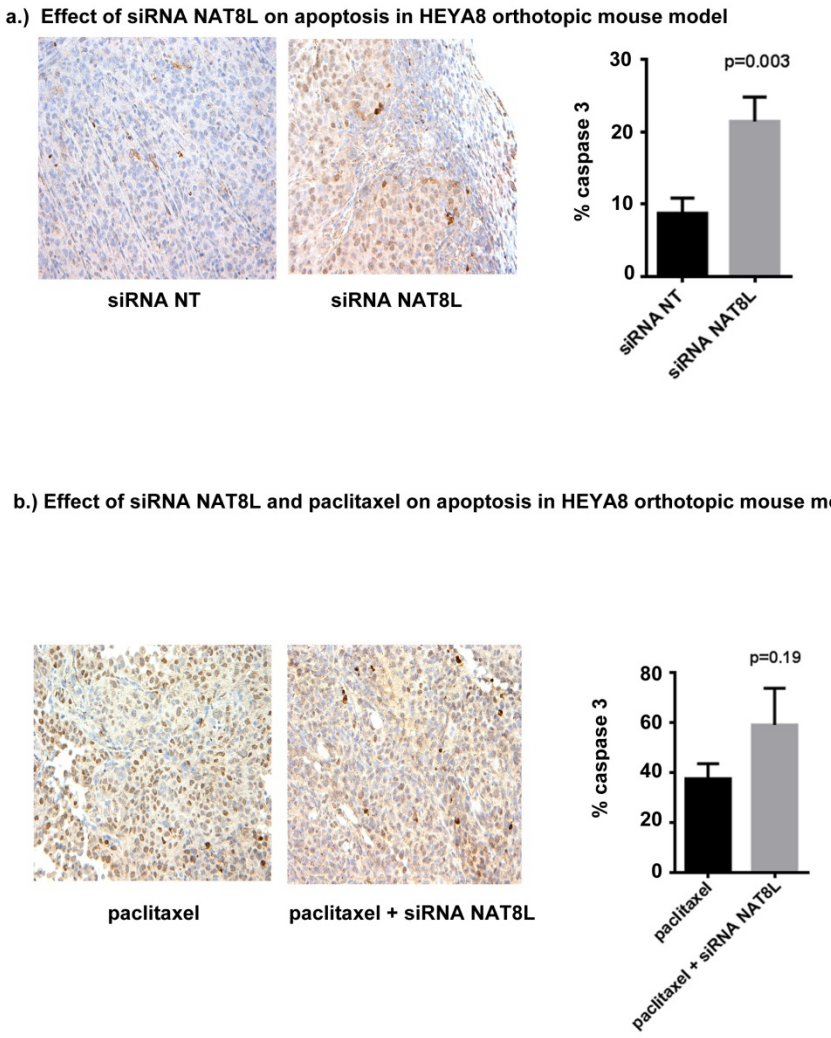


**Figure 36. Effect of siRNA NAT8L +/- paclitaxel on apoptosis in HEYA8 orthotopic mouse model.** Values are mean ±SEM.

To test the specificity and any possible off target effect of NAT8L siRNA, we did an experiment with two separate sequences of NAT8L siRNA in SKOV3 orthotopic mouse model. Our results showed that both NAT8L siRNA significantly reduced tumor burden. Our first sequence and second sequences decreased tumor burden by 70% and 76%, respectively (Figure 37). Furthermore, there were no significant differences in tumor burden between either NAT8L siRNA sequences.

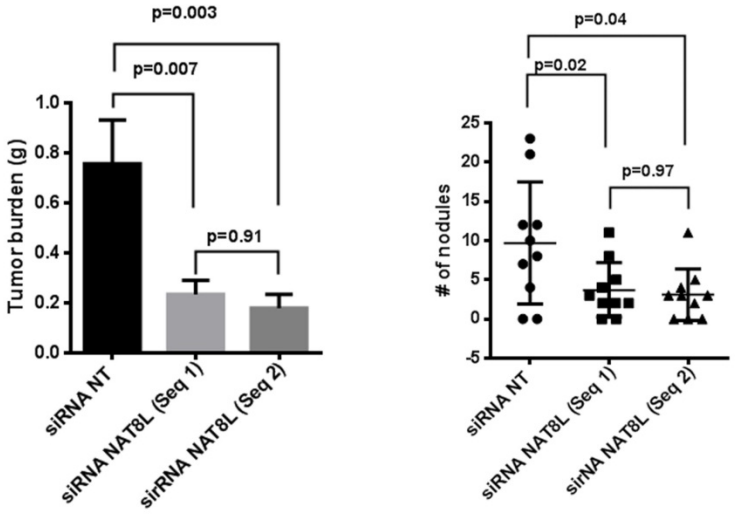


**Figure 37. SKOV3 orthotopic ovarian cancer mouse model.** Mice treated with DOPC NAT8L siRNA using two different sequences. Values are mean ±SEM.

To evaluate the generalizability of NAT8L siRNA , we evaluated its effect in an A375-SM orthotopic melanoma mouse model. Mice treated with NAT8L siRNA had a 62% decrease in tumor burden than the control mice. This indicates that NAT8L siRNA decreases tumor growth in melanoma cancer by inhibiting NAA production.

.

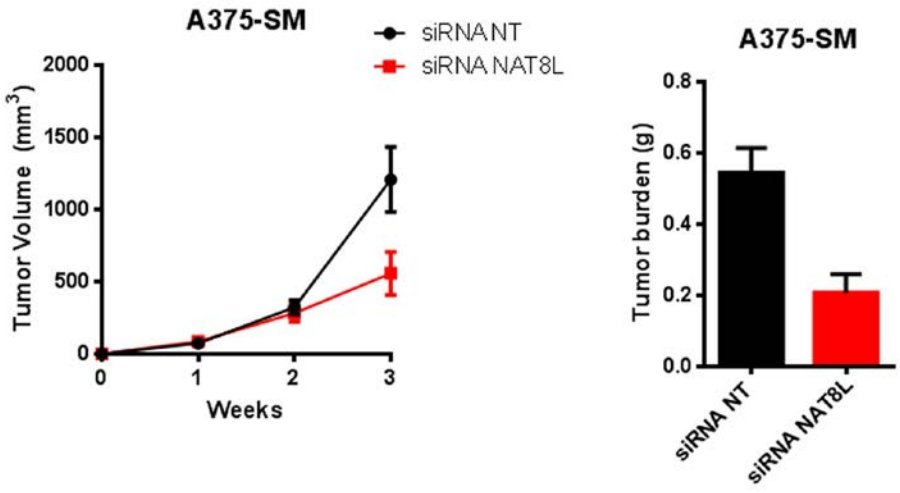


**Figure 38. A375-SM orthotopic melanoma mouse model.** Mice treated with DOPC NAT8L siRNA and NT (control) siRNA. Values are mean ±SEM.

## Discussion

### Clinical Relevance of NAA production

Our study is the largest metabolomics profile of high grade serous epithelial ovarian cancer (HGSOC) to date. We observed an increase in glycolytic intermediates seen in the "Warburg effect". Furthermore, nearly 75% of the alterations involved lipid and amino acid pathways. One of the most drastic up-regulations involved is the neuron biosynthesized NAA metabolite which is derived from acetylation of aspartic acid which we detected in cultured ovarian cancer cells. More importantly, high levels of NAA and its biosynthetic enzyme NAT8L leads to worsening patient survival. We observed that knockdown of NAT8L leads to significant decreases in tumor growth in an *in vitro* setting by decreasing tumor proliferation, cell cycle progression, increasing cellular apoptosis, and decreasing cancer cell invasion. In the In vivo setting, siRNA NAT8L decreased tumor proliferation and increased apoptosis. These findings along with the worsening clinical outcomes associated with high NAT8L gene expression in melanoma, breast, colon, lung squamous, renal clear cell, and uterine endometrial cancers provide compelling evidence that NAA production confers oncogenic properties, and functions as an oncometabolite.

The overwhelming majority of metabolites altered in HGSOC involved lipid and amino acid metabolic pathways when compared to the normal ovary. Eicosanoids and phospholipids were some of the highest fold changes in HGSOC highlighting the need for pro-inflammatory and pro-proliferative components. PGE2 is the most up-regulated eicosanoid in HGSOC tissues. PGE2 is the most abundant

prostaglandin in various cancers, and high levels are associated with worsening outcomes [183,184,185]. In colon cancer, PGE2 contributes to tumor growth by DNA methylation [186]. Interestingly, some essential diet derived fatty acids were elevated indicating, in addition to *de novo* lipogenesis, ovarian cancer cells also rely on the absorption of fatty acids from their microenvironment. This is in accordance with a recent study showing that breast and prostate cancers absorb diet derived fatty acids to promote tumor growth and proliferation[187]. In ovarian cancer tumors metastasized to the omentum, up-regulation of Fatty Acid Binding Protein 4 (FABP4) has been shown to significantly affect tumor growth and metastasis [123]. Thus, emphasizing the importance of fatty acid uptake in ovarian cancer.

Amino acid metabolism was the second most altered pathway in ovarian cancer with some of highest increases involving metabolites in the alanine/aspartate, glutamate/glutamine, and phenylalanine/tyrosine pathways suggesting that these are important amino acid pathways in HGSOC pathophysiology. There is emerging evidence that many cancers have dysregulated amino acid metabolism that lead to tumor aggressiveness. For example, cancer cells can divert glycolytic carbons into serine and glycine metabolic pathways [188]. The serine pathway has been found recently to be a major route for the conversion of glutamine to alpha-ketoglutarate for analeperosis in the TCA cycle to support tumor growth [66]. Glycine is used for *de novo* purine nucleotide synthesis in cancer cells [64].

Our analysis of HGSOC amino acid pathways showed that NAA involved in the aspartate/alanine pathway to be the most up regulated metabolites. The high up-regulation of NAA in ovarian cancer compared to the normal ovary is consistent with

recent metabolomics studies [162,163,189]. In a study by Fong et al, NAA was elevated in primary ovarian cancer and even in greater amount in omental metastatic tumors compared to the normal ovary [162]. Interestingly, the primary ovarian cancer samples were from stage I-IIIC patients and omental metastatic tumors were from stage IIIC-IV patients suggesting that higher levels of NAA would be detected in more advanced cancers. In a study by Ben Sellem et al, NMR analysis of serous, endometrioid, and mucinous cancers compared to the normal ovary showed specifically highest up-regulation of NAA in serous ovarian cancers. Furthermore, partial least square discriminant analysis showed a clear separation of high grade (grade III) serous ovarian cancers from the normal ovary when compared to grade I and II [189]. In a study by Kolwijck et al, aspiration of ovarian cyst fluid (OCF) from serous, mucinous, endometrial, and clear cell ovarian cancers showed that serous ovarian cancer had the largest concentrations of NAA. Furthermore, regardless of subtypes, patients with higher concentrations of NAA in OCF had more advanced stage disease (Stage III-IV). Interestingly, NAA concentrations of OCF were also comparable to the malignant ascites levels[163]. All of these studies suggest that high levels of NAA are associated with more advanced disease in ovarian cancer and the results of our study is the first direct evidence that high levels of NAA are in fact associated with worsening outcomes in HGSOC.

However, some of our data differ from these previous studies [162,163,189]. For example in our study of primary ovarian cancer samples (POC), NAA was up-regulated 28 fold vs. 3 fold in the study by Fong et al [162] when compared to the

normal ovary. Our POC were primarily from patients with advanced stage high grade epithelial ovarian cancers (Stages III-IV). Fong et al's POCs were mostly early stage ranging from Stage I-III. However, when they compared omental metastatic ovarian tumors (Stage IIIC-IV) to the normal ovary, they detected a dramatically 85 fold increase in NAA suggesting more aggressive tumors have higher levels of NAA. Second, the histopathologies of their ovarian adenocarcinomas were not specified, therefore making the metabolomics comparison to our HSOEC difficult. Finally, our sample size of POC was larger with 71 patients compared to 11 patients in their study. In the study by Kolwijck et al, aspiration from OCF did detect NAA in serous borderline and benign tumors, and they did not detect a difference between NAA concentration in OTC between the malignant, borderline, or benign serous tumors[163]. There are several issues with interpretation and comparisons with our study. First, this study was done in cystic fluid, and no tumor tissue was evaluated so it would be difficult to say where the source of NAA levels in serous borderline and benign tumors would be. Second, there were only 9 serous ovarian cancer patients OTC evaluated, and no details about the grade of the tumor were available. However, the authors did find significantly higher concentration of NAA in advanced stage disease compared to early stage disease. This suggests that higher levels of NAA would be associated with worsening prognosis. As we have shown in multiple large cohorts of ovarian cancer patients, at the gene-protein-metabolite level, high NAA production is significantly associated with worsening outcomes in HGSOC.

**Biologic relevance of NAA production**

This was the first time that the effects of NAT8L knockdown have been reported in cancer cells. We observed that the knockdown of the NAT8L leads to significant decreases in tumor growth in the *in vitro* and *in vivo* setting by decreasing tumor proliferation, cell cycle progression, invasion/migration, and increasing cellular apoptosis. Furthermore, knockdown of NAT8L resulted in up-regulation of the major metabolic regulator AMPK, and decreased activity of AKT and ACC in HEYA8 ovarian cancer cells. Metabolically, NAT8L knockdown decreased fatty acid levels in the cancer cell. These results suggest that abrogation of NAA biosynthesis switches cancer cells from an anabolic to a catabolic state, thus decreasing cancer's ability to proliferate and become more susceptible to cell death.

It is noteworthy that similar results of tumor inhibition by activating the catabolic state in tumors by activating AMPK activity. Drugs such as metformin have shown to activate AMPK activity, and cause cell cycle arrest and decreased cell proliferation in various cancers [124], metformin treated of several ovarian cancer cell lines caused cell cycle arrest and decreased cell proliferation. Metformin caused a significant increase in AMPK phosphorylation and ACC phosphorylation enhancing fatty acid beta-oxidation and decreased lipid synthesis. Interestingly, metformin's anti-proliferative effects were seen both through an AMPK dependent and independent pathways. In another study by Rattan et al [190], A2780 ovarian cancer orthotopic mice treated with metformin resulted in significant reduction of tumor growth with decreased tumor cell proliferation. Furthermore, metformin significantly increased cisplatin cytotoxicity. Moreover, the metformin treated group

had significantly increased activation of AMPK. In a study of the ovarian cancer cells SKOV3 [191], the FASN inhibitor drug C93 caused significant increase in AMPK activation and a decrease in ACC activity. As a result, fatty acid synthesis was decreased and glucose oxidation was increased possibly to conserve energy. This treatment worsened cell redox status causing cell death. Furthermore, C93 treatment of SKOV3 xenograft athymic mice showed significant anti-tumor effects and apoptosis.

Although siRNA NAT8L treatment had similar effects on AMPK activity as metformin and C93, there were some differences that we have noted from our study. The study by Rattan et al [124] showed anti-proliferative effects of metformin on various ovarian cancer cell lines (with the exception of SKOV3ip cell lines), unfortunately, no orthotopic model of these cell lines were included as validation in their study. In a separate study by Rattan et al [190], an orthotopic in vivo model of A2780 with metformin did show anti-tumor effects. However, there is a shortcoming for generalizability towards the more common high grade serous ovarian cancer; A2780 is an endometrioid ovarian cancer cell line. In the study by Zhou et al [191], the in vivo model was a xenograft model rather than orthotopic model affecting its generalizability. Furthermore, only one cell line was used for both in vitro and in vivo therapy. In our study, the therapeutic implications of siRNA NAT8L were tested in several in vivo models. We evaluated the effect of siRNA NAT8L in high grade serous and endometroid ovarian cancer cell lines. Furthermore, we evaluated the effect of siRNA NAT8L in several melanoma cell lines for generalizability.

**Study limitations**

Although we show compelling evidence that abrogating NAA production will have anti-tumor effects by switching cancer cells from a catabolic to anabolic state, the mechanism of how NAA contributes to cell anabolism and survival remains unknown at this point. Based on the protein and signaling alteration observed with knockdown of NAT8L, it would be helpful to profile HEYA8 cells to determine the metabolomics profile. This would give further insight into the mechanism of how NAA production affects cancer cells from gene, protein, and metabolic levels. Another limitation related to the mechanism of NAA functioning in cancer cell is the question why NAA and NAT8L are elevated in cancer cells. Our investigation is suggestive that NAA production is advantageous to cancer cells, and identifying the cause of NAA and NAT8L up-regulation elevation would be compelling to identify.

Another limitation of our study is based on the assumption that high levels of NAA would be present in other cancers that are associated with worse outcomes with high NAT8L gene expression. Although metabolomics profiling of human cancer tissues remains at its infancy, various metabolomics studies have shown significant up-regulation of NAA compared in invasive breast cancer and prostate cancer[65,192]. Furthermore, our clinical outcomes results of high NAT8L gene expression, and decreased tumor growth in our orthotopic melanoma mouse model treated with NAT8L siRNA, highly suggest that NAA levels would be high in several cancers promoting tumor growth.

**Implications**

From our study, we observed the increased expression of NAT8L in ovarian cancer compared to the normal ovary is a characteristic of this disease. Furthermore, from our clinical analysis, in vitro and in vivo experiments, we show that targeting NAT8L significantly inhibits tumor growth. Therefore, ovarian cancer is associated with the genetic up-regulation of the NAA biosynthetic machinery to promote growth and survival of the tumor. This unique characteristic of ovarian cancer not present in the normal ovarian tissue makes targeting NAT8L an attractive target to abrogating tumor growth and improving patient outcomes by blocking an important up-regulated cancer metabolic pathway. A better understanding of molecular mechanisms of why some cancers are more dependent on NAA production would help in improving the efficacy of targeting this pathway.

Furthermore, with the distinct elevation of NAA in ovarian cancer, there is promise that NAA may be used as a biomarker. With advances of clinical MRS technology, our metabolic results have implications for the possibility of NAA as a potential novel biomarker in tumors outside of the CNS. Recently, the novel oncometabolite 2-HG was shown to be detected in a non-invasive manner using MRS in glioma patients with IDH 1 and 2 mutations [193]. NAA would be an ideal marker in ovarian cancer due to its dramatic elevation compared to the normal ovary. It would be interesting to see if MRS technology could aid in diagnosis of ovarian cancer in woman who present with ovarian masses. Furthermore, the levels of NAA may be used in MRS techniques to assess response to

chemotherapy would be of use to assess. If NAA levels do decrease with therapy in ovarian cancer, then this holds great promise to use NAA as treatment biomarker.

Finally, our study reveals that NAA is not only unique to brain metabolism, but also in the metabolism of cancer. Since its discovery in 1956, NAA's biological role has remained unclear and elusive. The majority of studies related to NAA are in the area of NMR spectroscopy and its relationship to human brain pathologies. Diseases such as multiple sclerosis, cerebral vascular accidents, major head traumas, certain psychiatric conditions, and Canavan disease are all associated with deregulated NAA levels. More studies looking into the biology and biochemistry is needed to help understand the mechanism of this abundant metabolite in the human brain and cancers.

In conclusion, our study reveals that metabolic alteration in ovarian cancer involves mainly lipid and amino acid metabolic pathways. Targeting unique pathways such as NAA production seems to have promising effects in abrogating the results of this metabolic alteration by inhibiting tumor growth and metastasis. Furthermore, our clinical and biologic studies of several cancer types revealed that NAA production seems relevant not only in ovarian cancer but also in several cancers, and further understanding of its mechanism would not only contribute to understanding of its role in cancer but also further an understanding of its role in the human brain.

References

[1] R. Siegel, D. Naishadham, A. Jemal, Cancer statistics, 2012, CA Cancer J Clin 62 (2012) 10-29.

[2] R.L. Coleman, B.J. Monk, A.K. Sood, T.J. Herzog, Latest research and treatment of advanced-stage epithelial ovarian cancer, Nat Rev Clin Oncol 10 (2013) 211-224.

[3] K.H. Baumann, U. Wagner, A. du Bois, The changing landscape of therapeutic strategies for recurrent ovarian cancer, Future Oncol 8 (2012) 1135-1147.

[4] L. Huang, K.A. Cronin, K.A. Johnson, A.B. Mariotto, E.J. Feuer, Improved survival time: what can survival cure models tell us about population-based survival improvements in late-stage colorectal, ovarian, and testicular cancer?, Cancer 112 (2008) 2289-2300.

[5] R.E. Bristow, R.S. Tomacruz, D.K. Armstrong, E.L. Trimble, F.J. Montz, Survival effect of maximal cytoreductive surgery for advanced ovarian carcinoma during the platinum era: a meta-analysis, J Clin Oncol 20 (2002) 1248-1259.

[6] R.W. Hunter, N.D. Alexander, W.P. Soutter, Meta-analysis of surgery in advanced ovarian carcinoma: is maximum cytoreductive surgery an independent determinant of prognosis?, Am J Obstet Gynecol 166 (1992) 504-511.

[7] S.M. Eisenkop, R.L. Friedman, H.J. Wang, Complete cytoreductive surgery is feasible and maximizes survival in patients with advanced epithelial ovarian cancer: a prospective study, Gynecol Oncol 69 (1998) 103-108.

[8] M.J. Echarri Gonzalez, R. Green, F.M. Muggia, Intraperitoneal drug delivery for ovarian cancer: why, how, who, what, and when?, Oncology (Williston Park) 25 (2011) 156-165, 170.

[9] D. Hanahan, R.A. Weinberg, Hallmarks of cancer: the next generation, Cell 144 (2011) 646-674.

[10] M.G. Vander Heiden, L.C. Cantley, C.B. Thompson, Understanding the Warburg effect: the metabolic requirements of cell proliferation, Science 324 (2009) 1029-1033.

[11] O. Warburg, On respiratory impairment in cancer cells, Science 124 (1956) 269-270.

[12] D.A. Mankoff, J.F. Eary, J.M. Link, M. Muzi, J.G. Rajendran, A.M. Spence, K.A. Krohn, Tumor-specific positron emission tomography imaging in patients: [18F] fluorodeoxyglucose and beyond, Clin Cancer Res 13 (2007) 3460-3469.

[13] T.J. Berg JM, Stryer L., Biochemistry, 5th ed., W.H. Freeman, New York, 2002.

[14] P.S. Ward, C.B. Thompson, Metabolic reprogramming: a cancer hallmark even warburg did not anticipate, Cancer Cell 21 (2012) 297-308.

[15] D.C. Wallace, Mitochondria and cancer, Nat Rev Cancer 12 (2012) 685-698.

[16] R. Morais, K. Zinkewich-Peotti, M. Parent, H. Wang, F. Babai, M. Zollinger, Tumor-forming ability in athymic nude mice of human cell lines devoid of mitochondrial DNA, Cancer Res 54 (1994) 3889-3896.

[17] F. Weinberg, R. Hamanaka, W.W. Wheaton, S. Weinberg, J. Joseph, M. Lopez, B. Kalyanaraman, G.M. Mutlu, G.R. Budinger, N.S. Chandel, Mitochondrial

metabolism and ROS generation are essential for Kras-mediated tumorigenicity, Proc Natl Acad Sci U S A 107 (2010) 8788-8793.

[18] M. Brandon, P. Baldi, D.C. Wallace, Mitochondrial mutations in cancer, Oncogene 25 (2006) 4647-4662.

[19] I. Kurelac, G. Romeo, G. Gasparre, Mitochondrial metabolism and cancer, Mitochondrion 11 (2011) 635-637.

[20] C. Frezza, L. Zheng, O. Folger, K.N. Rajagopalan, E.D. MacKenzie, L. Jerby, M. Micaroni, B. Chaneton, J. Adam, A. Hedley, G. Kalna, I.P. Tomlinson, P.J. Pollard, D.G. Watson, R.J. Deberardinis, T. Shlomi, E. Ruppin, E. Gottlieb, Haem oxygenase is synthetically lethal with the tumour suppressor fumarate hydratase, Nature 477 (2011) 225-228.

[21] L. Dang, D.W. White, S. Gross, B.D. Bennett, M.A. Bittinger, E.M. Driggers, V.R. Fantin, H.G. Jang, S. Jin, M.C. Keenan, K.M. Marks, R.M. Prins, P.S. Ward, K.E. Yen, L.M. Liau, J.D. Rabinowitz, L.C. Cantley, C.B. Thompson, M.G. Vander Heiden, S.M. Su, Cancer-associated IDH1 mutations produce 2-hydroxyglutarate, Nature 462 (2009) 739-744.

[22] M. Xiao, H. Yang, W. Xu, S. Ma, H. Lin, H. Zhu, L. Liu, Y. Liu, C. Yang, Y. Xu, S. Zhao, D. Ye, Y. Xiong, K.L. Guan, Inhibition of alpha-KG-dependent histone and DNA demethylases by fumarate and succinate that are accumulated in mutations of FH and SDH tumor suppressors, Genes Dev 26 (2012) 1326-1338.

[23] S.C. Gupta, D. Hevia, S. Patchva, B. Park, W. Koh, B.B. Aggarwal, Upsides and downsides of reactive oxygen species for cancer: the roles of reactive

oxygen species in tumorigenesis, prevention, and therapy, Antioxid Redox Signal 16 (2012) 1295-1322.

[24] R.H. Burdon, Superoxide and hydrogen peroxide in relation to mammalian cell proliferation, Free Radic Biol Med 18 (1995) 775-794.

[25] C. Abate, L. Patel, F.J. Rauscher, 3rd, T. Curran, Redox regulation of fos and jun DNA-binding activity in vitro, Science 249 (1990) 1157-1161.

[26] G. Bonuccelli, D. Whitaker-Menezes, R. Castello-Cros, S. Pavlides, R.G. Pestell, A. Fatatis, A.K. Witkiewicz, M.G. Vander Heiden, G. Migneco, B. Chiavarina, P.G. Frank, F. Capozza, N. Flomenberg, U.E. Martinez-Outschoorn, F. Sotgia, M.P. Lisanti, The reverse Warburg effect: glycolysis inhibitors prevent the tumor promoting effects of caveolin-1 deficient cancer associated fibroblasts, Cell Cycle 9 (2010) 1960-1971.

[27] C.R. Santos, A. Schulze, Lipid metabolism in cancer, FEBS J 279 (2012) 2610-2623.

[28] G. Medes, A. Thomas, S. Weinhouse, Metabolism of neoplastic tissue. IV. A study of lipid synthesis in neoplastic tissue slices in vitro, Cancer Res 13 (1953) 27-29.

[29] J.A. Menendez, R. Lupu, Fatty acid synthase and the lipogenic phenotype in cancer pathogenesis, Nat Rev Cancer 7 (2007) 763-777.

[30] E.S. Pizer, F.D. Wood, H.S. Heine, F.E. Romantsev, G.R. Pasternack, F.P. Kuhajda, Inhibition of fatty acid synthesis delays disease progression in a xenograft model of ovarian cancer, Cancer Res 56 (1996) 1189-1193.

[31] E.S. Pizer, C. Jackisch, F.D. Wood, G.R. Pasternack, N.E. Davidson, F.P. Kuhajda, Inhibition of fatty acid synthesis induces programmed cell death in human breast cancer cells, Cancer Res 56 (1996) 2745-2747.

[32] G. Hatzivassiliou, F. Zhao, D.E. Bauer, C. Andreadis, A.N. Shaw, D. Dhanak, S.R. Hingorani, D.A. Tuveson, C.B. Thompson, ATP citrate lyase inhibition can suppress tumor cell growth, Cancer Cell 8 (2005) 311-321.

[33] A. Beckers, S. Organe, L. Timmermans, K. Scheys, A. Peeters, K. Brusselmans, G. Verhoeven, J.V. Swinnen, Chemical inhibition of acetyl-CoA carboxylase induces growth arrest and cytotoxicity selectively in cancer cells, Cancer Res 67 (2007) 8180-8187.

[34] A. Ramirez de Molina, R. Gutierrez, M.A. Ramos, J.M. Silva, J. Silva, F. Bonilla, J.J. Sanchez, J.C. Lacal, Increased choline kinase activity in human breast carcinomas: clinical evidence for a potential novel antitumor strategy, Oncogene 21 (2002) 4317-4322.

[35] E. Iorio, A. Ricci, M. Bagnoli, M.E. Pisanu, G. Castellano, M. Di Vito, E. Venturini, K. Glunde, Z.M. Bhujwalla, D. Mezzanzanica, S. Canevari, F. Podo, Activation of phosphatidylcholine cycle enzymes in human epithelial ovarian cancer cells, Cancer Res 70 (2010) 2126-2135.

[36] E. Rysman, K. Brusselmans, K. Scheys, L. Timmermans, R. Derua, S. Munck, P.P. Van Veldhoven, D. Waltregny, V.W. Daniels, J. Machiels, F. Vanderhoydonc, K. Smans, E. Waelkens, G. Verhoeven, J.V. Swinnen, De novo lipogenesis protects cancer cells from free radicals and

chemotherapeutics by promoting membrane lipid saturation, Cancer Res 70 (2010) 8117-8126.

[37] R.J. Deberardinis, J.J. Lum, C.B. Thompson, Phosphatidylinositol 3-kinase-dependent modulation of carnitine palmitoyltransferase 1A expression regulates lipid metabolism during hematopoietic cell growth, J Biol Chem 281 (2006) 37372-37380.

[38] Y. Liu, L.S. Zuckier, N.V. Ghesani, Dominant uptake of fatty acid over glucose by prostate cells: a potential new diagnostic and therapeutic approach, Anticancer Res 30 (2010) 369-374.

[39] L.S. Pike, A.L. Smift, N.J. Croteau, D.A. Ferrick, M. Wu, Inhibition of fatty acid oxidation by etomoxir impairs NADPH production and increases reactive oxygen species resulting in ATP depletion and cell death in human glioblastoma cells, Biochim Biophys Acta (2010).

[40] M. Buzzai, D.E. Bauer, R.G. Jones, R.J. Deberardinis, G. Hatzivassiliou, R.L. Elstrom, C.B. Thompson, The glucose dependence of Akt-transformed cells can be reversed by pharmacologic activation of fatty acid beta-oxidation, Oncogene 24 (2005) 4165-4173.

[41] J.D. Horton, Sterol regulatory element-binding proteins: transcriptional activators of lipid synthesis, Biochem Soc Trans 30 (2002) 1091-1095.

[42] M.S. Brown, J.L. Goldstein, The SREBP pathway: regulation of cholesterol metabolism by proteolysis of a membrane-bound transcription factor, Cell 89 (1997) 331-340.

[43] I. Shimomura, H. Shimano, J.D. Horton, J.L. Goldstein, M.S. Brown, Differential expression of exons 1a and 1c in mRNAs for sterol regulatory element binding protein-1 in human and mouse organs and cultured cells, J Clin Invest 99 (1997) 838-845.

[44] T. Porstmann, C.R. Santos, B. Griffiths, M. Cully, M. Wu, S. Leevers, J.R. Griffiths, Y.L. Chung, A. Schulze, SREBP activity is regulated by mTORC1 and contributes to Akt-dependent cell growth, Cell Metab 8 (2008) 224-236.

[45] A. Shamma, Y. Takegami, T. Miki, S. Kitajima, M. Noda, T. Obara, T. Okamoto, C. Takahashi, Rb Regulates DNA damage response and cellular senescence through E2F-dependent suppression of N-ras isoprenylation, Cancer Cell 15 (2009) 255-269.

[46] W.A. Freed-Pastor, H. Mizuno, X. Zhao, A. Langerod, S.H. Moon, R. Rodriguez-Barrueco, A. Barsotti, A. Chicas, W. Li, A. Polotskaia, M.J. Bissell, T.F. Osborne, B. Tian, S.W. Lowe, J.M. Silva, A.L. Borresen-Dale, A.J. Levine, J. Bargonetti, C. Prives, Mutant p53 disrupts mammary tissue architecture via the mevalonate pathway, Cell 148 (2012) 244-258.

[47] Y. Li, S. Xu, M.M. Mihaylova, B. Zheng, X. Hou, B. Jiang, O. Park, Z. Luo, E. Lefai, J.Y. Shyy, B. Gao, M. Wierzbicki, T.J. Verbeuren, R.J. Shaw, R.A. Cohen, M. Zang, AMPK phosphorylates and inhibits SREBP activity to attenuate hepatic steatosis and atherosclerosis in diet-induced insulin-resistant mice, Cell Metab 13 (2011) 376-388.

[48] A.K. Walker, R.L. Jacobs, J.L. Watts, V. Rottiers, K. Jiang, D.M. Finnegan, T. Shioda, M. Hansen, F. Yang, L.J. Niebergall, D.E. Vance, M. Tzoneva, A.C.

Hart, A.M. Naar, A conserved SREBP-1/phosphatidylcholine feedback circuit regulates lipogenesis in metazoans, Cell 147 (2011) 840-852.

[49] G. Wu, Amino acids: metabolism, functions, and nutrition, Amino Acids 37 (2009) 1-17.

[50] E. Curis, P. Crenn, L. Cynober, Citrulline and the gut, Curr Opin Clin Nutr Metab Care 10 (2007) 620-626.

[51] C.A. Hu, S. Khalil, S. Zhaorigetu, Z. Liu, M. Tyler, G. Wan, D. Valle, Human Delta1-pyrroline-5-carboxylate synthase: function and regulation, Amino Acids 35 (2008) 665-672.

[52] P. Manna, M. Sinha, P.C. Sil, Taurine plays a beneficial role against cadmium-induced oxidative renal dysfunction, Amino Acids 36 (2009) 417-428.

[53] J. Perla-Kajan, O. Stanger, M. Luczak, A. Ziolkowska, L.K. Malendowicz, T. Twardowski, S. Lhotak, R.C. Austin, H. Jakubowski, Immunohistochemical detection of N-homocysteinylated proteins in humans and mice, Biomed Pharmacother 62 (2008) 473-479.

[54] J. Escobar, J.W. Frank, A. Suryawan, H.V. Nguyen, S.R. Kimball, L.S. Jefferson, T.A. Davis, Physiological rise in plasma leucine stimulates muscle protein synthesis in neonatal pigs by enhancing translation initiation factor activation, Am J Physiol Endocrinol Metab 288 (2005) E914-921.

[55] K. Yao, Y.L. Yin, W. Chu, Z. Liu, D. Deng, T. Li, R. Huang, J. Zhang, B. Tan, W. Wang, G. Wu, Dietary arginine supplementation increases mTOR signaling activity in skeletal muscle of neonatal pigs, J Nutr 138 (2008) 867-872.

[56] G. Wu, F.W. Bazer, T.A. Davis, S.W. Kim, P. Li, J. Marc Rhoads, M. Carey Satterfield, S.B. Smith, T.E. Spencer, Y. Yin, Arginine metabolism and nutrition in growth, health and disease, Amino Acids 37 (2009) 153-168.

[57] P. Newsholme, L. Brennan, B. Rubi, P. Maechler, New insights into amino acid metabolism, beta-cell function and diabetes, Clin Sci (Lond) 108 (2005) 185-194.

[58] M. Tomasiak, Importance of the malate-aspartate shuttle for the reoxidation of glycolytically produced NADH and for cell aggregation in porcine blood platelets, Acta Biochim Pol 34 (1987) 269-284.

[59] W.J. Fu, T.E. Haynes, R. Kohli, J. Hu, W. Shi, T.E. Spencer, R.J. Carroll, C.J. Meininger, G. Wu, Dietary L-arginine supplementation reduces fat mass in Zucker diabetic fatty rats, J Nutr 135 (2005) 714-721.

[60] C.V. Dang, Glutaminolysis: supplying carbon or nitrogen or both for cancer cells?, Cell Cycle 9 (2010) 3884-3886.

[61] M. Yuneva, N. Zamboni, P. Oefner, R. Sachidanandam, Y. Lazebnik, Deficiency in glutamine but not glucose induces MYC-dependent apoptosis in human cells, J Cell Biol 178 (2007) 93-105.

[62] R.J. DeBerardinis, A. Mancuso, E. Daikhin, I. Nissim, M. Yudkoff, S. Wehrli, C.B. Thompson, Beyond aerobic glycolysis: transformed cells can engage in glutamine metabolism that exceeds the requirement for protein and nucleotide synthesis, Proc Natl Acad Sci U S A 104 (2007) 19345-19350.

[63] A.R. Mullen, W.W. Wheaton, E.S. Jin, P.H. Chen, L.B. Sullivan, T. Cheng, Y. Yang, W.M. Linehan, N.S. Chandel, R.J. DeBerardinis, Reductive

carboxylation supports growth in tumour cells with defective mitochondria, Nature 481 (2012) 385-388.

[64] M. Jain, R. Nilsson, S. Sharma, N. Madhusudhan, T. Kitami, A.L. Souza, R. Kafri, M.W. Kirschner, C.B. Clish, V.K. Mootha, Metabolite profiling identifies a key role for glycine in rapid cancer cell proliferation, Science 336 (2012) 1040-1044.

[65] A. Sreekumar, L.M. Poisson, T.M. Rajendiran, A.P. Khan, Q. Cao, J. Yu, B. Laxman, R. Mehra, R.J. Lonigro, Y. Li, M.K. Nyati, A. Ahsan, S. Kalyana-Sundaram, B. Han, X. Cao, J. Byun, G.S. Omenn, D. Ghosh, S. Pennathur, D.C. Alexander, A. Berger, J.R. Shuster, J.T. Wei, S. Varambally, C. Beecher, A.M. Chinnaiyan, Metabolomic profiles delineate potential role for sarcosine in prostate cancer progression, Nature 457 (2009) 910-914.

[66] R. Possemato, K.M. Marks, Y.D. Shaul, M.E. Pacold, D. Kim, K. Birsoy, S. Sethumadhavan, H.K. Woo, H.G. Jang, A.K. Jha, W.W. Chen, F.G. Barrett, N. Stransky, Z.Y. Tsun, G.S. Cowley, J. Barretina, N.Y. Kalaany, P.P. Hsu, K. Ottina, A.M. Chan, B. Yuan, L.A. Garraway, D.E. Root, M. Mino-Kenudson, E.F. Brachtel, E.M. Driggers, D.M. Sabatini, Functional genomics reveal that the serine synthesis pathway is essential in breast cancer, Nature 476 (2011) 346-350.

[67] J. Ye, A. Mancuso, X. Tong, P.S. Ward, J. Fan, J.D. Rabinowitz, C.B. Thompson, Pyruvate kinase M2 promotes de novo serine synthesis to sustain mTORC1 activity and cell proliferation, Proc Natl Acad Sci U S A 109 (2012) 6904-6909.

[68] O.D. Maddocks, C.R. Berkers, S.M. Mason, L. Zheng, K. Blyth, E. Gottlieb, K.H. Vousden, Serine starvation induces stress and p53-dependent metabolic remodelling in cancer cells, Nature 493 (2013) 542-546.

[69] M.M. Mihaylova, R.J. Shaw, The AMPK signalling pathway coordinates cell growth, autophagy and metabolism, Nat Cell Biol 13 (2011) 1016-1023.

[70] B. Xiao, M.J. Sanders, E. Underwood, R. Heath, F.V. Mayer, D. Carmena, C. Jing, P.A. Walker, J.F. Eccleston, L.F. Haire, P. Saiu, S.A. Howell, R. Aasland, S.R. Martin, D. Carling, S.J. Gamblin, Structure of mammalian AMPK and its regulation by ADP, Nature 472 (2011) 230-233.

[71] J.S. Oakhill, R. Steel, Z.P. Chen, J.W. Scott, N. Ling, S. Tam, B.E. Kemp, AMPK is a direct adenylate charge-regulated protein kinase, Science 332 (2011) 1433-1435.

[72] R.J. Shaw, M. Kosmatka, N. Bardeesy, R.L. Hurley, L.A. Witters, R.A. DePinho, L.C. Cantley, The tumor suppressor LKB1 kinase directly activates AMP-activated kinase and regulates apoptosis in response to energy stress, Proc Natl Acad Sci U S A 101 (2004) 3329-3335.

[73] A. Woods, S.R. Johnstone, K. Dickerson, F.C. Leiper, L.G. Fryer, D. Neumann, U. Schlattner, T. Wallimann, M. Carlson, D. Carling, LKB1 is the upstream kinase in the AMP-activated protein kinase cascade, Curr Biol 13 (2003) 2004-2008.

[74] S.A. Hawley, D.A. Pan, K.J. Mustard, L. Ross, J. Bain, A.M. Edelman, B.G. Frenguelli, D.G. Hardie, Calmodulin-dependent protein kinase kinase-beta is

an alternative upstream kinase for AMP-activated protein kinase, Cell Metab 2 (2005) 9-19.

[75] K.A. Anderson, T.J. Ribar, F. Lin, P.K. Noeldner, M.F. Green, M.J. Muehlbauer, L.A. Witters, B.E. Kemp, A.R. Means, Hypothalamic CaMKK2 contributes to the regulation of energy balance, Cell Metab 7 (2008) 377-388.

[76] P. Tamas, S.A. Hawley, R.G. Clarke, K.J. Mustard, K. Green, D.G. Hardie, D.A. Cantrell, Regulation of the energy sensor AMP-activated protein kinase by antigen receptor and Ca2+ in T lymphocytes, J Exp Med 203 (2006) 1665-1670.

[77] G. Herrero-Martin, M. Hoyer-Hansen, C. Garcia-Garcia, C. Fumarola, T. Farkas, A. Lopez-Rivas, M. Jaattela, TAK1 activates AMPK-dependent cytoprotective autophagy in TRAIL-treated epithelial cells, EMBO J 28 (2009) 677-685.

[78] D.G. Hardie, F.A. Ross, S.A. Hawley, AMPK: a nutrient and energy sensor that maintains energy homeostasis, Nat Rev Mol Cell Biol 13 (2012) 251-262.

[79] R.J. Shaw, K.A. Lamia, D. Vasquez, S.H. Koo, N. Bardeesy, R.A. Depinho, M. Montminy, L.C. Cantley, The kinase LKB1 mediates glucose homeostasis in liver and therapeutic effects of metformin, Science 310 (2005) 1642-1646.

[80] S.A. Hawley, F.A. Ross, C. Chevtzoff, K.A. Green, A. Evans, S. Fogarty, M.C. Towler, L.J. Brown, O.A. Ogunbayo, A.M. Evans, D.G. Hardie, Use of cells expressing gamma subunit variants to identify diverse mechanisms of AMPK activation, Cell Metab 11 (2010) 554-565.

[81] D.G. Hardie, Neither LKB1 nor AMPK are the direct targets of metformin, Gastroenterology 131 (2006) 973; author reply 974-975.

[82] D.G. Hardie, AMP-activated protein kinase as a drug target, Annu Rev Pharmacol Toxicol 47 (2007) 185-210.

[83] S.B. Rothbart, A.C. Racanelli, R.G. Moran, Pemetrexed indirectly activates the metabolic kinase AMPK in human carcinomas, Cancer Res 70 (2010) 10299-10309.

[84] J.W. Zmijewski, S. Banerjee, H. Bae, A. Friggeri, E.R. Lazarowski, E. Abraham, Exposure to hydrogen peroxide induces oxidation and activation of AMP-activated protein kinase, J Biol Chem 285 (2010) 33154-33164.

[85] S. Ditch, T.T. Paull, The ATM protein kinase and cellular redox signaling: beyond the DNA damage response, Trends Biochem Sci 37 (2012) 15-22.

[86] X. Fu, S. Wan, Y.L. Lyu, L.F. Liu, H. Qi, Etoposide induces ATM-dependent mitochondrial biogenesis through AMPK activation, PLoS One 3 (2008) e2009.

[87] C. Ji, B. Yang, Y.L. Yang, S.H. He, D.S. Miao, L. He, Z.G. Bi, Exogenous cell-permeable C6 ceramide sensitizes multiple cancer cell lines to Doxorubicin-induced apoptosis by promoting AMPK activation and mTORC1 inhibition, Oncogene 29 (2010) 6557-6568.

[88] T. Sanli, A. Rashid, C. Liu, S. Harding, R.G. Bristow, J.C. Cutz, G. Singh, J. Wright, T. Tsakiridis, Ionizing radiation activates AMP-activated kinase (AMPK): a target for radiosensitization of human cancer cells, Int J Radiat Oncol Biol Phys 78 (2010) 221-229.

[89] D.M. Gwinn, D.B. Shackelford, D.F. Egan, M.M. Mihaylova, A. Mery, D.S. Vasquez, B.E. Turk, R.J. Shaw, AMPK phosphorylation of raptor mediates a metabolic checkpoint, Mol Cell 30 (2008) 214-226.

[90] A. Kalender, A. Selvaraj, S.Y. Kim, P. Gulati, S. Brule, B. Viollet, B.E. Kemp, N. Bardeesy, P. Dennis, J.J. Schlager, A. Marette, S.C. Kozma, G. Thomas, Metformin, independent of AMPK, inhibits mTORC1 in a rag GTPase-dependent manner, Cell Metab 11 (2010) 390-401.

[91] D.F. Egan, D.B. Shackelford, M.M. Mihaylova, S. Gelino, R.A. Kohnz, W. Mair, D.S. Vasquez, A. Joshi, D.M. Gwinn, R. Taylor, J.M. Asara, J. Fitzpatrick, A. Dillin, B. Viollet, M. Kundu, M. Hansen, R.J. Shaw, Phosphorylation of ULK1 (hATG1) by AMP-activated protein kinase connects energy sensing to mitophagy, Science 331 (2011) 456-461.

[92] J. Kim, M. Kundu, B. Viollet, K.L. Guan, AMPK and mTOR regulate autophagy through direct phosphorylation of Ulk1, Nat Cell Biol 13 (2011) 132-141.

[93] D. Nakada, T.L. Saunders, S.J. Morrison, Lkb1 regulates cell cycle and energy metabolism in haematopoietic stem cells, Nature 468 (2010) 653-658.

[94] D. Carling, V.A. Zammit, D.G. Hardie, A common bicyclic protein kinase cascade inactivates the regulatory enzymes of fatty acid and cholesterol biosynthesis, FEBS Lett 223 (1987) 217-222.

[95] R. Sato, J.L. Goldstein, M.S. Brown, Replacement of serine-871 of hamster 3-hydroxy-3-methylglutaryl-CoA reductase prevents phosphorylation by AMP-activated kinase and blocks inhibition of sterol synthesis induced by ATP depletion, Proc Natl Acad Sci U S A 90 (1993) 9261-9265.

[96] M.J. Watt, A.G. Holmes, S.K. Pinnamaneni, A.P. Garnham, G.R. Steinberg, B.E. Kemp, M.A. Febbraio, Regulation of HSL serine phosphorylation in skeletal muscle and adipose tissue, Am J Physiol Endocrinol Metab 290 (2006) E500-508.

[97] M. Ahmadian, M.J. Abbott, T. Tang, C.S. Hudak, Y. Kim, M. Bruss, M.K. Hellerstein, H.Y. Lee, V.T. Samuel, G.I. Shulman, Y. Wang, R.E. Duncan, C. Kang, H.S. Sul, Desnutrin/ATGL is regulated by AMPK and is required for a brown adipose phenotype, Cell Metab 13 (2011) 739-748.

[98] K. Sakamoto, G.D. Holman, Emerging role for AS160/TBC1D4 and TBC1D1 in the regulation of GLUT4 traffic, Am J Physiol Endocrinol Metab 295 (2008) E29-37.

[99] W.C. Huang, X. Li, J. Liu, J. Lin, L.W. Chung, Activation of androgen receptor, lipogenesis, and oxidative stress converged by SREBP-1 is responsible for regulating growth and progression of prostate cancer cells, Mol Cancer Res 10 (2012) 133-142.

[100] W. Li, Y. Tai, J. Zhou, W. Gu, Z. Bai, T. Zhou, Z. Zhong, P.A. McCue, N. Sang, J.Y. Ji, B. Kong, J. Jiang, C. Wang, Repression of endometrial tumor growth by targeting SREBP1 and lipogenesis, Cell Cycle 11 (2012) 2348-2358.

[101] W. Mair, I. Morantte, A.P. Rodrigues, G. Manning, M. Montminy, R.J. Shaw, A. Dillin, Lifespan extension induced by AMPK and calcineurin is mediated by CRTC-1 and CREB, Nature 470 (2011) 404-408.

[102] Z. Feng, W. Hu, E. de Stanchina, A.K. Teresky, S. Jin, S. Lowe, A.J. Levine, The regulation of AMPK beta1, TSC2, and PTEN expression by p53: stress, cell and tissue specificity, and the role of these gene products in modulating the IGF-1-AKT-mTOR pathways, Cancer Res 67 (2007) 3043-3053.

[103] M.M. Mihaylova, D.S. Vasquez, K. Ravnskjaer, P.D. Denechaud, R.T. Yu, J.G. Alvarez, M. Downes, R.M. Evans, M. Montminy, R.J. Shaw, Class IIa histone deacetylases are hormone-activated regulators of FOXO and mammalian glucose homeostasis, Cell 145 (2011) 607-621.

[104] Y. Gu, S. Lin, J.L. Li, H. Nakagawa, Z. Chen, B. Jin, L. Tian, D.A. Ucar, H. Shen, J. Lu, S.N. Hochwald, F.J. Kaye, L. Wu, Altered LKB1/CREB-regulated transcription co-activator (CRTC) signaling axis promotes esophageal cancer cell migration and invasion, Oncogene 31 (2012) 469-479.

[105] T. Komiya, A. Coxon, Y. Park, W.D. Chen, M. Zajac-Kaye, P. Meltzer, T. Karpova, F.J. Kaye, Enhanced activity of the CREB co-activator Crtc1 in LKB1 null lung cancer, Oncogene 29 (2010) 1672-1680.

[106] P. Marks, R.A. Rifkind, V.M. Richon, R. Breslow, T. Miller, W.K. Kelly, Histone deacetylases and cancer: causes and therapies, Nat Rev Cancer 1 (2001) 194-202.

[107] Integrated genomic analyses of ovarian carcinoma, Nature 474 (2011) 609-615.

[108] K. Bensaad, A. Tsuruta, M.A. Selak, M.N. Vidal, K. Nakano, R. Bartrons, E. Gottlieb, K.H. Vousden, TIGAR, a p53-inducible regulator of glycolysis and apoptosis, Cell 126 (2006) 107-120.

[109] S.P. Mathupala, Y.H. Ko, P.L. Pedersen, Hexokinase II: cancer's double-edged sword acting as both facilitator and gatekeeper of malignancy when bound to mitochondria, Oncogene 25 (2006) 4777-4786.

[110] S.P. Mathupala, C. Heese, P.L. Pedersen, Glucose catabolism in cancer cells. The type II hexokinase promoter contains functionally active response elements for the tumor suppressor p53, J Biol Chem 272 (1997) 22776-22780.

[111] S. Suzuki, T. Tanaka, M.V. Poyurovsky, H. Nagano, T. Mayama, S. Ohkubo, M. Lokshin, H. Hosokawa, T. Nakayama, Y. Suzuki, S. Sugano, E. Sato, T. Nagao, K. Yokote, I. Tatsuno, C. Prives, Phosphate-activated glutaminase (GLS2), a p53-inducible regulator of glutamine metabolism and reactive oxygen species, Proc Natl Acad Sci U S A 107 (2010) 7461-7466.

[112] A. Saleem, P.J. Adhihetty, D.A. Hood, Role of p53 in mitochondrial biogenesis and apoptosis in skeletal muscle, Physiol Genomics 37 (2009) 58-66.

[113] P. Jiang, W. Du, X. Wang, A. Mancuso, X. Gao, M. Wu, X. Yang, p53 regulates biosynthesis through direct inactivation of glucose-6-phosphate dehydrogenase, Nat Cell Biol 13 (2011) 310-316.

[114] A. Carracedo, L.C. Cantley, P.P. Pandolfi, Cancer metabolism: fatty acid oxidation in the limelight, Nat Rev Cancer 13 (2013) 227-232.

[115] T. Ide, L. Brown-Endres, K. Chu, P.P. Ongusaha, T. Ohtsuka, W.S. El-Deiry, S.A. Aaronson, S.W. Lee, GAMT, a p53-inducible modulator of apoptosis, is critical for the adaptive response to nutrient stress, Mol Cell 36 (2009) 379-392.

[116] S. Farber, E.C. Cutler, J.W. Hawkins, J.H. Harrison, E.C. Peirce, 2nd, G.G. Lenz, The Action of Pteroylglutamic Conjugates on Man, Science 106 (1947) 619-621.

[117] B.A. Chabner, T.G. Roberts, Jr., Timeline: Chemotherapy and the war on cancer, Nat Rev Cancer 5 (2005) 65-72.

[118] M.C. Li, R. Hertz, D.M. Bergenstal, Therapy of choriocarcinoma and related trophoblastic tumors with folic acid and purine antagonists, N Engl J Med 259 (1958) 66-74.

[119] M.G. Vander Heiden, Targeting cancer metabolism: a therapeutic window opens, Nat Rev Drug Discov 10 (2011) 671-684.

[120] M.A. Weiser, M.E. Cabanillas, M. Konopleva, D.A. Thomas, S.A. Pierce, C.P. Escalante, H.M. Kantarjian, S.M. O'Brien, Relation between the duration of remission and hyperglycemia during induction chemotherapy for acute lymphocytic leukemia with a hyperfractionated cyclophosphamide, vincristine, doxorubicin, and dexamethasone/methotrexate-cytarabine regimen, Cancer 100 (2004) 1179-1185.

[121] J.A. Meyerhardt, P.J. Catalano, D.G. Haller, R.J. Mayer, J.S. Macdonald, A.B. Benson, 3rd, C.S. Fuchs, Impact of diabetes mellitus on outcomes in patients with colon cancer, J Clin Oncol 21 (2003) 433-440.

[122] J. Yun, C. Rago, I. Cheong, R. Pagliarini, P. Angenendt, H. Rajagopalan, K. Schmidt, J.K. Willson, S. Markowitz, S. Zhou, L.A. Diaz, Jr., V.E. Velculescu, C. Lengauer, K.W. Kinzler, B. Vogelstein, N. Papadopoulos, Glucose

deprivation contributes to the development of KRAS pathway mutations in tumor cells, Science 325 (2009) 1555-1559.

[123] K.M. Nieman, H.A. Kenny, C.V. Penicka, A. Ladanyi, R. Buell-Gutbrod, M.R. Zillhardt, I.L. Romero, M.S. Carey, G.B. Mills, G.S. Hotamisligil, S.D. Yamada, M.E. Peter, K. Gwin, E. Lengyel, Adipocytes promote ovarian cancer metastasis and provide energy for rapid tumor growth, Nat Med 17 (2011) 1498-1503.

[124] R. Rattan, S. Giri, L.C. Hartmann, V. Shridhar, Metformin attenuates ovarian cancer cell growth in an AMP-kinase dispensable manner, J Cell Mol Med 15 (2011) 166-178.

[125] C. Algire, L. Amrein, M. Zakikhani, L. Panasci, M. Pollak, Metformin blocks the stimulative effect of a high-energy diet on colon carcinoma growth in vivo and is associated with reduced expression of fatty acid synthase, Endocr Relat Cancer 17 (2010) 351-360.

[126] M. Buzzai, R.G. Jones, R.K. Amaravadi, J.J. Lum, R.J. DeBerardinis, F. Zhao, B. Viollet, C.B. Thompson, Systemic treatment with the antidiabetic drug metformin selectively impairs p53-deficient tumor cell growth, Cancer Res 67 (2007) 6745-6752.

[127] K. Brusselmans, E. De Schrijver, G. Verhoeven, J.V. Swinnen, RNA interference-mediated silencing of the acetyl-CoA-carboxylase-alpha gene induces growth inhibition and apoptosis of prostate cancer cells, Cancer Res 65 (2005) 6719-6725.

[128] N.M. Al-Saffar, H. Troy, A. Ramirez de Molina, L.E. Jackson, B. Madhu, J.R. Griffiths, M.O. Leach, P. Workman, J.C. Lacal, I.R. Judson, Y.L. Chung, Noninvasive magnetic resonance spectroscopic pharmacodynamic markers of the choline kinase inhibitor MN58b in human carcinoma models, Cancer Res 66 (2006) 427-434.

[129] H. Yan, D.W. Parsons, G. Jin, R. McLendon, B.A. Rasheed, W. Yuan, I. Kos, I. Batinic-Haberle, S. Jones, G.J. Riggins, H. Friedman, A. Friedman, D. Reardon, J. Herndon, K.W. Kinzler, V.E. Velculescu, B. Vogelstein, D.D. Bigner, IDH1 and IDH2 mutations in gliomas, N Engl J Med 360 (2009) 765-773.

[130] D.W. Parsons, S. Jones, X. Zhang, J.C. Lin, R.J. Leary, P. Angenendt, P. Mankoo, H. Carter, I.M. Siu, G.L. Gallia, A. Olivi, R. McLendon, B.A. Rasheed, S. Keir, T. Nikolskaya, Y. Nikolsky, D.A. Busam, H. Tekleab, L.A. Diaz, Jr., J. Hartigan, D.R. Smith, R.L. Strausberg, S.K. Marie, S.M. Shinjo, H. Yan, G.J. Riggins, D.D. Bigner, R. Karchin, N. Papadopoulos, G. Parmigiani, B. Vogelstein, V.E. Velculescu, K.W. Kinzler, An integrated genomic analysis of human glioblastoma multiforme, Science 321 (2008) 1807-1812.

[131] P.S. Ward, J. Patel, D.R. Wise, O. Abdel-Wahab, B.D. Bennett, H.A. Coller, J.R. Cross, V.R. Fantin, C.V. Hedvat, A.E. Perl, J.D. Rabinowitz, M. Carroll, S.M. Su, K.A. Sharp, R.L. Levine, C.B. Thompson, The common feature of leukemia-associated IDH1 and IDH2 mutations is a neomorphic enzyme

activity converting alpha-ketoglutarate to 2-hydroxyglutarate, Cancer Cell 17 (2010) 225-234.

[132] M.E. Figueroa, O. Abdel-Wahab, C. Lu, P.S. Ward, J. Patel, A. Shih, Y. Li, N. Bhagwat, A. Vasanthakumar, H.F. Fernandez, M.S. Tallman, Z. Sun, K. Wolniak, J.K. Peeters, W. Liu, S.E. Choe, V.R. Fantin, E. Paietta, B. Lowenberg, J.D. Licht, L.A. Godley, R. Delwel, P.J. Valk, C.B. Thompson, R.L. Levine, A. Melnick, Leukemic IDH1 and IDH2 mutations result in a hypermethylation phenotype, disrupt TET2 function, and impair hematopoietic differentiation, Cancer Cell 18 (2010) 553-567.

[133] S. Zhao, Y. Lin, W. Xu, W. Jiang, Z. Zha, P. Wang, W. Yu, Z. Li, L. Gong, Y. Peng, J. Ding, Q. Lei, K.L. Guan, Y. Xiong, Glioma-derived mutations in IDH1 dominantly inhibit IDH1 catalytic activity and induce HIF-1alpha, Science 324 (2009) 261-265.

[134] B. Yang, C. Zhong, Y. Peng, Z. Lai, J. Ding, Molecular mechanisms of "off-on switch" of activities of human IDH1 by tumor-associated mutation R132H, Cell Res 20 (2010) 1188-1200.

[135] C.D. Dinardo, K.J. Propert, A.W. Loren, E. Paietta, Z. Sun, R.L. Levine, K.S. Straley, K. Yen, J.P. Patel, S. Agresta, O. Abdel-Wahab, A.E. Perl, M.R. Litzow, J.M. Rowe, H.M. Lazarus, H.F. Fernandez, D.J. Margolis, M.S. Tallman, S.M. Luger, M. Carroll, Serum 2-hydroxyglutarate levels predict isocitrate dehydrogenase mutations and clinical outcome in acute myeloid leukemia, Blood (2013).

[136] P.S. Ariyannur, J.R. Moffett, P. Manickam, N. Pattabiraman, P. Arun, A. Nitta, T. Nabeshima, C.N. Madhavarao, A.M. Namboodiri, Methamphetamine-induced neuronal protein NAT8L is the NAA biosynthetic enzyme: implications for specialized acetyl coenzyme A metabolism in the CNS, Brain Res 1335 (2010) 1-13.

[137] E. Wiame, D. Tyteca, N. Pierrot, F. Collard, M. Amyere, G. Noel, J. Desmedt, M.C. Nassogne, M. Vikkula, J.N. Octave, M.F. Vincent, P.J. Courtoy, E. Boltshauser, E. van Schaftingen, Molecular identification of aspartate N-acetyltransferase and its mutation in hypoacetylaspartia, Biochem J 425 (2010) 127-136.

[138] I. Becker, J. Lodder, V. Gieselmann, M. Eckhardt, Molecular characterization of N-acetylaspartylglutamate synthetase, J Biol Chem 285 (2010) 29156-29164.

[139] T.B. Patel, J.B. Clark, Synthesis of N-acetyl-L-aspartate by rat brain mitochondria and its involvement in mitochondrial/cytosolic carbon transport, Biochem J 184 (1979) 539-546.

[140] G. Tahay, E. Wiame, D. Tyteca, P.J. Courtoy, E. Van Schaftingen, Determinants of the enzymatic activity and the subcellular localization of aspartate N-acetyltransferase, Biochem J 441 (2012) 105-112.

[141] Z.H. Lu, G. Chakraborty, R.W. Ledeen, D. Yahya, G. Wu, N-Acetylaspartate synthase is bimodally expressed in microsomes and mitochondria of brain, Brain Res Mol Brain Res 122 (2004) 71-78.

[142] T.E. Bates, M. Strangward, J. Keelan, G.P. Davey, P.M. Munro, J.B. Clark, Inhibition of N-acetylaspartate production: implications for 1H MRS studies in vivo, Neuroreport 7 (1996) 1397-1400.

[143] C.G. Janson, S.W. McPhee, J. Francis, D. Shera, M. Assadi, A. Freese, P. Hurh, J. Haselgrove, D.J. Wang, L. Bilaniuk, P. Leone, Natural history of Canavan disease revealed by proton magnetic resonance spectroscopy (1H-MRS) and diffusion-weighted MRI, Neuropediatrics 37 (2006) 209-221.

[144] N. De Stefano, P.M. Matthews, D.L. Arnold, Reversible decreases in N-acetylaspartate after acute brain injury, Magn Reson Med 34 (1995) 721-727.

[145] K. Kantarci, C.R. Jack, Jr., Y.C. Xu, N.G. Campeau, P.C. O'Brien, G.E. Smith, R.J. Ivnik, B.F. Boeve, E. Kokmen, E.G. Tangalos, R.C. Petersen, Regional metabolic patterns in mild cognitive impairment and Alzheimer's disease: A 1H MRS study, Neurology 55 (2000) 210-217.

[146] C. Demougeot, P. Garnier, C. Mossiat, N. Bertrand, M. Giroud, A. Beley, C. Marie, N-Acetylaspartate, a marker of both cellular dysfunction and neuronal loss: its relevance to studies of acute brain injury, J Neurochem 77 (2001) 408-415.

[147] M.H. Baslow, Evidence that the tri-cellular metabolism of N-acetylaspartate functions as the brain's "operating system": how NAA metabolism supports meaningful intercellular frequency-encoded communications, Amino Acids 39 (2010) 1139-1145.

[148] J.R. Moffett, B. Ross, P. Arun, C.N. Madhavarao, A.M. Namboodiri, N-Acetylaspartate in the CNS: from neurodiagnostics to neurobiology, Prog Neurobiol 81 (2007) 89-131.

[149] E. Bitto, C.A. Bingman, G.E. Wesenberg, J.G. McCoy, G.N. Phillips, Jr., Structure of aspartoacylase, the brain enzyme impaired in Canavan disease, Proc Natl Acad Sci U S A 104 (2007) 456-461.

[150] A.F. D'Adamo, Jr., J.C. Smith, C. Woiler, The occurrence of N-acetylaspartate amidohydrolase (aminoacylase II) in the developing rat, J Neurochem 20 (1973) 1275-1278.

[151] M.H. Baslow, R.F. Suckow, V. Sapirstein, B.L. Hungund, Expression of aspartoacylase activity in cultured rat macroglial cells is limited to oligodendrocytes, J Mol Neurosci 13 (1999) 47-53.

[152] A.F. D'Adamo, Jr., F.M. Yatsu, Acetate metabolism in the nervous system. N-acetyl-L-aspartic acid and the biosynthesis of brain lipids, J Neurochem 13 (1966) 961-965.

[153] R. Burri, C. Steffen, N. Herschkowitz, N-acetyl-L-aspartate is a major source of acetyl groups for lipid synthesis during rat brain development, Dev Neurosci 13 (1991) 403-411.

[154] G. Chakraborty, P. Mekala, D. Yahya, G. Wu, R.W. Ledeen, Intraneuronal N-acetylaspartate supplies acetyl groups for myelin lipid synthesis: evidence for myelin-associated aspartoacylase, J Neurochem 78 (2001) 736-745.

[155] J.B. Clark, N-acetyl aspartate: a marker for neuronal loss or mitochondrial dysfunction, Dev Neurosci 20 (1998) 271-276.

[156] M.H. Baslow, J. Hrabe, D.N. Guilfoyle, Dynamic relationship between neurostimulation and N-acetylaspartate metabolism in the human visual cortex: evidence that NAA functions as a molecular water pump during visual stimulation, J Mol Neurosci 32 (2007) 235-245.

[157] M. Yudkoff, D. Nelson, Y. Daikhin, M. Erecinska, Tricarboxylic acid cycle in rat brain synaptosomes. Fluxes and interactions with aspartate aminotransferase and malate/aspartate shuttle, J Biol Chem 269 (1994) 27414-27420.

[158] A.P. Burlina, B. Schmitt, U. Engelke, R.A. Wevers, A.B. Burlina, E. Boltshauser, Hypoacetylaspartia: clinical and biochemical follow-up of a patient, Adv Exp Med Biol 576 (2006) 283-287; discussion 361-283.

[159] Y. Furukawa-Hibi, A. Nitta, H. Fukumitsu, H. Somiya, K. Toriumi, S. Furukawa, T. Nabeshima, K. Yamada, Absence of SHATI/Nat8l reduces social interaction in mice, Neurosci Lett 526 (2012) 79-84.

[160] P. Leone, D. Shera, S.W. McPhee, J.S. Francis, E.H. Kolodny, L.T. Bilaniuk, D.J. Wang, M. Assadi, O. Goldfarb, H.W. Goldman, A. Freese, D. Young, M.J. During, R.J. Samulski, C.G. Janson, Long-term follow-up after gene therapy for canavan disease, Sci Transl Med 4 (2012) 165ra163.

[161] R. Matalon, P.L. Rady, K.A. Platt, H.B. Skinner, M.J. Quast, G.A. Campbell, K. Matalon, J.D. Ceci, S.K. Tyring, M. Nehls, S. Surendran, J. Wei, E.L. Ezell, S. Szucs, Knock-out mouse for Canavan disease: a model for gene transfer to the central nervous system, J Gene Med 2 (2000) 165-175.

[162] M.Y. Fong, J. McDunn, S.S. Kakar, Identification of metabolites in the normal ovary and their transformation in primary and metastatic ovarian cancer, PLoS One 6 (2011) e19963.

[163] E. Kolwijck, R.A. Wevers, U.F. Engelke, J. Woudenberg, J. Bulten, H.J. Blom, L.F. Massuger, Ovarian cyst fluid of serous ovarian tumors contains large quantities of the brain amino acid N-acetylaspartate, PLoS One 5 (2010) e10293.

[164] E.A. Boss, S.H. Moolenaar, L.F. Massuger, H. Boonstra, U.F. Engelke, J.G. de Jong, R.A. Wevers, High-resolution proton nuclear magnetic resonance spectroscopy of ovarian cyst fluid, NMR Biomed 13 (2000) 297-305.

[165] E. Kolwijck, U.F. Engelke, M. van der Graaf, A. Heerschap, H.J. Blom, M. Hadfoune, W.A. Buurman, L.F. Massuger, R.A. Wevers, N-acetyl resonances in in vivo and in vitro NMR spectroscopy of cystic ovarian tumors, NMR Biomed 22 (2009) 1093-1099.

[166] R.W. Tothill, A.V. Tinker, J. George, R. Brown, S.B. Fox, S. Lade, D.S. Johnson, M.K. Trivett, D. Etemadmoghadam, B. Locandro, N. Traficante, S. Fereday, J.A. Hung, Y.E. Chiew, I. Haviv, D. Gertig, A. DeFazio, D.D. Bowtell, Novel molecular subtypes of serous and endometrioid ovarian cancer linked to clinical outcome, Clin Cancer Res 14 (2008) 5198-5208.

[167] D. Bogunovic, D.W. O'Neill, I. Belitskaya-Levy, V. Vacic, Y.L. Yu, S. Adams, F. Darvishian, R. Berman, R. Shapiro, A.C. Pavlick, S. Lonardi, J. Zavadil, I. Osman, N. Bhardwaj, Immune profile and mitotic index of metastatic

melanoma lesions enhance clinical staging in predicting patient survival, Proc Natl Acad Sci U S A 106 (2009) 20429-20434.

[168] G. Jonsson, C. Busch, S. Knappskog, J. Geisler, H. Miletic, M. Ringner, J.R. Lillehaug, A. Borg, P.E. Lonning, Gene expression profiling-based identification of molecular subtypes in stage IV melanomas with different clinical outcome, Clin Cancer Res 16 (2010) 3356-3367.

[169] W. Hu, C. Lu, H.H. Dong, J. Huang, D.Y. Shen, R.L. Stone, A.M. Nick, M.M. Shahzad, E. Mora, N.B. Jennings, S.J. Lee, J.W. Roh, K. Matsuo, M. Nishimura, B.W. Goodman, R.B. Jaffe, R.R. Langley, M.T. Deavers, G. Lopez-Berestein, R.L. Coleman, A.K. Sood, Biological roles of the Delta family Notch ligand Dll4 in tumor and endothelial cells in ovarian cancer, Cancer Res 71 (2011) 6030-6039.

[170] C.N. Landen, T.J. Kim, Y.G. Lin, W.M. Merritt, A.A. Kamat, L.Y. Han, W.A. Spannuth, A.M. Nick, N.B. Jennnings, M.S. Kinch, D. Tice, A.K. Sood, Tumor-selective response to antibody-mediated targeting of alphavbeta3 integrin in ovarian cancer, Neoplasia 10 (2008) 1259-1267.

[171] R.N. Buick, R. Pullano, J.M. Trent, Comparative properties of five human ovarian adenocarcinoma cell lines, Cancer Res 45 (1985) 3668-3676.

[172] J. Yoneda, H. Kuniyasu, M.A. Crispens, J.E. Price, C.D. Bucana, I.J. Fidler, Expression of angiogenesis-related genes and progression of human ovarian carcinomas in nude mice, J Natl Cancer Inst 90 (1998) 447-454.

[173] R.C. Bast, Jr., M. Feeney, H. Lazarus, L.M. Nadler, R.B. Colvin, R.C. Knapp, Reactivity of a monoclonal antibody with human ovarian carcinoma, J Clin Invest 68 (1981) 1331-1337.

[174] D.H. Lau, A.D. Lewis, M.N. Ehsan, B.I. Sikic, Multifactorial mechanisms associated with broad cross-resistance of ovarian carcinoma cells selected by cyanomorpholino doxorubicin, Cancer Res 51 (1991) 5181-5187.

[175] L. Li, J.E. Price, D. Fan, R.D. Zhang, C.D. Bucana, I.J. Fidler, Correlation of growth capacity of human tumor cells in hard agarose with their in vivo proliferative capacity at specific metastatic sites, J Natl Cancer Inst 81 (1989) 1406-1412.

[176] S. Huang, D. Jean, M. Luca, M.A. Tainsky, M. Bar-Eli, Loss of AP-2 results in downregulation of c-KIT and enhancement of melanoma tumorigenicity and metastasis, EMBO J 17 (1998) 4358-4369.

[177] H. Kuramoto, S. Tamura, Y. Notake, Establishment of a cell line of human endometrial adenocarcinoma in vitro, Am J Obstet Gynecol 114 (1972) 1012-1019.

[178] C.N. Landen, Jr., C. Lu, L.Y. Han, K.T. Coffman, E. Bruckheimer, J. Halder, L.S. Mangala, W.M. Merritt, Y.G. Lin, C. Gao, R. Schmandt, A.A. Kamat, Y. Li, P. Thaker, D.M. Gershenson, N.U. Parikh, G.E. Gallick, M.S. Kinch, A.K. Sood, Efficacy and antivascular effects of EphA2 reduction with an agonistic antibody in ovarian cancer, J Natl Cancer Inst 98 (2006) 1558-1570.

[179] P.H. Thaker, L.Y. Han, A.A. Kamat, J.M. Arevalo, R. Takahashi, C. Lu, N.B. Jennings, G. Armaiz-Pena, J.A. Bankson, M. Ravoori, W.M. Merritt, Y.G. Lin,

L.S. Mangala, T.J. Kim, R.L. Coleman, C.N. Landen, Y. Li, E. Felix, A.M. Sanguino, R.A. Newman, M. Lloyd, D.M. Gershenson, V. Kundra, G. Lopez-Berestein, S.K. Lutgendorf, S.W. Cole, A.K. Sood, Chronic stress promotes tumor growth and angiogenesis in a mouse model of ovarian carcinoma, Nat Med 12 (2006) 939-944.

[180] W.M. Merritt, Y.G. Lin, W.A. Spannuth, M.S. Fletcher, A.A. Kamat, L.Y. Han, C.N. Landen, N. Jennings, K. De Geest, R.R. Langley, G. Villares, A. Sanguino, S.K. Lutgendorf, G. Lopez-Berestein, M.M. Bar-Eli, A.K. Sood, Effect of interleukin-8 gene silencing with liposome-encapsulated small interfering RNA on ovarian cancer cell growth, J Natl Cancer Inst 100 (2008) 359-372.

[181] A.K. Sood, E.A. Seftor, M.S. Fletcher, L.M. Gardner, P.M. Heidger, R.E. Buller, R.E. Seftor, M.J. Hendrix, Molecular determinants of ovarian cancer plasticity, Am J Pathol 158 (2001) 1279-1288.

[182] A.P. Simopoulos, Essential fatty acids in health and chronic disease, Am J Clin Nutr 70 (1999) 560S-569S.

[183] B. Rigas, I.S. Goldman, L. Levine, Altered eicosanoid levels in human colon cancer, J Lab Clin Med 122 (1993) 518-523.

[184] D. Wang, R.N. Dubois, Cyclooxygenase-2: a potential target in breast cancer, Semin Oncol 31 (2004) 64-73.

[185] T.L. McLemore, W.C. Hubbard, C.L. Litterst, M.C. Liu, S. Miller, N.A. McMahon, J.C. Eggleston, M.R. Boyd, Profiles of prostaglandin biosynthesis

in normal lung and tumor tissue from lung cancer patients, Cancer Res 48 (1988) 3140-3147.

[186] D. Xia, D. Wang, S.H. Kim, H. Katoh, R.N. DuBois, Prostaglandin E2 promotes intestinal tumor growth via DNA methylation, Nat Med 18 (2012) 224-226.

[187] N.B. Kuemmerle, E. Rysman, P.S. Lombardo, A.J. Flanagan, B.C. Lipe, W.A. Wells, J.R. Pettus, H.M. Froehlich, V.A. Memoli, P.M. Morganelli, J.V. Swinnen, L.A. Timmerman, L. Chaychi, C.J. Fricano, B.L. Eisenberg, W.B. Coleman, W.B. Kinlaw, Lipoprotein lipase links dietary fat to solid tumor cell proliferation, Mol Cancer Ther 10 (2011) 427-436.

[188] J.W. Locasale, A.R. Grassian, T. Melman, C.A. Lyssiotis, K.R. Mattaini, A.J. Bass, G. Heffron, C.M. Metallo, T. Muranen, H. Sharfi, A.T. Sasaki, D. Anastasiou, E. Mullarky, N.I. Vokes, M. Sasaki, R. Beroukhim, G. Stephanopoulos, A.H. Ligon, M. Meyerson, A.L. Richardson, L. Chin, G. Wagner, J.M. Asara, J.S. Brugge, L.C. Cantley, M.G. Vander Heiden, Phosphoglycerate dehydrogenase diverts glycolytic flux and contributes to oncogenesis, Nat Genet 43 (2011) 869-874.

[189] D. Ben Sellem, K. Elbayed, A. Neuville, F.M. Moussallieh, G. Lang-Averous, M. Piotto, J.P. Bellocq, I.J. Namer, Metabolomic Characterization of Ovarian Epithelial Carcinomas by HRMAS-NMR Spectroscopy, J Oncol 2011 (2011) 174019.

[190] R. Rattan, R.P. Graham, J.L. Maguire, S. Giri, V. Shridhar, Metformin suppresses ovarian cancer growth and metastasis with enhancement of cisplatin cytotoxicity in vivo, Neoplasia 13 (2011) 483-491.

[191] W. Zhou, W.F. Han, L.E. Landree, J.N. Thupari, M.L. Pinn, T. Bililign, E.K. Kim, A. Vadlamudi, S.M. Medghalchi, R. El Meskini, G.V. Ronnett, C.A. Townsend, F.P. Kuhajda, Fatty acid synthase inhibition activates AMP-activated protein kinase in SKOV3 human ovarian cancer cells, Cancer Res 67 (2007) 2964-2971.

[192] J. Budczies, C. Denkert, B.M. Muller, S.F. Brockmoller, F. Klauschen, B. Gyorffy, M. Dietel, C. Richter-Ehrenstein, U. Marten, R.M. Salek, J.L. Griffin, M. Hilvo, M. Oresic, G. Wohlgemuth, O. Fiehn, Remodeling of central metabolism in invasive breast cancer compared to normal breast tissue - a GC-TOFMS based metabolomics study, BMC Genomics 13 (2012) 334.

[193] C. Choi, S.K. Ganji, R.J. DeBerardinis, K.J. Hatanpaa, D. Rakheja, Z. Kovacs, X.L. Yang, T. Mashimo, J.M. Raisanen, I. Marin-Valencia, J.M. Pascual, C.J. Madden, B.E. Mickey, C.R. Malloy, R.M. Bachoo, E.A. Maher, 2-hydroxyglutarate detection by magnetic resonance spectroscopy in IDH-mutated patients with gliomas, Nat Med 18 (2012) 624-629.

## Vita

Behrouz was born in Tehran, Iran on June 23rd, 1978, the son of a computer scientist Dr. Mansour Zand, his father, and Behshid Zand, his mother. His family moved to the United States when he was 8 years old, and was raised in Omaha, Nebraska. After graduating from Millard North High School, Omaha, NE, he enrolled in the University of Nebraska, Lincoln, NE. He received two Bachelor of Arts degrees in chemistry and psychology with a minor in biochemistry in 2003. He was then accepted into the University Of Nebraska College Of Medicine, and graduated with a Doctor of Medicine in 2007. He entered the Obstetrics and Gynecology residency program at Baylor College of Medicine, Houston, Texas, completing his training in 2011. In July 2011, he began a fellowship in Gynecologic Oncology at M.D. Anderson Cancer Center. His two-year Master's program during this fellowship was mentored by Dr. Anil Sood and focused on ovarian cancer metabolomics and the role of novel metabolites in ovarian carcinoma. During his research years, he also investigated a prolactin receptor antagonist, G129R, as a novel drug for therapy in uterine cancers. Behrouz has been married to Sara Razavi-Zand, an attorney, since 2007. They recently welcomed a new son Aria in July of 2012.